Vrije Universiteit Brussel
FACULTEIT INGENIEURSWETENSCHAPPEN

Universidad Pública de Navarra
Nafarroako Unibertsitate Publikoa
ETSIIT

PROOF-OF-CONCEPT DEMONSTRATION OF SMART OPTICAL IMAGING SYSTEMS

Gloria Esteban García

Promotor: Prof. Heidi Otteveare
Copromotor: Ir. Gebirie Yizengaw Belay

Academic year: 2012-2013

Abstract

This thesis focuses on the proof-of concept demonstration of smart optical imaging systems. Two systems have been investigated: first, a three-channel multi-resolution imaging system and in second place, a refocusing imaging system.

The three-channel multi-resolution optical imaging system (Static System) has already been investigated by Ir. Gebirie. Y. Belay. The system possesses three optical channels with different resolutions and fields of view. The first channel has the highest resolution and the lowest field of view; the third optical channel has contrary properties, that is, the widest field of view and the lowest resolution. The second optical channel has intermediate properties.
The experiments accomplished show that the system performs according to the expectations (simulations) and the quality of the images captured by the system is good. It has been observed two phenomena: distortion in the second optical channel and crosstalk in the third optical channel. The influence of misalignment errors of the components has been analyzed as well. The system is robust to longitudinal movements of the components, especially the first optical channel. Nevertheless, the system is less sensitive to rotational movements, becoming important the achievement of a good angular alignment.

The refocusing system is a voltage-tunable refocusing optical imaging system. The voltage applied to an electrically tunable liquid lens allows obtaining a sharp image for a large range of object positions. This fact is an added value with respect to the Static System, where the object distances range is limited.

The refocusing optical imaging system (Dynamic System) was designed by Lien Smeesters (et al.) and consists of two optical channels. The first channel is the third optical channel of the Static System and the second channel is the refocusing channel. This channel is compound of two passive lenses and the voltage-tunable liquid lens (Varioptic Arctic 320) in-between the two passive lenses. Each passive lens is composed of two aspheric surfaces (concave and convex). The lenses have been fabricated in PMMA by ultraprecision diamond tooling and they have been characterized (surface profile) by means of a measurement coordinate machine (Werth UA 400).

After the characterization of the lenses, a setup of the channel with refocusing capability has been built up. In this setup it has been necessary to modify the distance between the tunable lens and the second passive lens, and between the second lens and the image sensor (uEye CMOS camera detector) with regards to the design specifications. Indeed, the fabricated lenses are not identical to the designed lens surfaces; there is one surface that has not been fabricated with the parameters of the design.

The mounted refocusing channel performs well and the quality (contrast and ability to resolve fine details) of the captured images is high. In the experiments realized the working distances (object position) go from 0.15 m to 3 m, which is similar to the distance span obtained in the simulations for almost all the voltage values considered (from 51.1 Vrms to 60. The depth of field and depth of focus for different object distances and detector distances has been measured founding that the largest depth of field are obtained for low voltage values. In the experiments has been also observed that the tunable lens behaves hysterically (the optimal distance position where the image is sharp varies depending on the turning direction of the voltage, i.e., from higher to lower voltages values or viceversa.

Table of Contents

List of Figures

List of Tables

I. Introduction

1. Motivation for developing new smart optical imaging systems

Nowadays, the world is immersed in the *Knowledge and Information Society.* The insertion of cameras in mobile phones and other portable devices (by the way, these gadgets are becoming smaller and thinner) has caused that taking a picture or recording a video is quite quotidian. It is pretty common to find out a surveillance camera when one raises his/her head up[1]. Security has been converted into a primary issue; especially concerning people identification, so face recognition plays an important role. Furthermore, imaging systems have application in medicine (e.g. an endoscopy), in biology (e.g. microscopy), in satellite imaging (e.g. meteorology), in astronomy (e.g. telescope) or in photography and cinematography, of course. In short, imaging systems are present in **many domains**.

In most of these **applications,** it is interesting to have a global vision of a scenario, i.e., having general situation awareness and being able to focus on a region of interest. Or being concentrated in an area and yet keeping an eye on what is happening in the surroundings. In the terminology of imaging system's field, these aspects are translated in the combination of different **resolutions** (degree of resolving details) and **field of views** (extent of the perceived area). Other facet to bear in mind is the concept of **miniaturization**. The current tendency is to make devices as small as possible such that they are easily transportable and can be integrated in a major system without difficulty.

The aforementioned features conforms the idea of the wanted system: a compact, miniaturized optical imaging system that is able to give different resolutions and subtended areas (field angles) at the same time.

The first paragraph verses about various applications of imaging systems, artificial imaging systems. And, what happens with natural imaging systems? Well, there is no necessity of going too far away; what does make reading this text possible? The eyes and precisely, the human eye has **multi-resolution** capabilities. It is possible to contemplate a landscape and, in a certain moment, point the gaze in a bird obtaining accurate vision. The eye possesses a region in the retina called fovea where the resolution is high; the maximum is reached at the centre (foveola) where the cones (the photoreceptor cells responsible for colour vision) are densely packed. The number of cones reduces (whereas the number of rods, which are more sensitive to the light, increases) towards the outskirts so the acuity diminishes. The rest of the retina allows peripheral vision, gives event awareness.

The human vision is an example of **single** aperture eyes. Alternatively, many insects have **compound** eyes, i.e. many lenses in a small volume. Each *ommatidia* (individual "eye units") is located in a convex surface, thus pointing in slightly different directions such that the perceived image is a contribution of **multiple** inputs. As a result, the viewed angle is quite large and a fast movement can be detected simply; conversely, the resolution is low. This eye type inspires compact systems fabricated at wafer scale thanks to the current micro-optical technology [1-3]. This fact brings an advantage with respect to the classical imaging systems used to achieve a wide field of view (e.g. fish-eye lenses), which has its archetype in single aperture eyes and are quite bulky and expensive. This paragraph highlights the fact that human-made imaging systems mimic nature.

[1] *Big Brother is watching you...*

All in all, the aspiration is the invention of a system that combines the benefits and features of compound eyes (wide FOV, multichannel, compactness) and single aperture eyes (high sensitivity and resolution). The numerous fields (and therefore there are many applications) in which imaging system are present motivates the implementation of such a smart system.
What can be found? The next section gives a brief explanation, a rough outline in that regard.

2. State-of-the art

The imaging systems found in the literature combining different resolutions and field angles (such that it is possible to have detailed information of a region of interest without losing the general overview) have been demonstrated to be quite bulky and complex, what makes difficult their utilization in applications that require a compact system. As an example, two demonstrated approaches whose main purpose is surveillance will be presented. The first one is a cooperative distributed system for outdoor surveillance based on fixed and mobile cameras [3]. The second approach consists of a multi-channel, agile, computationally enhanced camera based on the PANOPTES (Processing Arrays of Nyquist-limited Observations to Produce a Thin Electro-optic Sensor) architecture [4].

The first considered imaging system consists of a stationary camera and an active pan-tilt zoom camera has been demonstrated to monitor the entire scene and obtain high-resolution images of a certain region of interest. The stationary camera had low resolution, imaging a wide area to detect and locate moving objects. The object position was then used to determine which direction the pan-tilt camera had to move to image the object of interest at a much higher resolution. The implemented system is able to provide automatic change detection at multiple zoom levels as main feature. Video shot with small zoom factor is used to monitor the entire scene from fixed camera, while medium and high zoom factor are used to improve the interpretation of the scene. Both the stationary and the active pan-tilt zoom cameras were connected to computers for movement and image processing tasks. A client/server approach has been used to connect the two PCs and to enable the cooperation of the two sensors with standard TCP/IP communication channels. This solution permits to decentralize computational units and to locate sensors in the more appropriate sites without logistic constraints.

The immediate given figure depicts an overview of the discussed system. Two main issues have been considered in the architecture design: first, the analysis of the monitored scenes with different levels of resolution (with the possibility of focusing the attention of the system on a particular region); second, monitor a wider area of interest.

Figure 1. Physical architecture of the system [3]

In another approach, multiple channels were used to first take different portions of the scene and then a high-resolution image was extracted by applying higher resolution reconstruction algorithms (e.g., super-resolution algorithm) on the image taken by the low-resolution channels. The imaging system comprises of five optical channels which use the same focal plane array. In the centre is the optical channel with wide field of view (FOV) for providing situational awareness. The other four optical channels have narrow field of view and are situated at the corners. Each of these four channels incorporates two flat adjustable mirrors: the mirrors closest to the focal plane array along the optical path just fold the optical path, whereas the mirrors closest to the object (furthest from the centre of the focal plane array) are rotated, thereby providing steerable field of view. There are several steering patterns of the narrow FOV channels. The operator can move all four narrow FOVs independently and look at four different locations within the wide FOV scene simultaneously with larger magnification, or can group them in some specific pattern and point to a desired location in the scene with wide extended view. There is also an o*n-board computer* that controls the narrow FOV steering mirrors, focal plane array image acquisition and several data processing tasks (collection and transfer for storage). Image reconstruction, analysis and enhancement are performed off-line on the collected imagery using algorithms specifically developed for this application.

In the figure given below is shown the conceptual layout of the modified PANOPTES system (prototype) (a) and the main parts of the prototype system (b).

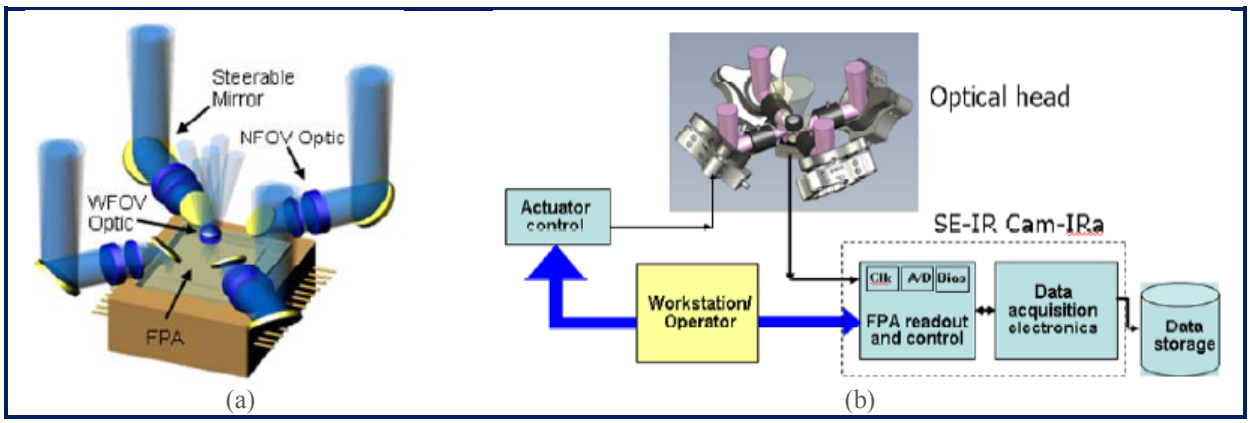

Figure 2. (a) Conceptual layout of the imager. (b) Main components of the PANOPTES prototype [4].

These approaches are not appropriate for purposes in which a reduced size is the principal requirement. As concerning compactness and miniaturization, the fields of micro-optics and active optics could be an excellent place to have a look and being inspired by new potential solutions. Some demonstrated implementations can serve as a model; for instance, artificial compound eyes [6] or a lens with a constant total field of view and real-time variable resolution in certain zones of interest [7]. The next section presents the B-PHOT approach, which will be the subject of this thesis.

3. B-PHOT approaches: a three-channel multi-resolution smart optical imaging system and a refocusing optical imaging system.

In order to tackle the challenge of creating such a desired (described in the first section) smart imaging system, the line of attack adopted consists of, in first place, the design of a three-channel optical imaging system. The channels have different angular resolution and field of view (FOV) in such a way that there is one channel (first optical channel) that has high resolution and narrow FOV; another channel (third optical channel) with inverse features, that is, low resolution and wide FOV; finally, the last channel (second optical channel) has intermediate properties. The function of the third optical channel is related to event awareness; motion detection is a possible purpose. A potential use of the first optical channel is face recognition as this channel allows resolving fine details. Possible, potential because the application is not unique; different processing algorithms can be implemented. The chosen application is in-car-pedestrian detection by implementing a Viola-Jones algorithm. The second optical channel is necessary for the correct functioning of the Viola-Jones algorithm as this algorithm needs consecutive processing steps which require increasing angular resolutions (in each step) for face recognition procedure [8]. The three channels share the same image sensor. The designed imaging system can be fabricated in two polymer plates at wafer scale; indeed, the lenses have been manufactured by diamond tooling. All the components (four lens surface arrays, each one with three lenses in it, so there are twelve surfaces in total; an aperture stop of absorbing material and a tube, acting as baffle board, for crosstalk reduction) have been assembled using guiding pins and alignment holes. The three optical channels coexist in the same plate, such that each of the three lenses composing the array corresponds to one optical channel. In other words, each optical channel is composed of four aspheric lenses. The lens arrays are grouped in pairs originating a 'lens-stack' in such a way that there are two lens-stacks. The image sensor used is a commercial (uEye) CMOS sensor.

This system will be named as '*Static System'* (following paragraphs clarify why) and it is discussed in the third chapter of this dissertation. The system is being investigated and developed by *Ir. Gebirie Yizengaw Belay* (thesis supervisor) together with other B-PHOT members [9]. In addition, this optical imaging system is framed inside the 3SIS project[2], being one of the layers of a stacked 3D imager thought for automotive pedestrian detection.
The Static System is able to resolve fine details in a small zone of interest, through the channel that has the highest angular resolution, while controlling the surrounding region with the widest field of view channel. Nevertheless, the system is static (here the reason☺), fixed as regards to working distances: depending on where the object of interest with respect to the system is situated, the image could be blurred if the object is out of focus. Therefore, a good improvement is to provide the system with autofocusing functionality.

[2] https://projects.imec.be/3sis/

The integration of a tunable lens in the high resolution channel is a good way of obtaining such desired **refocusing capability**. The best option is to utilize an electrically liquid tunable lens since its integration is easier and it is feasible to attain a compact system (wafer scale design). Mechanical tuning has been rejected due to the requirements of integration and compactness are not fulfilled.

The proposal is a design of a bi-channel imaging system with one of the channels performing refocusing faculty by means of voltage-tunable configuration. The first channel corresponds to the third optical channel of the Static System which has the widest FOV and lowest resolution of the three channels. In turn, the second optical channel is wanted to have high angular resolution and narrow FOV. As far as the first channel is already designed, the refocusing channel (second optical channel) must adapt to the characteristics of the first channel. This fact imposes some constraints in the design of the second channel as it has to create a perfect entity with the other channel. Furthermore, there are other simulations whose purpose was to study the effect of the relative position between the lens elements on the performance and thus, find out the most suitable (optimized) configuration. This configuration has become the best when the tunable lens is in-between two passive lenses (is a system with three elements). It is necessary to mention that the configuration of the first channel (third channel of the Static System) has an aperture stop in between the two lens array-stacks. The final design for the second channel is as follows: two passive lenses and the tunable lens in-between, similar to the composition of the first channel, but instead of the aperture stop, the tunable lens is found now. The pursued target is that the coincident elements are made in one piece of the same material facilitating the alignment and not degrading the robustness of the system.

All works related to the refocusing system have been accomplished by Ir. *Lien Smeesters* in her master thesis whose title is *Integration of tunable lenses in micro - optical smart camera systems.*

This system, alternatively, will be referenced as 'Dynamic System' as it has refocusing capacity. Currently, only the second channel can be tested. The lenses of this channel have been fabricated, but the integration with the other channel in order to make up the designed refocusing imaging system has not been realized yet. The work that has been carried out in this thesis consists, essentially, of the proof-of-concept demonstration of the second optical channel belonging to the designed refocusing imaging system. Chapter IV verses about it. The references made to several simulations and configurations in this chapter correspond to the ones appearing in the cited master thesis of Lien Smeesters.

4. Rational of this thesis

The work that has been accomplished in this thesis is mainly experimental and is framed inside a bigger project in the field of optics and imaging systems. It is a stage in a process to achieve a final objective, and this work is the continuation of two already existing projects. Two smart imaging systems ('Static System' and 'Dynamic system', described in the previous section) have been designed and fabricated, so the next step is to check their real performance by means of several proof-of-concept demonstrations (as the title of this text denotes).

As specific tasks, in the case of the Static System, the study of its behaviour and tolerance analysis (how misalignment errors in the optical components affect its performance) have

been carried out. The undertakings for the Dynamic System are the characterization of the fabricated lenses (surface profiles) with advanced measurement tools and the comparison of the experimental and simulated performances. It has been also necessary to get acquainted with liquid tunable lenses (working principle and operation) given that is responsible for the refocusing capability of the second investigated system. In order to measure quantitatively the quality of the systems, the modulation transfer function (MTF) has been calculated experimentally.

The experimental results will be useful to determine the optimal way of fabricating such smart imaging systems and improve the possible malfunctions; as well as, to anticipate solutions to matters that were not considered in the design. In other words, this work will provide inputs, feedback to achieve better systems.

5. Thesis Structure

This thesis is composed by five chapters.

The first chapter introduces the context in which this Thesis is encompassed and its motivation. A general view of the current imaging system panorama (State-of-the-Art) together with the approaches carried out in B-PHOT. The rational of this thesis is also included in this first chapter.

The second chapter is about relevant definitions and concepts for this thesis. These concepts are related to optical properties and performances of the investigated systems. The concept of modulation transfer function (MTF) is developed more deeply. Apart from the concept itself and some measurement methods, it is also explained how the MTF has been applied to quantify the quality of the captured images by the systems subject of this thesis.

The next two chapters are about the optical imaging systems subject of this thesis.

Chapter III is about the Static System. First, the system is introduced and described. Afterwards, the optical performance of the system is presented. Then, the accomplished analysis of the influence of misalignment errors in the performance of the system is discussed. The conclusions of the performance of the Static System close the chapter.

In Chapter IV several aspects related to the Dynamic System are treated. In the first part of the chapter is explained an experiment made to study the behaviour and operating principle of the tunable lens. Then, the Dynamic system is described. The results of the characterization of the fabricated lenses are explained. The chapter also includes the proof-of-concept demonstration of the refocusing imaging system.

Finally, the last chapter summarizes the accomplished work and gives the conclusions of the obtained results. Additionally, some perspectives are proposed.

II. Relevant concepts and definitions for this thesis work

This chapter collects a set of terms which are necessary along this text to provide helpful information to understand some results and have essential knowledge. First of all, a table with several definitions is presented. Secondly, in the first section, there is an assortment of concepts that are related to some optical properties or to the performance of the studied systems. The second and closing section is dedicated to the Modulation Transfer Function (MTF). This topic has a considerable weight in the accomplished work for this thesis. An explanation of the concept is included followed by a brief description of some measurement methods. The section finalizes with the description of how the MTF has been utilized to measure the optical quality of an image captured with the imaging systems under investigation.

Table 1. Field specific terms definitions

Term	Definition
Astigmatism	Aberrations that are caused by different focuses of two perpendicular planes (tangential and sagittal). The image of a point source is not a point, but takes the form of two separated lines.
Coma	Aberration caused by variation of magnification over the entrance pupil.
Distortion	Aberration of a lens or optical system due to variations in the magnification with the lateral distance from the optical axis.
Spherical aberration	Aberration that causes a blurred image, because the light rays, that are striking a mirror or lens at different heights, are focused at different points on the optical axis.
Chromatic aberration	Aberration that is caused by the focusing of the light rays of different wavelengths at different points on the optical axis.
Diffraction	Deviation of a direction of propagation of a beam of light, which occurs when the light rays passes the edge of an obstacle, such as a diaphragm.
Aperture stop and Field stop	Physical pieces of hardware that limits rays that can propagate through the system. The aperture stop limits the light-gathering ability, and the field stop limits the field of view. The image of the aperture stop is the '***pupil***' and the image of the field stop is the '***window***'.
Clear aperture	Diameter of the widest on-axis light beam, that passes through the aperture stop and reaches the detector.
Focal length	The distance between the principal plane and the focal point of a lens.
F-number	The ratio of the focal length and the diameter of the lens.
Field of view	Solid angle that can be viewed through an optical instrument.
Meridional ray	Ray that is restricted to the plane that contains the system's optical axis and the object point, from which the ray originated. It is also called a *tangential ray*.
Marginal ray	The meridional ray that starts at the point where the object crosses the optical axis. It touches the edge of the aperture stop of the system, and crosses the optical axis at the locations where an image is formed.
Point spread function	The irradiance at the image plane which is produced by a point source at the input of the optical system.
Refocusing system	System with a constant magnification and image distance, that focuses on different object distances, by adaptations of the focal length.
Zooming system	System with a constant image and object distance, that gives different magnifications, by adaptations of the focal length.

1. Definitions and concepts of interest for the investigated imaging systems

Field of View (FOV)

The extent of the object which a lens actually images is called the **field of view** and is specified as the actual size for near objects or by the angle between the extreme principal rays. There are three possible ways to measure the field of view: horizontally, vertically or diagonally.

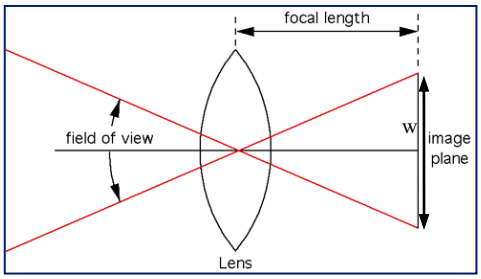

Figure 3. Horizontal field of view [10]

The field of view depends on the focal length which is defined as the distance between the principal plane and the focal point of a lens. From Figure 3 it can be extracted that $FOV = 2 \cdot \arctan\left(\frac{w/2}{f}\right)$, where w is the width of the image sensor and f is the focal length. If a wide field of view is desired the focal length of the lens must be short. Alternatively, having a big sensor size is another option although the size is not infinite, there are physical limits. According to this, the sensor size could be a possible limitation for studying, for instance, the performance of an imaging system. In fact, this matter is found in the characterization of the static system.

The FOV is determined by the field stop: the element limiting the size or angular breadth of the object that can be imaged by an optical system.

The Static System (three-channel multiresolution imaging system) possesses three different fields of view in the same device. The same is true for the angular resolution; this concept is explained following. The static system is discussed in more detail in the third chapter of this master thesis.

Angular Resolution

Angular resolution is the minimum angular distance for which two adjacent objects can be distinguished from each other. It is the ability of an optical instrument to resolve between two closely spaced objects or in another way, the ability to produce separable images of different objects points.

The resolution limit is given by the Rayleigh criterion which states that "*two images are just resolvable when the centre of the diffraction pattern of one is directly over the first minimum of the diffraction pattern of the other.*" The first minimum is at the angle for which $\boldsymbol{\sin(\theta) = 1.22\lambda/D \approx \Delta\theta}$, where λ is the wavelength of light and D is the diameter of the lens aperture. Thus, the resolution is determined, between others, by the aperture stop of the system. The smaller the angle, the better the resolution is. If the angular separation of two objects is $\Delta\varphi$, and $\Delta\varphi \gg \Delta\theta$, the images will be distinct and easily resolved.

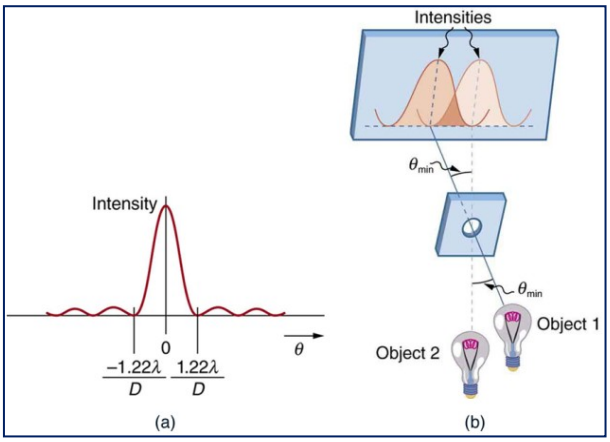

Figure 4. (a) Diffraction pattern for a circular aperture. (b) Rayleigh criterion for resolving two point objects. The overlap of the two diffraction patterns is such that the maximum of one pattern falls in the first minimum of the other one [11].

The first minimum of the diffraction pattern of a circular aperture corresponds to the first zero of a first order Bessel function and it is called "Airy Disk". Because of diffraction from the system stop, an aberration-free optical system does not image a point as a point but more as a spot. An airy disk is produced having a bright central core surrounded by diffraction rings.

The radius of the Airy disk is given by $q_1 = 1.22\,\frac{R\lambda}{2a} \approx \mathbf{1.22}\,\frac{\boldsymbol{f\lambda}}{\boldsymbol{D}}$ where D is the aperture diameter, i.e. $D = 2a$ and f is the focal length which is approximately equal to the distance between the point and the centre of the aperture, i.e. $f \approx R$ (this case is valid when the object is at infinity).

When the object is at a finite distance, the spatial distance between the two object points is used to determine the spatial resolution of the system. Assume Δl is the centre to centre separation of the images, the **limit of resolution** is$\boldsymbol{\Delta l_{min} = 1.22\,\frac{f\lambda}{D}}$. The *spatial resolution* is obtained by multiplying the angular resolution in radians and the object distance.

Typically for the two explained terms, angular resolution and field of view a trade-off should be made. The consecution of a wide field of view, for instance, compromises how the angular resolution will be. For classical imaging systems it is difficult to combine a high resolution and a large field of view at the same time. If having a high resolution and a wide field of view is desired, a big sensor with nanopixels (the size of the pixel is in nanometres) is needed. This small pixel pitch is the main constraint to not fulfil both desired features. New approaches like the one presented in this thesis can change the latter.

Depth of Field (DOF)

The depth of field is defined as the range of object distances within which objects are imaged with acceptable sharpness.

For a given image plane a system shows a sharp image for only one object plane. If the object is before or behind this object plane the image in the given image plane is not sharp.

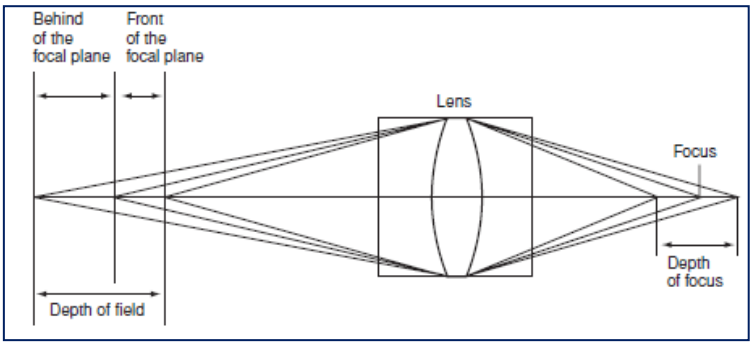

Figure 5. Depth of Field definition [12].

The depth of field is affected by the lens focal length, the aperture and the subject distance. If the other two factors remain the same a deeper depth of field is obtained by having a smaller aperture or a shorter focal length. For example, if the lens focal length and the shooting distance (being the case of a camera) stay the same, the depth of field is much deeper at F# of 16 than at F# of 1.4. The other case, comparing a 55 mm lens with a 200 mm lens at the same aperture and shooting distance, depth of field is deeper with the 55 mm lens.

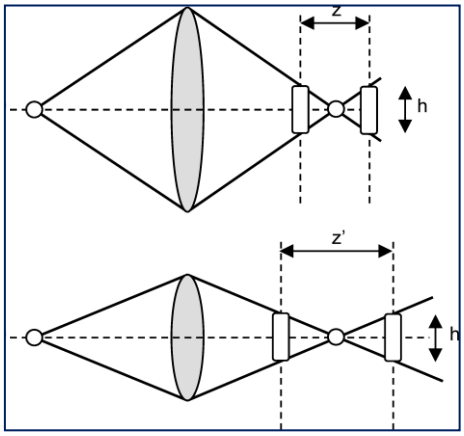

Figure 6. Influence of lens aperture in the depth of field for a fixed focal length [13].

From figure 6 it is noticed that, for a given focal length, the depth of field is worse for a lens with larger aperture; there is a compromise to be made: a larger aperture leads to more light in the image, but to a smaller depth of field (and in general more aberrations).
An infinite depth of field is obtained by employing a small hole in a screen: all objects are imaged sharply because one object point corresponds to only one ray through the system. Unfortunately, the image will be dark.

If the image sensor is shifted instead of the object, the concept of **depth of focus** appears instead of depth of field. The depth of focus describes the distances over which light is focused at the camera's sensor and is also called "focus spread". The depth of focus is the extent of the region around the image plane in which the image will appear acceptably sharp. This depends on the magnification. The concept is depicted in Figure 5.
The concept of depth of focus is used in the study carried out for understanding the working principle of the tunable lens. (Chapter IV)

Distortion

Distortion is the phenomena that each off-axis image point has different transverse magnification. Thus, the location of the off-axis image point may be differing from its ideal location predicted by paraxial imaging (in the same image plane).

The distortion causes the image of a straight line at the edge to be arched out, i.e. *barrel or negative distortion* or to be arched in, i.e. *positive* or *pincushion distortion*. The reason is that the image scale or magnification is not constant throughout the entire image field.

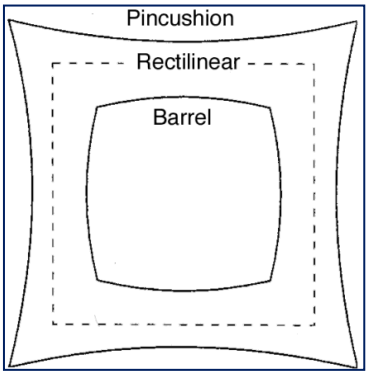

Figure 7. Pincushion and Barrel distortion [14]

The amount of distortion is the displacement of the image from the paraxial position, and can be expressed either directly or as a percentage of the ideal image height. The paraxial and real image heights can be expressed as a product of the focal length and tangent of the subtended field angles, i.e. the paraxial (ideal) image height, $h'_1 = ftan\theta_1$ and the real image height, $h'_2 = ftan\theta_2$, for an infinitely distant object. Then, the distortion is the difference of the real and paraxial image heights, given by $h'_2 - h'_1 = f(tan\theta_2 - tan\theta_1)$.

The amount of distortion ordinarily increases as the image size increases; the distortion itself usually increases as the cube of the image height (percentage distortion increases as the square). Thus, if a centred rectilinear object is imaged by a system affected with distortion, it can be seen that the images of the corners will be displaced more (in proportion) than the images of the points making up the sides.

Thinking of a whole imaging system, a potential cause of distortion is the position of the aperture diaphragm with respect to the lens. This is an issue to keep in mind when designing a new imaging system.

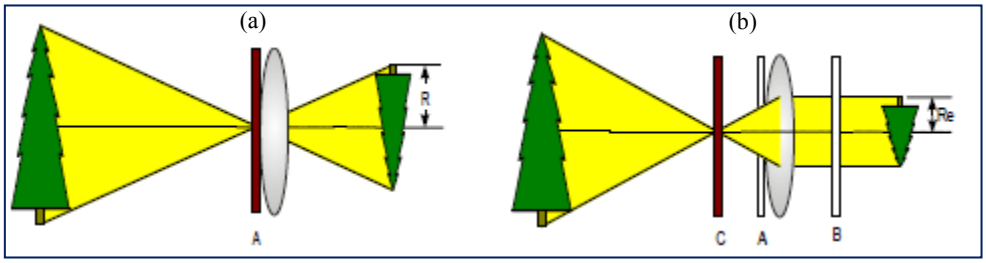

Figure8. Influence of aperture diaphragm on distortion. (a) Image without distortion. (b) Barrel distorted image [15].

The principal ray –the ray that passes through the centre of the aperture stop determines the location of the image. This ray is depicted by the lines that bound the yellow shaded region. When the aperture is sited at position A with respect to the lens (Figure 8 (a)), the principal ray passes through the optical centre and leaves the lens at the same angle as it entered. The result is a non-distorted image (orthoscopic). When the aperture stop moves behind or forward, the principal ray is refracted. If the diaphragm is positioned in front of a positive lens (position C) barrel distortion is noticed (Figure 8 (b)) whereas if the diaphragm is behind the lens (position B) pincushion distortion occurs. When the stop is in front, the object distance measured along the chief ray (i.e., the one passing through the centre of the aperture) will be greater that it was in the orthoscopic case. Thus, the distance from the object to the focal point will increase and the transversal magnification will be smaller. A rear stop produces the

opposite effect such that the transversal magnification for an off-axis point will be larger than without the stop in the back of the lens (positive). If the lens is negative, the mentioned diaphragm position will result in the inverse effect. In addition, the interchange of the object and the image will change the sign of the distortion for a given lens and a stop.

In multi-lenses systems, it is common to use a stop midway between identical lens elements in order to suppress distortion. The distortion from the first lens will cancel the contribution from the second lens. For an ideal performance the magnification has to be equal to unity, which means the object and image distances have to be identical.

From the concepts above mentioned in this section, the following conclusion can be drawn: there is a compromise, interdependency between the treated concepts as they depend on the same property, for example the focal length or the aperture. The improvement of one aspect causes deterioration of the other one. It is important to find a good balance or give major priority to one of them based on the specific requirement of the desired system yet optimizing the other features.

2. Modulation Transfer Function

2.1. Understanding the concept of Modulation Transfer Function

Determining the quality of an optical system or element is critical to know how it will perform. One quality criterion is associated with the limit of resolution: the larger the resolution, the better the performance.

One way of quantifying this quality is by means of the *Modulation Transfer Function* (MTF). **MTF** is defined as the normalized magnitude of the Fourier Transform of the imaging system's *Point Spread Function*, which describes the degree of spreading of an image of a point object. This definition does not provide a practical understanding and the purpose of this subsection is not to going into mathematics, so what is underneath the concept?

Modulation is the process whereby one or more properties of a waveform are varied. A useful example to explain the modulation idea is to consider a sinusoidal distribution representing the irradiance values of an image which is introduced in the system.

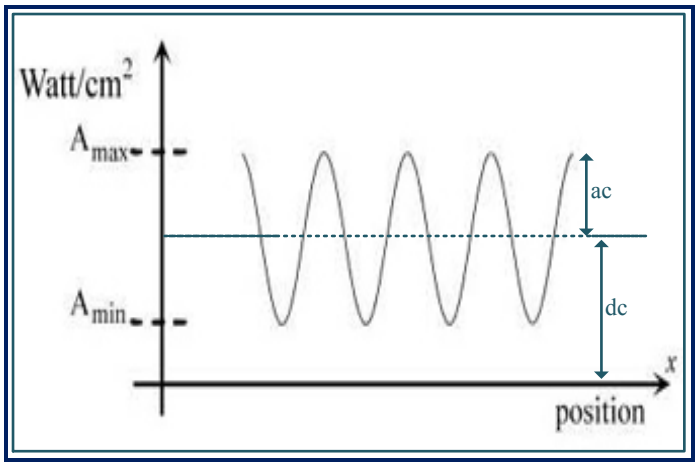

Figure 9. Concept of modulation [16]

Modulation is defined as the amplitude of the irradiance variation divided by the bias level:

$$M \equiv \frac{A_{max}-A_{min}}{A_{max}+A_{min}} = \frac{ac}{dc} \qquad (1)$$

The modulation takes values between 0 and 1. When the waveform has a minimum value of zero ($A_{min} = 0$), the modulation is equal to unity whatever the maximum irradiance level is. The $M = 0$ condition means that, although there is still a nonzero image-irradiance level, there is no spatial variation of that irradiance ($A_{max} = A_{min}$). Low levels of modulation are harder to discern against the unavoidable levels of noise inherent in any practical system.
An easy way to understand it is thinking of a white and black rectangular bars target. The output of an ideal optical system is identical to the input. However, in real systems the resulting image will be somewhat degraded due to aberrations and diffraction phenomena, in addition to assembling and alignment errors in the optics. In the image, bright highlights will not appear as bright as they do in the object, and dark or shadowed areas will not be as black as those observed in the original patterns. The limited spatial resolution of the optical system results in a decrease in the modulation M of the image relative to what was in the object distribution (Figure 10).

If the width of the lines decreases, there are more line pairs (black and white lines) in the same space and it is more difficult to distinguish them from each other and as such the modulation index will be lower. Therefore, the modulation is dependent on the spatial frequency. The spatial frequency is expressed in line pairs or cycles per unit of length, [lp/mm] or [cycles/mm], as well as cycles per pixel [C/P] and line widths per picture height [LW/PH] which are more used in digital sensors.

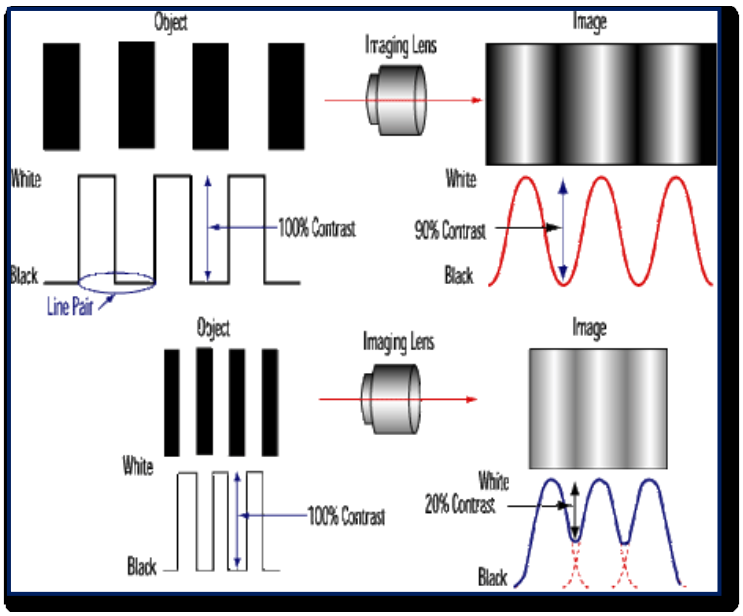

Figure 10. Contrast comparison at object and image planes [17].

The MTF can be seen as a description of how much the optical system modulates the input as a function of the spatial frequency, in other words, what is the response of the system. The MTF can be defined as the ratio between the modulation of the image and the modulation of the object.

$$MTF(\nu) \equiv \frac{M_i}{M_o} \qquad (2)$$

T
he representation of the MTF will be a decreasing curve as frequency increases according to the above paragraphs.

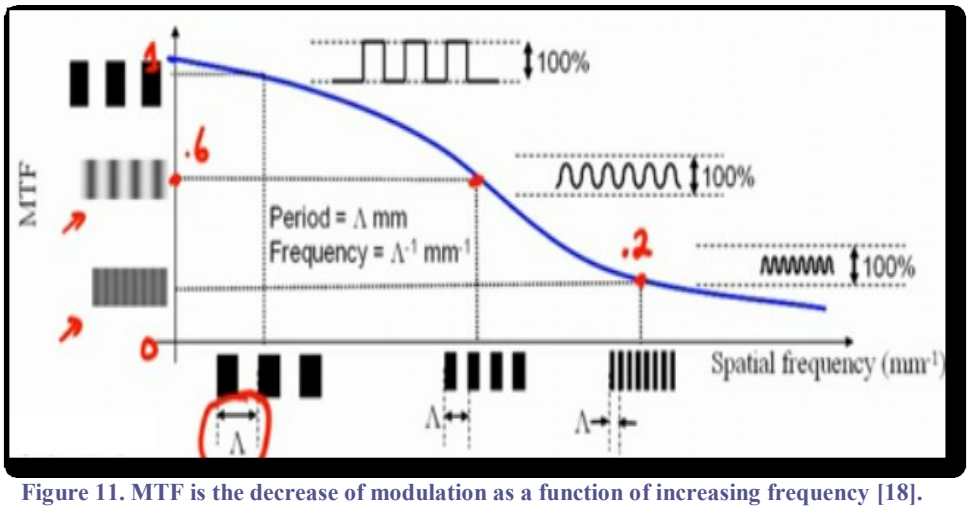

Figure 11. MTF is the decrease of modulation as a function of increasing frequency [18].

Figure 11 summarizes the concept perfectly. It is clear that there is a relationship between the distances of the black-white bars, i.e. the spatial frequency and how the imaging system shows the object in the resulted image. The closer the lines to one another, the more difficult to distinguish them and the more blurred the image is.

2.2. Measuring methods

There is not a single manner of calculating the MTF. Next, a brief description of some of these methods is presented.

In order to explain the MTF concept in the preceding section (2.1), one type of target has been introduced which allows measuring the MTF. The target consists of a set of black and white bars with different spacings in order to have a vast range of frequencies.
An example of a "bar pattern" target is the *USAF 1951* resolution target. The pattern consists of groups of three bars and decreasing spacing in power of 2 according to the following formula:

$$frequency(lp/mm) = 2^{group+(element-1)/6} \qquad (3)$$

The largest bar that the imaging system cannot discern is the limit of the resolving power of the imaging system.

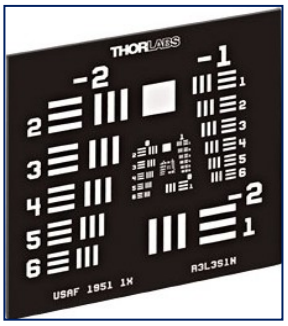

Figure 12. USAF 1951 resolution target chart from Thorlabs

Every group is composed of six elements and the number of groups varies from seven to nine depending on the specific chart.

The MTF can be calculated directly from this target by using its definition. (eq. 2)

A second type of target consists of gray scale patterns of different frequency and is the denominated "sine-wave target".

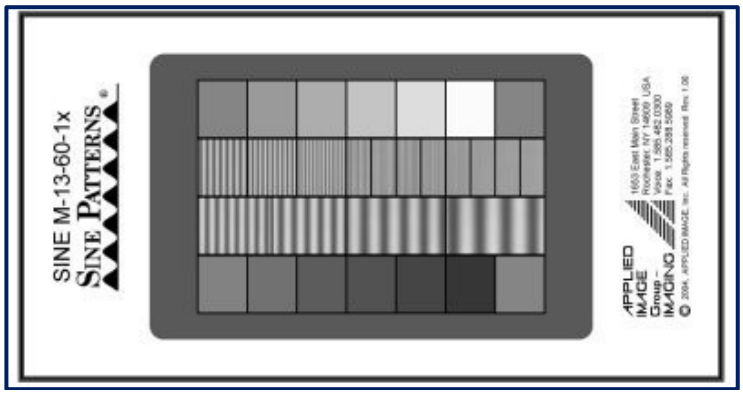

Figure 13. M-13-60 sine-wave target from Applied Image Inc. The upper and lower rows in each test pattern array contain the gray scales, usually together with data of the approximate density. The four corners areas have a 0.7 density and are useful for checking uniformity of illumination. The inner rows contain the sinusoidal areas with the associated spatial frequency. Nominal modulation of the sinusoidal areas is 60%.

There are two methods of measuring the MTF with this target: one directly based on the definition of MTF (eq. 2) and another one using Fourier analysis, knowing that the modulation is equal to the ratio of the fundamental frequency component and the DC component. This last method is more robust to the noise since the Fourier transform suppresses the random noise effectively [19].

Another technique applied to measure the MTF is *Slanted-Edge* method. It is a widely extended method and probably the most used. The main idea is to study the response of a system to a step function. This step function is obtained by having two different areas such that there is a contrast edge compared with the background. As the name indicates, the edge must be slanted. In the case that the sensor is not spatially invariant, the relative positions of the test edge and the matrix of the sensor are conditioned. In order to avoid the boundary of the test target does not match the pixel axis of the sensor array, the test target must be slightly slanted by a small angle. Practical angles are used from 5º up to 10º, but it is not critical. It is enough if the angle ensures that the test image projection on the sensor grid will affect geometrically in different way each successive row or column of the pixel array [20].

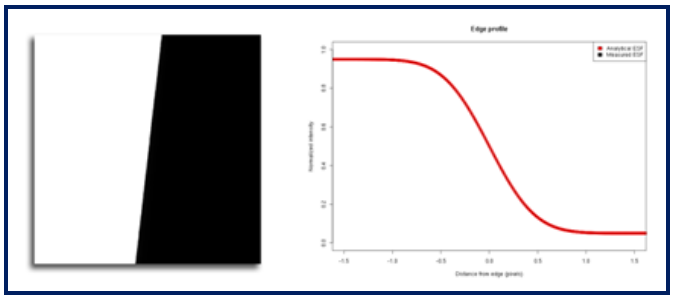

Figure 14. Example of a region of interest of one target to be analyzed by Slanted-Edge Method and the respective edge profile.

The analysis is done starting from the Edge Spread Function (ESF) and calculating the Fourier Transform of the derivative of the ESF, meaning the MTF.

2.3. Experimental MTF

This section describes the procedure used to analyze the quality of images captured by the studied imaging system, in other words the MTF. It also includes the respective MATLAB code reference although in a qualitative way.

2.3.1. Aspects to consider in the calculation of the MTF

The USAF 1951 resolution target is the chosen test target. The way of calculating the MTF is as follows: Each element of the different bar groups of the USAF plate is selected and the corresponding modulation is calculated from the maximum and minimum intensity values (based on its definition given in eq.1) for that particular element, which represents a single spatial frequency. This procedure is repeated for all the elements that are resolved. Thus, the modulation for a certain range of discrete spatial frequencies is obtained. As can be observed in Figure 15 the size of the elements diminishes as the group number increases (in agreement with the increasing range of spatial frequency values). Therefore, it is necessary to vary the magnification depending on the object spacing, being needed to move the object. However, the relationship between the object and image size in the different position should be constant.

The first consequence is that, it is not possible to calculate the MTF from a single image, more images are required. These are images of group-2 and -1, group 0 and 1 and group 2 and 3. The object has to be situated further or closer to the imaging system depending on which groups are intended to image. The magnification is given by the ratio of the image's height and the object's height or the ratio between the distances of the image and the object with respect to the principal planes of the imaging system. Then, it could be said that, there exists a correlation between the height of an element and the distance of the object. The sensor size has influence on the image magnification too. Actually, it is the image height which determinates the magnification, nevertheless if the height of the magnified image is too large, it will be truncated by the limited size of the image sensor.

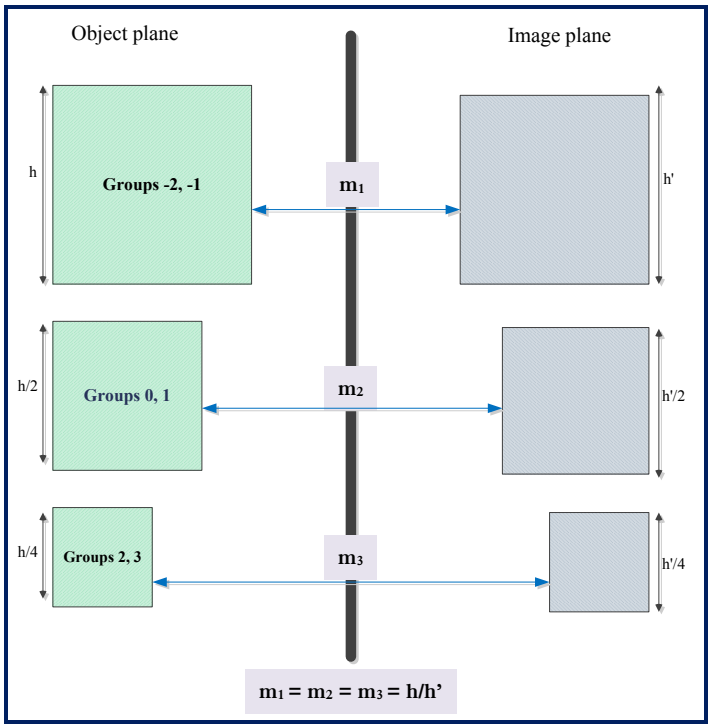

Figure 15. The magnification must be constant regardless the group in the USAF 1951 resolution target.

Suppose that the height of one element belonging to groups 2/3 is half of the height of one element of groups 0/1 which, at the same time, is half of an element of groups -2/-1 whose height is *h*. This relationship between the heights should be identical in the case of the respective images, what implies that the magnification in the three cases is the same; it is constant.

The proportionality between distances has its equivalence in the frequency domain. The magnification can be expressed as a quotient of spatial frequencies.

In short, it is necessary to modify the object distance in order to avoid the effects of magnification in the measurement. Magnification influences indirectly the resolution because the subtended angle changes although the resolution limit of the imaging system is fixed. Furthermore, it is important to keep in mind the fact that the position of the detector must change to adapt to the object distances changes.

2.3.2. Description of the real procedure

A MATLAB script[3] has been written to calculate the MTF. The process flow is depicted in the figure below. For every sample which corresponds to one element and thus one frequency, the respective modulation is calculated. The result of the calculation is affected by noise and hence reducing its effect is indispensable.

Starting from the intensity values, it is possible to take the maximum and minimum values and calculate the mean of those values, separately for the maximum and the minimum. Subtracting the mean from the maximum and minimum values gives the error, how much the values deviate from the mean value. Finally, the average of the error is calculated, getting what in Figure 16 appears like $\bar{e}_{max}$ and $\bar{e}_{min}$. The reason for having two differentiated errors is found in the definition of modulation: if the error is unique it has no influence in the numerator as it cancelled in the subtraction; on the contrary, it occurs in the denominator since the effect of the noise is assumed to be additive so the modulation will be lower. Unique means that instead of considering two error values (one for high intensity values and other for low intensity values), the error is only calculated from low intensity values. These values would belong to background areas and not to the elements. Thus, the noise would be considered as 'background noise' in such a way the respective error will be subtracted from the whole image (all the intensity values) instead of treat each element separately. Treating the noise individually for every sample instead of applying a correction in the overall image is better as the accuracy is greater.

The noise treatment and the error quantification of such a noise (or other error sources) is not a trivial issue since the modulation value is affected by this error. This fact could cause an overestimation of the image quality as the calculated MTF values are higher than the actual values.

[3]The MATLAB code can be found in the Appendix A.

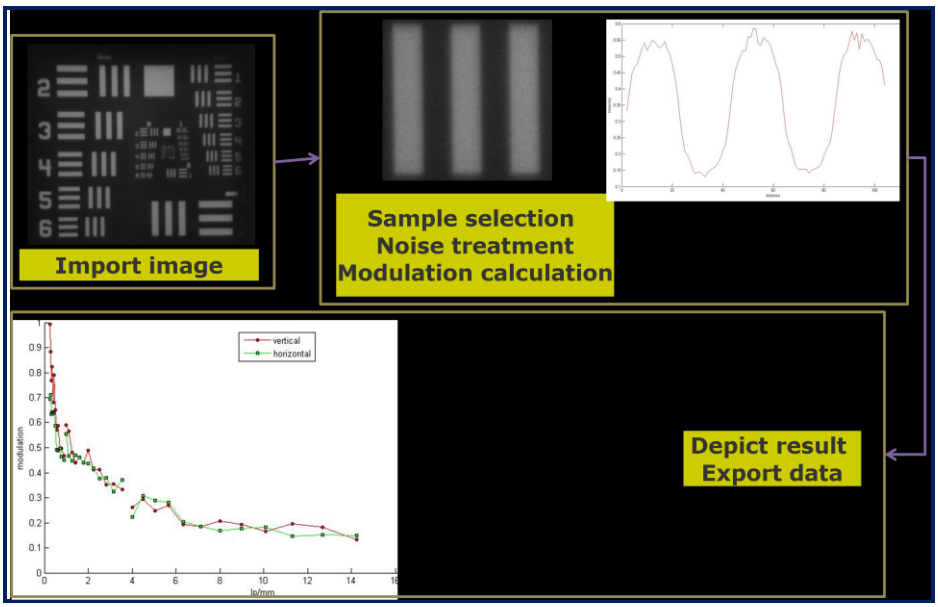

Figure 16. Flow diagram of the MATLAB script for calculating the MTF

Next, some examples of cases that can appear in the calculation process are depicted.

Example 1: high modulation value

The contrast is clear and the histogram ratifies it, most of the values are gathered in two intensity values. It is observed that the two considered errors are different and they have, therefore, unequal effect.

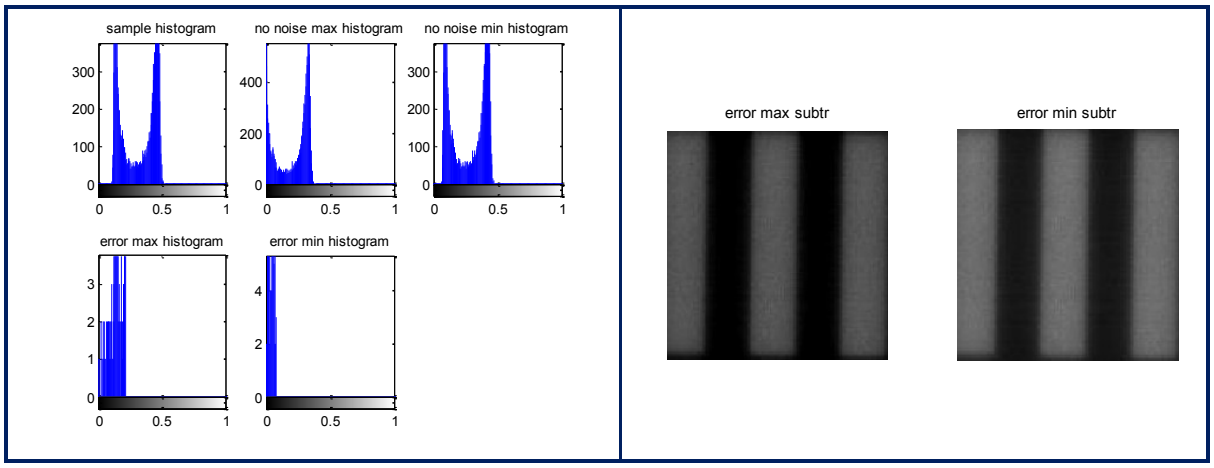

Example 2: medium modulation value

The range of intensity values is wider and it is more difficult to distinguish the beginning of one line and the end of the counterpart. In this case, it could happen that the minimum intensity value is close to zero and the maximum intensity value is low obtaining a relatively high modulation index. For instance, the maximum intensity is 0.29 and the minimum is 0.04 what gives a modulation of 76%. A closer value could have been obtained in an image with higher black-white visual contrast. Nevertheless, looking at their edge profile it will be more abrupt in the second case.

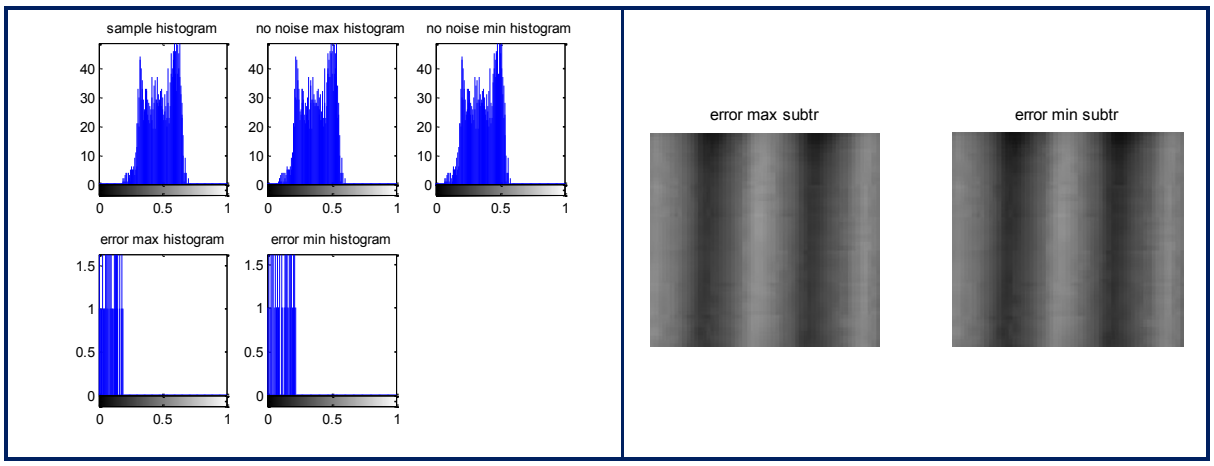

Example 3: low modulation value

In this example the values are almost equal to one value; the uniform distribution shows it clearly. The maximum and minimum value will be very close.

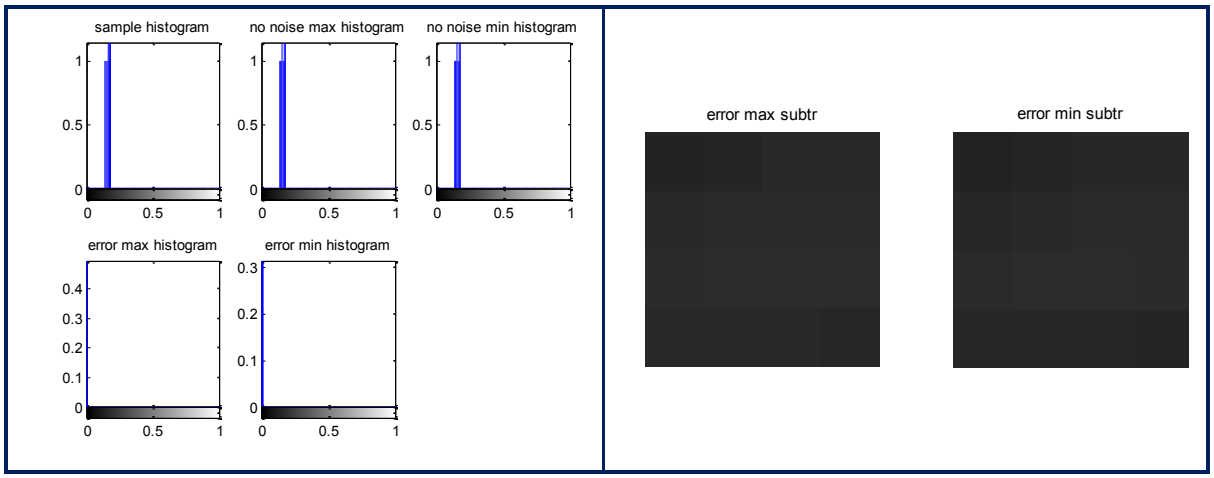

When selecting the sample in the processing, special care must be taken with the edges of an image; it is recommended to pay attention not to pick an outside value. The black background intensity is often lower than the black bar intensity and taking the latter into account, the fact that the minimum intensity value is used for calculating the modulation, could lead to erroneous results (!)

III. A three-channel multiresolution imaging system (Static System)

This chapter discusses the experimental performances of the three-channel multi-resolution imaging system and its sensitivity to the different parameters changes. In the first section, a brief revision of the optical design of the imaging system is presented. The experimental performance of the imaging system is described in the second section. The final section is dedicated to the sensitivity (tolerance analysis) of the imaging system which includes sensitivity to changes in image distance, air spacing, position of the aperture stop, position of the lens stacks, etc. An in depth analysis of the optical performance of the imaging system has been done for all perturbations.

1. Description of the three-channel multiresolution imaging system

This system is able to resolve fine details of a region of interest through the high resolution channel while controlling the surrounding region or give event awareness through the widest FOV channel at the same time. The optical system is designed by G. Y. Belay et al. is composed of three optical channels with different angular resolution and field of view and has diffraction limited performance ensuring good overall image quality.

The first optical channel has the highest angular resolution (0.0096º) and the smallest field of view (2x3.5º). Whereas, the third optical channel has opposite properties, i.e. the smallest angular resolution (0.078º) and the highest field of view (2x40º). The second optical channel has intermediate properties and shares the same size of image sensor segment as the first channel.

A significant aspect of the imaging system is that it is possible to implement different image processing algorithms at different segments of the image sensor, which is shared by the three channels, to obtain smart imaging functionality. The image sensor has 1440x960 pixels and a pixel pitch of 10 µm. The first and second segments (first and second channels respectively) have 480x480 pixels; whereas, the third channel duplicates this amount, i.e. 960x960 pixels.
If, for instance, the Viola-Jones algorithm is implemented it is required that the ratio of angular resolution in the various imaging channels needs to be factor of $\sqrt{2}$ [8].

The system can be fabricated at wafer scale to obtain a compact and low cost imaging device. In fact, this is an optical sub-system which is part of an advanced 3D-stacked image sensor where all image processing capabilities and intelligence is contained within the same package. As figure 18 shows the system consists of two separate lens arrays (four lens surface arrays), aperture stops for each channel and a tube with clearly distinct channel division. They are assembled by using guiding pins and alignment holes.

Each optical channel consists of four aspherical lens surfaces; as a result we have 12 surfaces in total in the three channels. Three of the lens surfaces (one surface per channel) make one array which resulted in four lens surface arrays overall. In such a way the three optical channels are integrated into a single imaging entity. The aperture stop of the first channel is positioned at the first surface in order to get minimal lens size; the aperture stops of the second and third channels are situated at the centre of the two lenses. This results in a symmetrical system which can easily be integrated with the first channel.

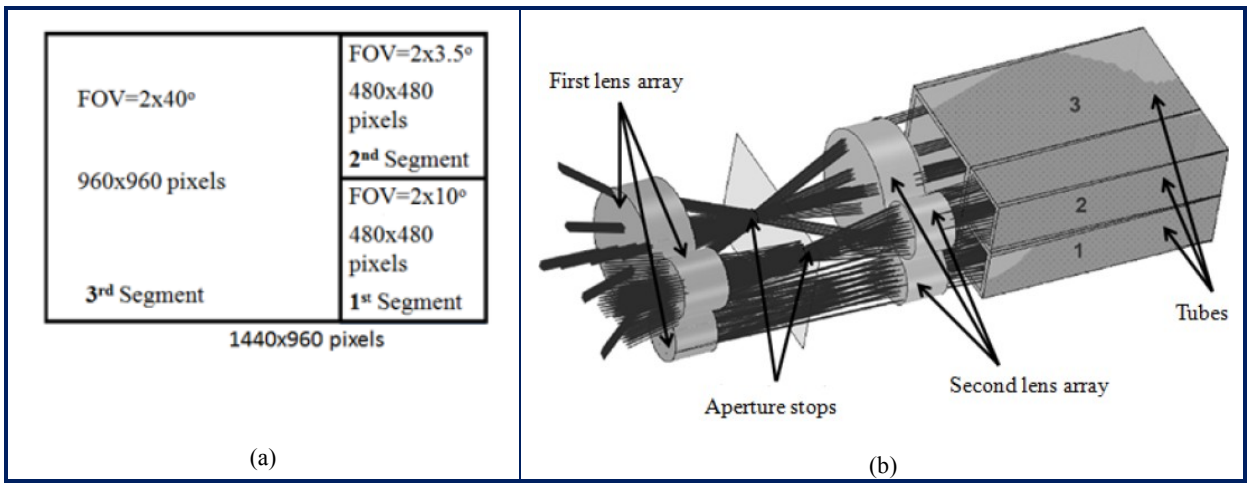

Figure 17. (a) Image sensor segments of the three optical channels. (b) Design of a three-optical channel imaging system. [9]

The tube is required to reduce crosstalk, i.e. rays coming from the neighbouring optical channels appear within the image segment of one optical channel. It extends from the image sensor to the last surface of the second lens array acting as a field stop and limiting the angular extent captured by the channels.

2. Optical performance of the three optical channels

As a first step, it is necessary to check the system performance. Which image quality can be obtained in every channel? Is it according to what is expected? In order to answer these questions and demonstrate the proof-of-concept, an experimental set-up consisting of an illumination source, an object (USAF 1951 resolution target), the optical imaging system and a CMOS detector (uEye camera) together with a display screen has been established.

The USAF 1951 resolution target has a distribution of horizontal and vertical white and black bars of different dimensions, from larger to smaller size along the area. Each block of lines constitutes an element and corresponds to a spatial frequency. Six elements form a group having a total of nine groups (from -2 to 7). The USAF has already been described in the second section of chapter II.

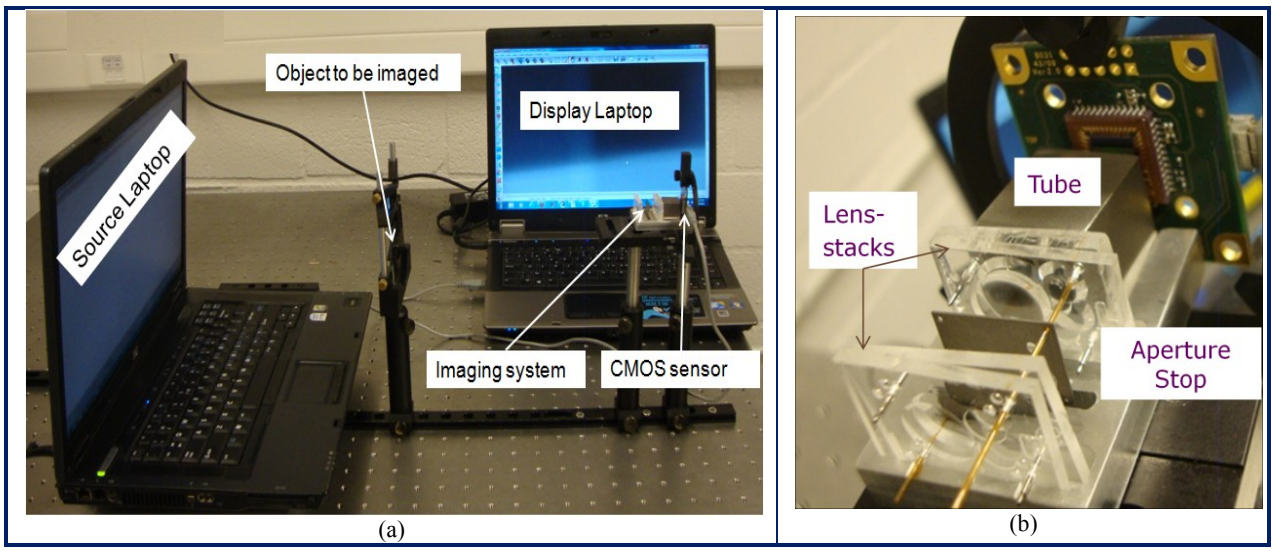

Figure 18. (a) Experimental set-up. (b) Detail of the system.

According to Figure 18 the illumination source is a laptop in which the screen appears totally or partially white. This is because sometimes it is better to have black background in the edges in order to reduce the surroundings noise but always giving enough amount of light to the object. It is very important to have a uniform illumination as it has influence on the image quality. That is why the screen of the laptop is chosen as a source because it emits light uniformly distributed within a wide area.

The CMOS sensor takes light from the environment. The amount of spurious light must be as low as possible and one way to reduce it is by avoiding the light originating from the laptop, that means, the illumination should be as much collimated as possible; the idea is to add directivity to the rays. The approach used to tackle this problem was putting some white papers around the screen similar as a horn antenna. This solution is combined with the white screen area mentioned in the above paragraph. Maybe it would have been better to utilize black papers to reduce the reflection from the white paper. There could be a problem in the way the rays reflect, meaning in which direction; however, the distribution of the emitting light source is uniform and the reflected rays will not change this fact, the light is still diffusing. What is more, black paper absorbs the ray lights so some power will be lost.

Another significant point is the distance between the different components. For instance, in order to get an image of groups -2 and -1 of the USAF 1951 resolution target with the first channel it is necessary that the object is situated far away from (around 1 m) the system; whereas, for the third channel this distance reduces to 30 cm. That is necessary for calculating the MTF[4]. Similarly, the distance between the system (tube) and the detector is different for both cases. For the first channel, there must be a separation of 4 mm; this distance almost turns to zero for the third channel where the detector is very close to the system, nearly touching. This difference increases when going to inner groups being almost ten times larger for groups 2 and 3 (47 mm for channel 1 and 9 mm for channel 3). Note that the spatial frequency of groups 2 and 3 is also approximately ten times large.

These aspects are in accordance with the optical properties (FOV, focal length, angular resolution ...) of the channels. The focal lengths of channel 1 and channel 3 are 29.9 mm and 2.65 mm respectively. If the object is moved closer to the system and obtaining a good image is intended, the detector must be placed further since the focal length is constant. A shorter focal length leads to a wider FOV and a lower magnification. As a consequence of these properties and in line with the behaviour described previously, for a particular position of the detector it is not feasible to obtain a sharp image in the three channels at the same time; in the setup when an image captured by the first optical channel, for example, was optimal the image obtained with the others channels was blurred. The following example will try to illustrates what wants to be expressed: Let suppose that an observer has general awareness of a scene (channel 3) and something “grab their eye” so they directs the attention to channel 1 in order to have detailed information, e.g. a face. The system is fixed in one position. Does the observer be able to distinguish the face features? For certain object distances it will be possible.

Next the description of the behaviour of the three channels will be summarized. At this point, it is relevant to remark the fact that besides the experimental results, there is also much perceptive information (sometimes a bit tricky to capture and reflect in a tangible manner).

[4] The method to calculate the MTF is explained in section 2.3 of chapter II

Channel 1

This channel has the best resolution and lowest field of view, so it is expected to capture a detailed image. It is relatively easy to capture a good quality image with this channel; once the first channel is focussed well,[5] it is just needed to play with distances, from the system to the camera or to the object. It is feasible to reach groups 4 and 5 which correspond to spatial frequencies up to 60 lp/mm, precisely 57.02 lp/mm. Despite the designed system is able to reach higher frequencies (up to 135 cycles/mm), the setup conditions entail some restrictions[6]: it is not possible to locate the resolution target as close as required, another limitation is the camera's dimension since the detector cannot capture the whole image. As it is known, the closer the object is, the greater magnification is and smaller the subtended angle.

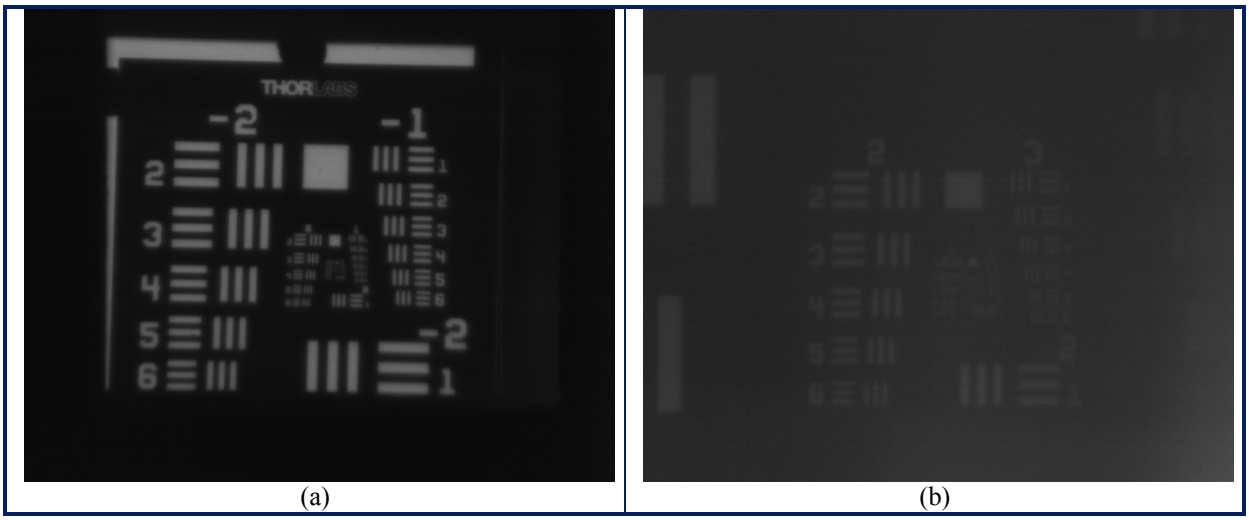

Figure 19. (a) Images from channel 1 are clear and detailed. (b) The noise is more perceptible for higher frequencies.

As has been said previously, the first channel can resolve fine details. However, the noise degrades the image quality especially at higher frequencies. The signal to noise ratio (SNR) becomes smaller as the spatial frequency increases. This matter has to do with the device capturing the images: a CMOS image sensor. CMOS image sensors are sensible to the noise (suffer from high read noise[7] and non-uniformity) as it works with active pixels. As a result, the SNR and the dynamic range are low (lower than CCDs). Dynamic range quantifies the sensors ability to adequately image both high lights and dark shadows in a scene. In order to capture an image of groups 2 and 3 it is necessary to bring the object closer and move the detector further (so the relationship between conjugate planes is maintained). Due to the detector is far away from the system (around 5 cm) and the light spreads when leaves the tube, the amount of light captured by a pixel is very small. Assuming that the energy distribution is uniform and that there are not loses in the way between the object plane and the image plane, the power in the detector will be equal to the power in the object (elements of groups 2 and 3). Because of magnification, the area of the image will be larger than the object area (the height and the width of the image with respect to the object area will be multiplied by the magnification). Therefore, the intensity reaching the detector (image plane) will be

[5] Since the detector is small to record the images captured by the three channels together, not it is necessary to move the system and/or the detector and find out the optimal position.

[6] These restrictions are applicable to all the channels.

[7] During readout, voltage information from each pixel is directly communicated to the appropriate amplifier/ADC, a row of pixels at a time. Each active pixel has an individual readout structure, having a noise distribution.

multiplied by the reciprocal of the square of the magnification, resulting in a low intensity value. The input signal level is close to the noise values.

If the object has an area $S_o = \omega_o \cdot h_o$ (ω_o is the width and h_o the height), and the magnification is m, the area of the image will be equal to $S_i = m\omega_o \cdot mh_o = m^2 S_o$. The power is equal in both sides (object plane and image plane), such that $S_o \cdot I_o = m^2 S_o \cdot I_i$ and therefore, $I_i = {}^{I_o}/_{m^2}$ (with I_o and I_i the intensity in the object and in the image, respectively).

Actually, the intensity capture by a pixel will be even lower, since there are propagation loses. Is the first channel more sensitive to noise than the other two channels? In view of the result and taking into account the fact that channels two and three do not show this behaviour, the answer could be affirmative but it is not. The noise affects equally the system although the features of the first channel turn this fact more noticeable (the magnification is lower for channels. 2 and 3, and the detector is positioned closer when capturing the respective images)

Channel 3

This channel has opposite characteristics compared to the first channel: the resolution of this channel is the lowest and the field of view is the largest. What does it mean? If the object is far away from the system the resolving ability will be pretty poor and the details will be slightly distinguishable. On the other hand, there will be awareness of the surroundings; it will be possible to watch what is going on within a wide area. In practical terms: the USAF has to be closer to the system in order to get an image which is good enough for the MTF calculation. Furthermore, the maximum number of line pairs or cycles per millimetre will be lower; in fact the last element of the third group is the limit in the setup.

Apart from the distance, the tilt of the system has a relevant role in having a sharp image. As a consequence of misalignment or off-axis position the system must be slightly rotated in the horizontal plane, i.e., a plane parallel to or containing the optical axis (sagittal plane). The angle is very small in comparison to the field of view (2x40º) so the tilt is tolerable from FOV point of view, and just provokes a shift in the axis.

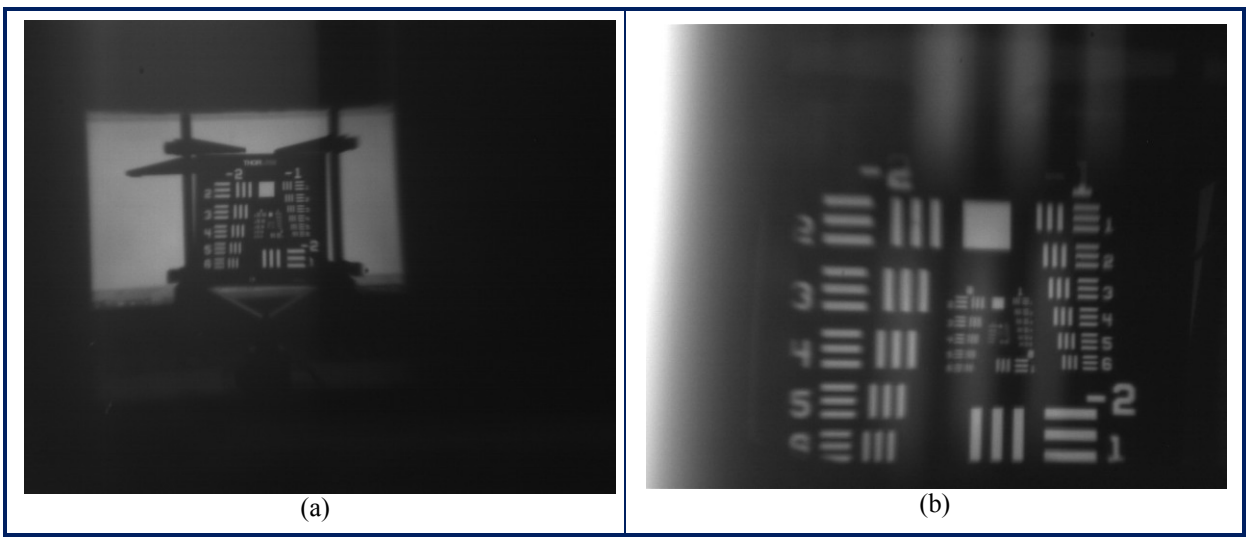

(a) (b)

Figure 20. (a) Sample of larger FOV. (b) Crosstalk

Crosstalk is present in this optical channel: ray lights coming from the two other channels cause interferences in the image caught by the third channel.

Slanting the system is one way to solve this problem: with a rotation of -3.93º from the optical axis the 'ghost images' disappear. Nevertheless, the image quality gets worst since some fraction of the image is out of the optimal distance to the detector. Moreover, it is important to keep in mind that the channel is not isolated, it is part of an integrated system and thus, any change in a element will have an effect, significant or not, in the whole system. At this point, one question arises: which one has more influence in the image quality, the crosstalk or the blur inherent to the tilt? It is necessary to study in which way the crosstalk affects to the image quality and if it could be considered as noise (and be modelled). In such a case, as regards to the MTF calculation, the crosstalk could be treated as error to subtract (the statement does not imply that the error is linear). On the other hand, in the case of the tilt the blur is partial, which means that only the quality of certain parts of the image is degraded. Depending on how large is that affected area, this handicap could be tolerable.

The tube is supposed to avoid the crosstalk but there are air gaps between the tube and other components of the system (the second lens-stack and the detector) and the light coming from other channels interferes with the ray lights in the channel of interest. To avoid this situation the tube should be larger. Indeed, in previous experiments carried out by G.Y. Belay the tube was larger and crosstalk was not observed.

The third channel behaves according the expectations in function of its optical properties.

Channel 2

This optical channel has intermediate properties between the first and third channel. In this case it is not so easy to obtain a good image: the detector has to be very close to the system and finding the optimal position is not as simple and immediate as for the first channel.

The images by this channel have pincushion distortion as can be seen in figure 21, i.e., it is positive which means that the real image location is farther than the ideal image from the axis. In most lenses, the magnification between the object and the image is constant for specific conjugate planes, or very slightly changing, creating systems with almost no distortion. Distortion can be described as a variable magnification across the full field of view of a lens. Although distortion does not directly affect the image quality (the image is perceived as sharp and the contrast is high), it sometimes has an indirect effect by producing other aberrations as there are changes in the ideal paraxial position of the points and these new circumstances give rise to the presence of aberrations [21].

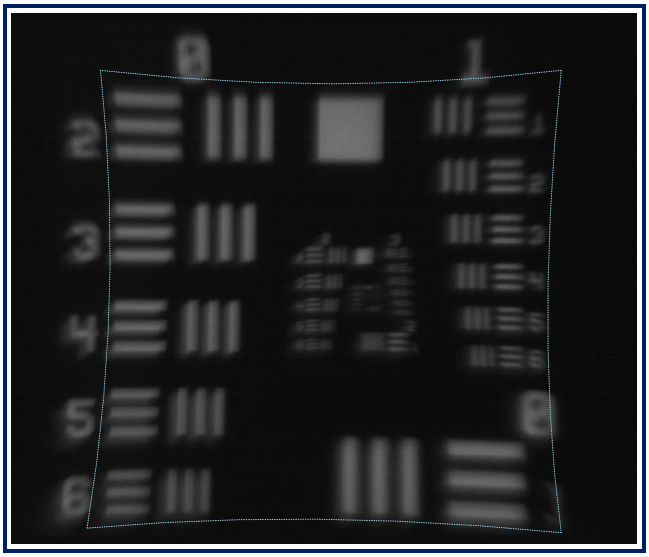

Figure 21. Pincushion distortion appears in the image.

This optical channel does not play a main role in the system from an application point of view. For in-car-pedestrian detection applications, the Viola-Jones algorithm works with different consecutive processing steps which require increasing resolution; in such a way that the images obtained by the second optical channel will be used in a second processing step after the first processing step with the large FOV images.

The system has been thought to work at relatively large distances and the maximum distance in the set-up is a bit more than one metre. To have an idea of how large these distances can be the depth of field is a good reference. The depths of field for the designed system are [9m, ∞] for the first channel, [2m, ∞] for the second optical channel and [0.2m, ∞] for third one. Is the crosstalk really important when the scenario is for example 25 metres away from the system? Are these malfunctions truly determinant in a real application? The system has been tested at 4 m and 6 m and works well so the crosstalk will not be a problem.

3. Sensitivity (tolerance) analysis of the three-channel imaging system

The purpose of the tolerance analysis is to investigate how the misalignment errors (of the components) influence the system's performance and therefore, the image quality.

3.1. Finding out the optimal position of the components

There are different parameters that play an important role in determining the image quality of the imaging system. Among these parameters, the positions of the lens-stacks, the aperture stop and the tube are considered for the tolerance analysis. One of the components will be moved while the others remain fixed. The movement is longitudinal along the optical axis.

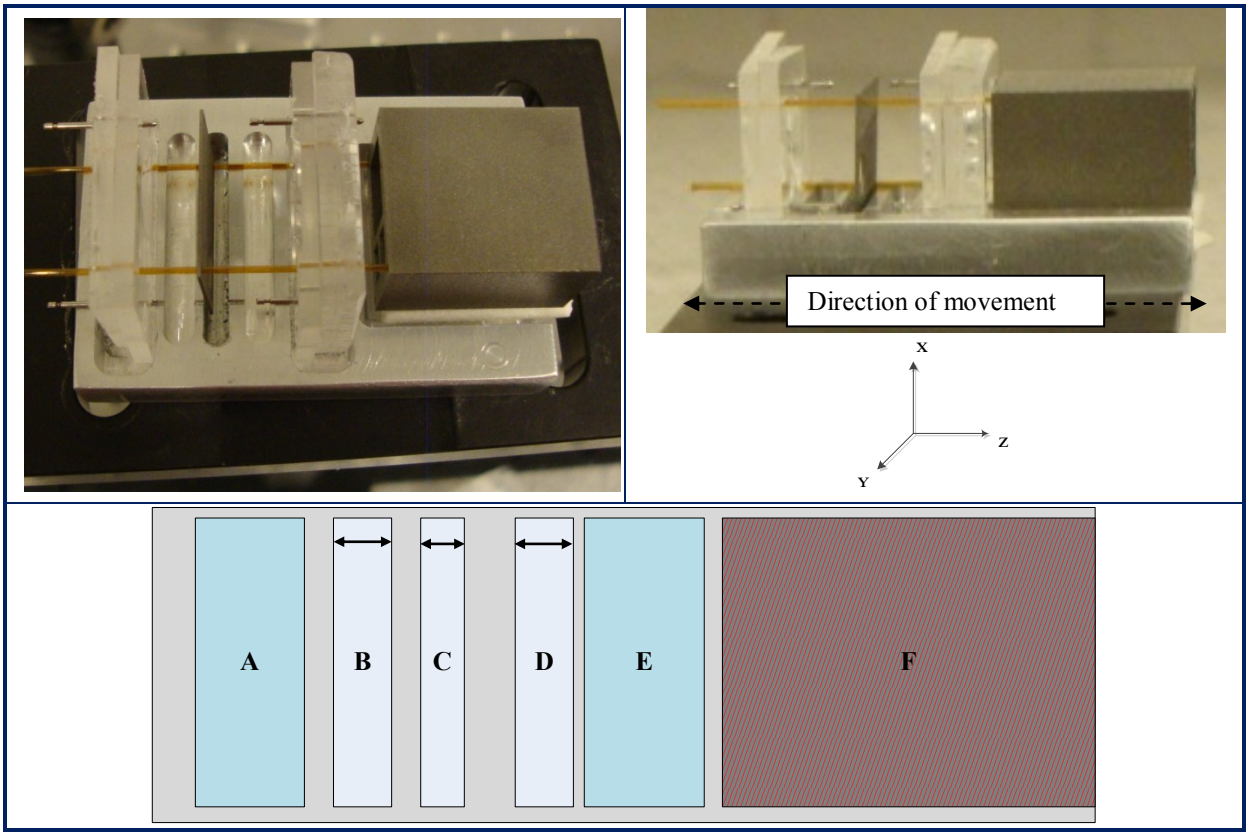

Figure 22. Different perspectives of the system: top and cross section. The slots have been labelled as A, B, C, D, E and F. The bottom image is not in scale.

3.1.1. Movement of the aperture stop

In first place, the aperture stop will be positioned in the slots B, C and D respectively (see figure 22). There is some space in the slots so the aperture stop can be located at the left, the right edges or at the centre of the slot. The dimensions are the following ones: slot B 3.0 mm, slot C 2.5 mm, slot D 3.1 mm; the distance between slots B and C is 1.15 mm and between slots C and D, 2.783 mm.

Inside one slot, the position of the aperture stop does not matter. The obtained result, either quantitatively (MTF analysis) or qualitatively (direct visual inspection), barely varies when the aperture is at the left, the centre or at the right side. This is depicted in figure 23, where representative sample images captured by the three channels (when the aperture stop is in the slot D) are shown. The MTF analysis is not included but it has been done. Maybe, it is necessary to have a look to the Phase Transfer Function and check if there is any phase change originating from the aberrations if any.

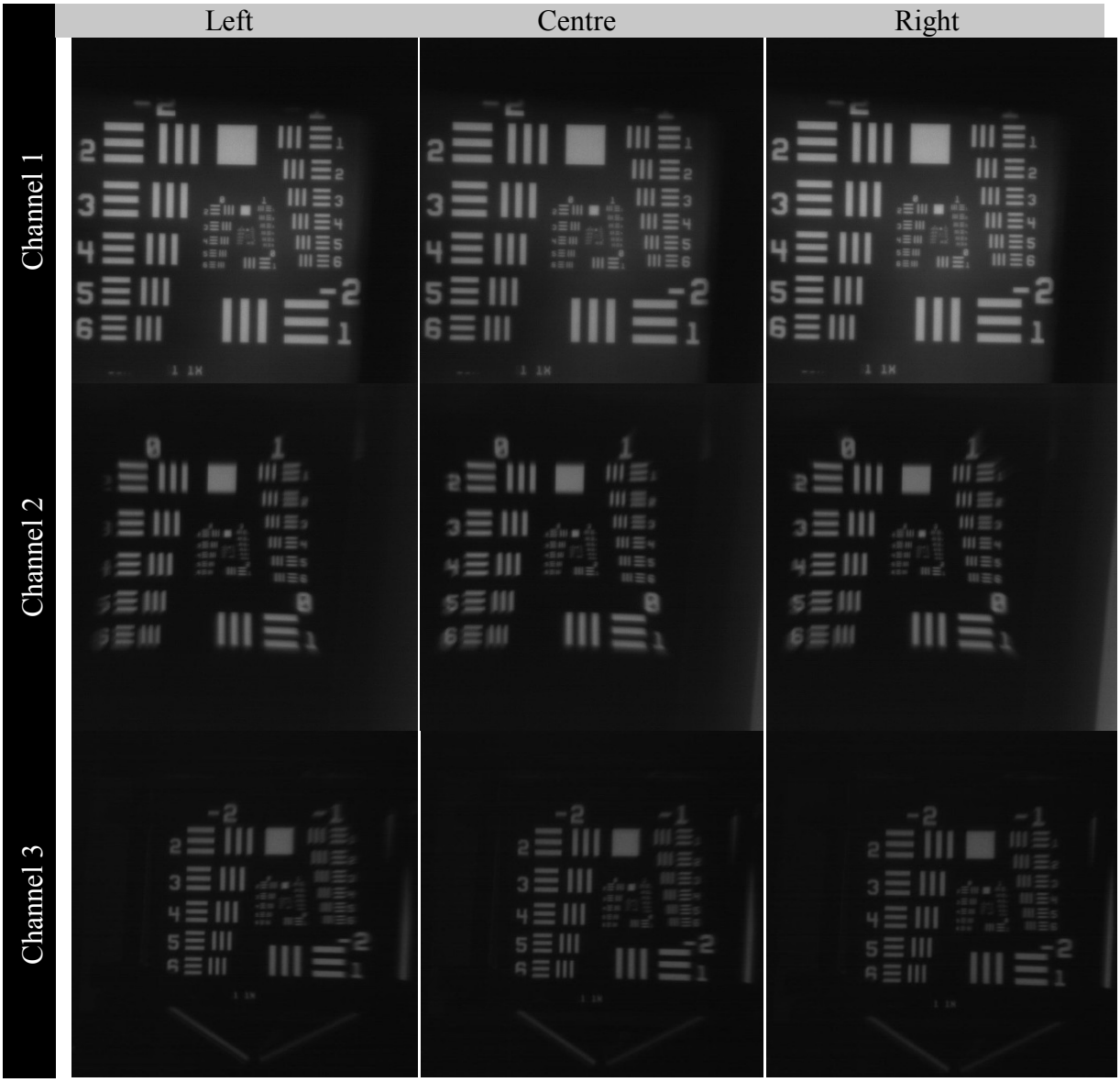

Figure 23. Examples for slot D with the aperture stop located in the left, centre and right.

For the third channel, there is a slight difference in the sharpness of the group -1 at the three different positions. The alignment of the system was perturbed in the case of the left image and as result, the image quality is blurred. The system varies a bit its position when the aperture stop was displaced, so the conditions were not exactly the same for the three captures.

Unlike the previous case where the range of positions of the aperture stop is quite small (the length of the slots B, C or D) and the difference in the captured images was insignificant, the effects of locating the aperture stop in another slot are more noticeable and relevant as the image quality is concerned. There is also a dependence on the optical channel as they perform in a different manner. Down-pages the different results are given.

The **first optical channel** is the less sensitive or more robust one to alterations. Whatever the position of the aperture stop, the image quality is not degraded. There is a little change in the brightness without repercussion on the resolving power.

Table 2. Images of the different groups of the USAF resolution target by the first channel with the aperture stop positioned in slots B, C and D right.

Slot B	Slot C	Slot D
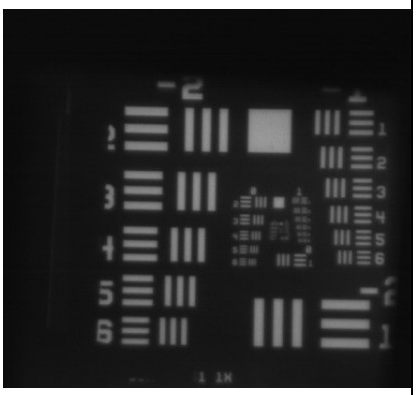	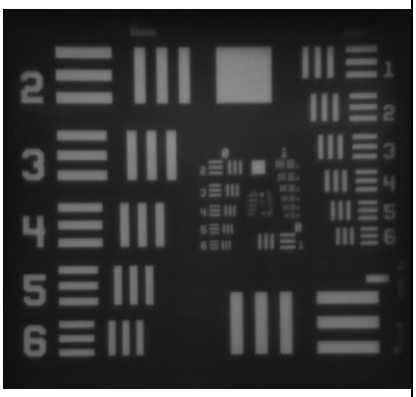	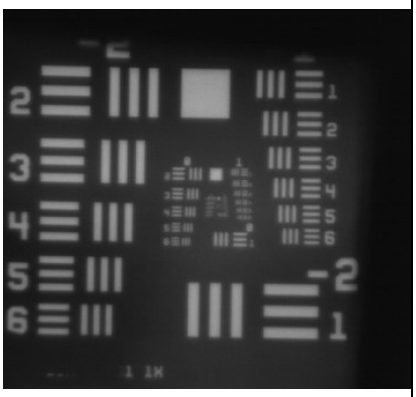
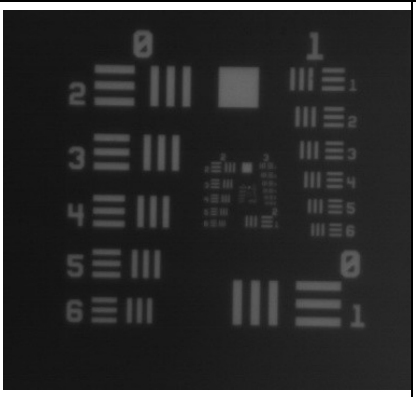	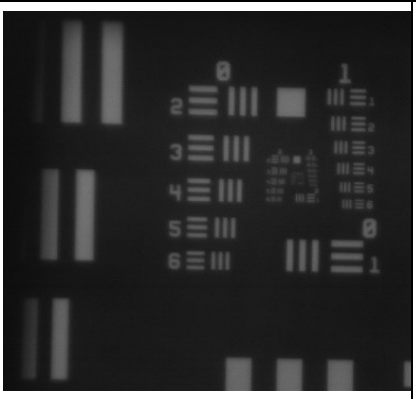	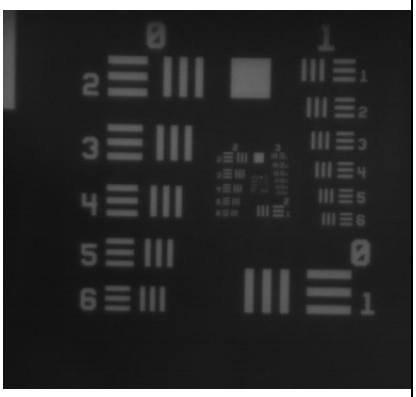
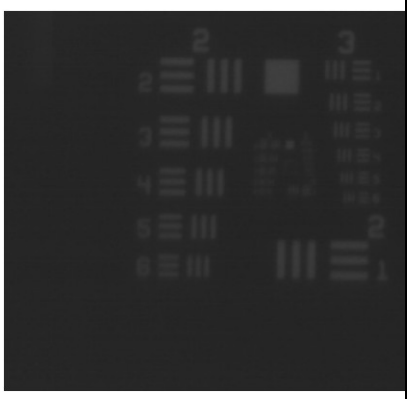	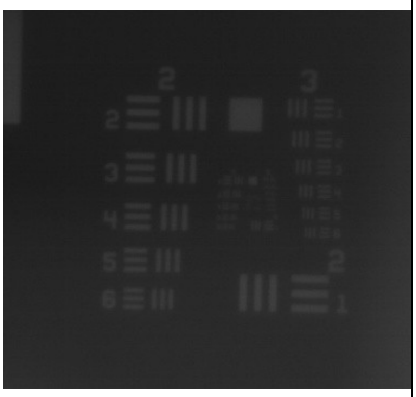	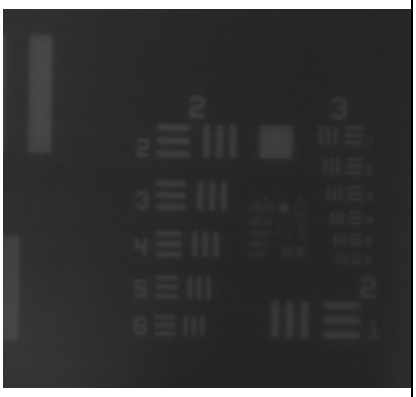

The MTF analysis corresponds to what is seen in the captured images at the first impression. The three MTF curves depicted in figure 24 have the same tendency and they almost overlap. The modulation values decrease faster at lower frequencies then the curves tend to flatten; the variation for inner groups (higher spatial frequencies) is slower.

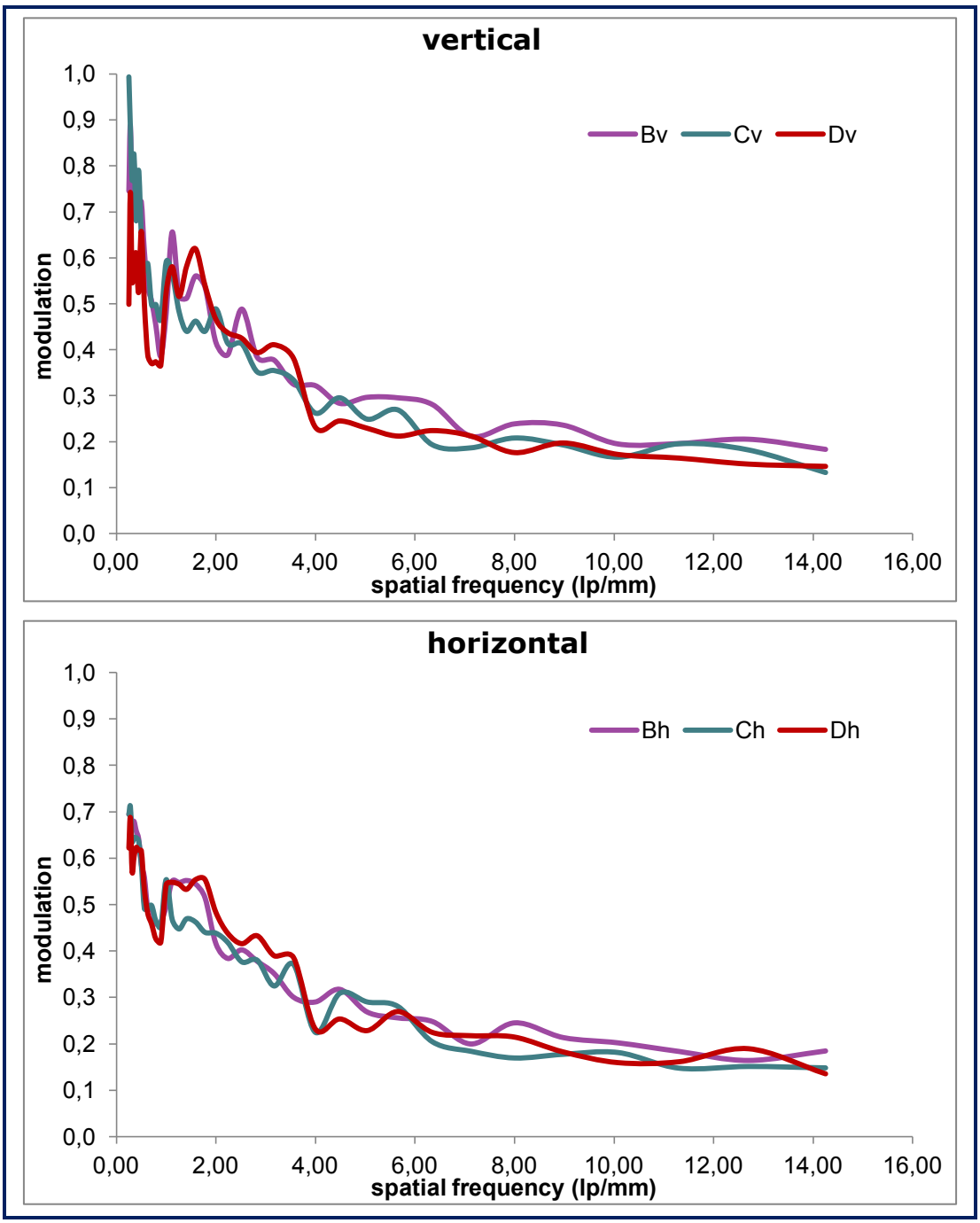

Figure 24. MTF graphs for the first optical channel when the aperture stop is located in the slots B, C and D right.

A modulation index less than 20%, is low for the working frequencies considering that this channel reaches up to 135 cycles/mm. Nevertheless, the bars in the image look distinguishable for a human eye... The main reason is, probably, the noise which reduces the contrast causing an important degradation in the image quality and affecting the MTF calculation. Furthermore, a modulation value up to 5% can be considered as still acceptable, which means 20% is not a bad value, after all.

For the **second optical channel**, there is a difference depending on the slot in which the aperture stop is placed. The best result is found for slot D as the next pictures show.

Table 3. Images of the different groups of the USAF resolution target by the second channel with the aperture stop positioned in slots B, C and D right.

Slot B	Slot C	Slot D
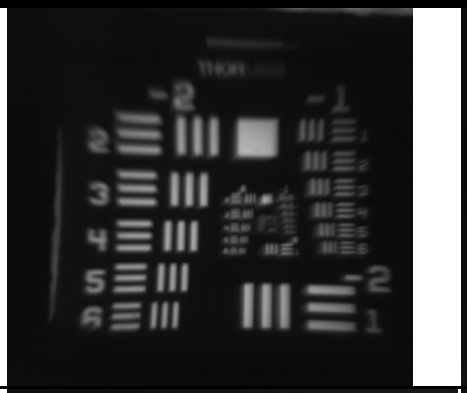		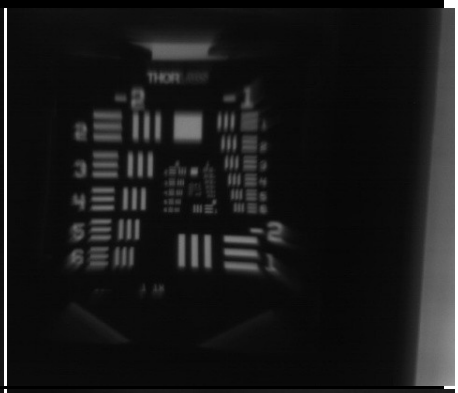
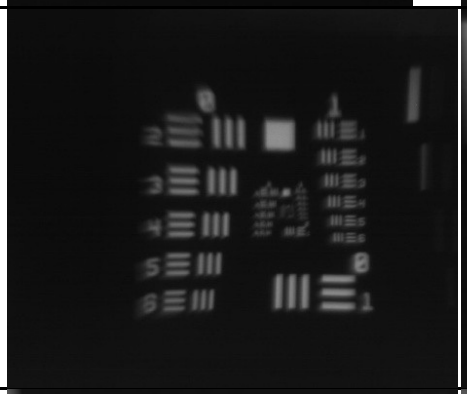	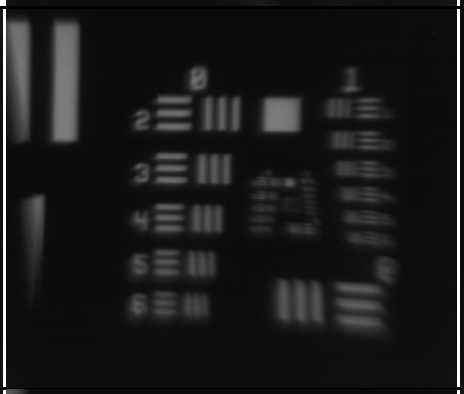	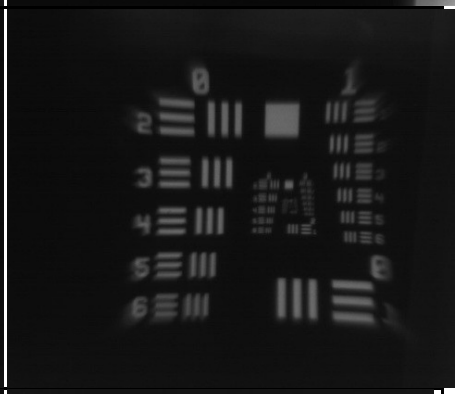
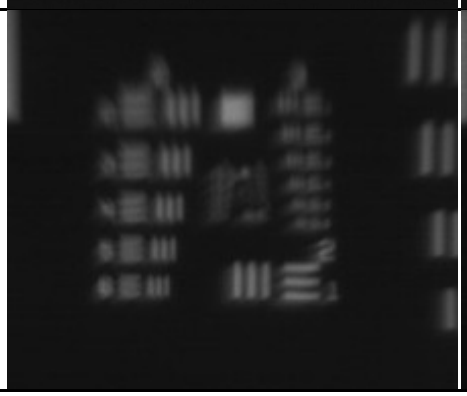		

The distortion is clearly visible, especially in groups 0 and 1. The object distance have to do with the why: for that distance the bundle of rays experience more deviation from the constant transverse magnification. The field angle subtended by the USAF plate varies with the object distance and the distortion varies with the field angle (the distortion is maximum in the extremes of the field of view). That means the distortion is changing with object distance. For those particular groups the corner points might be the extreme field pointes where the distortion of this channel is highest.

This aberration is a bit less significant in the central slot. One way to reduce distortion is to have symmetrical systems and this is what happens when the aperture stop is located in the central slot or slot C.

What do the numbers say? Let's have a look to the MTF graphs.

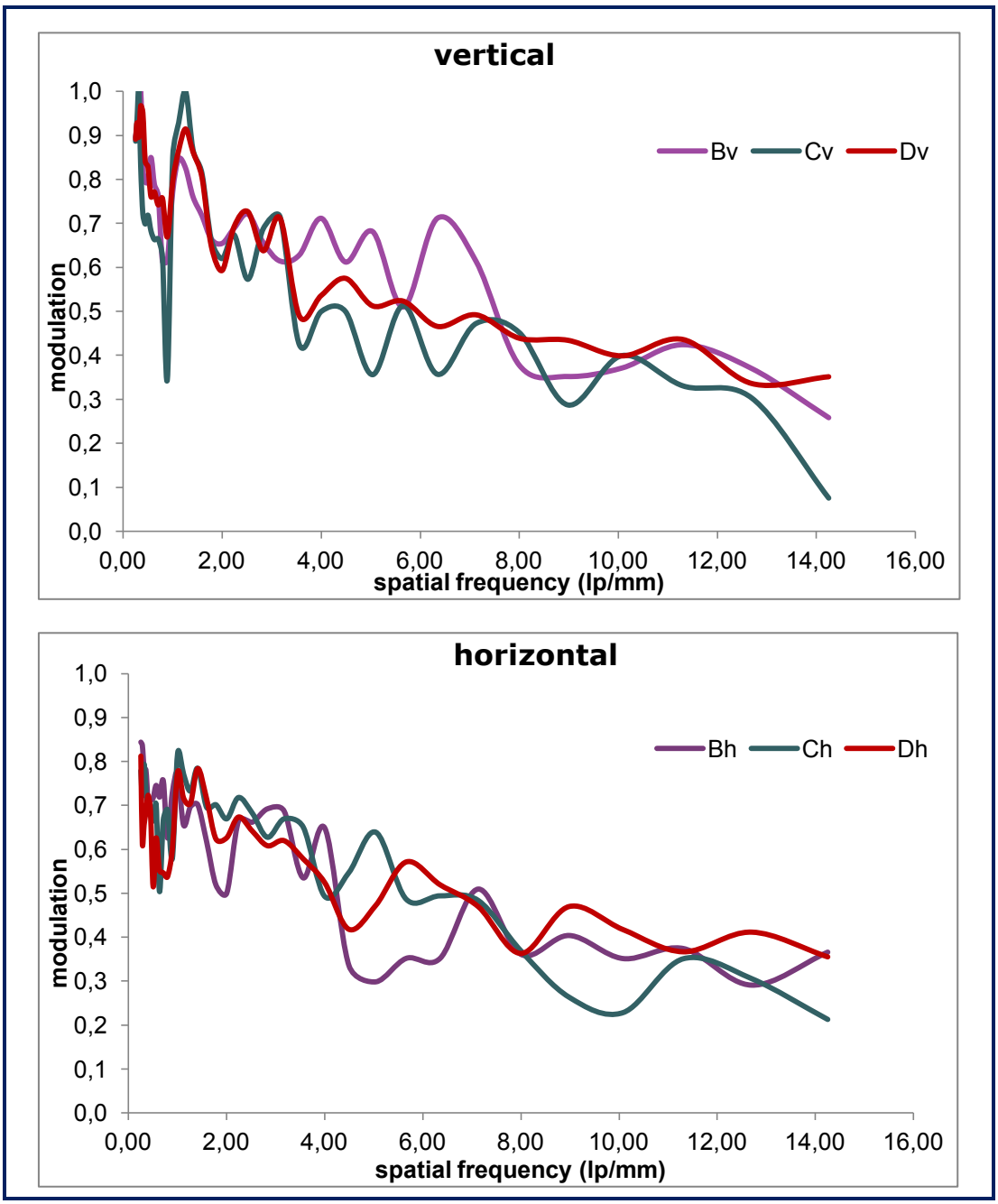

Figure 25. MTF curves for the second channel when the aperture stop is located in the slots B, C and D right.

Observing the above figure, it does not give the circumstance of having such a big difference as could be expected from the images, the curves are pretty comparable. Nevertheless, the correspondence between the qualitative and quantitative results is moderately high. Actually, there are good and bad data points.

For example, the -2 and -1 groups of the slot C are quite blurred and the curve B decreases quite fast and reaches lower values in the respective range of frequencies. It is true that in the case of the horizontal analysis, the descent is not so drastic. Apparently, the group 2 for slot B is worse than its equivalent in the slot D but the MTF is saying the opposite, B's quality is higher than D's; what is happening? This discrepancy obeys to the way of calculating the function: take the maximum and minimum intensity values. Imagine the case in which the minimum value is zero or approximately zero, the modulation will be unity. Or whether the operation between both intensity values is such that the element with

poorer visual quality has the highest modulation; normally, when the denominator is small, tends to zero.

The **third optical channel** is more robust to the variation of the position of the aperture stop but another handicap exists: the tilt. There is certain dependence on the general alignment of the system with the optical axis. Sometimes, the imaging system does not have to be at 0º, tilting the system to the left or to the right is required.

Table 4. Images of the different groups of the USAF resolution target by the third channel with the aperture stop positioned in slots B, C and D right.

Slot B	Slot C	Slot D
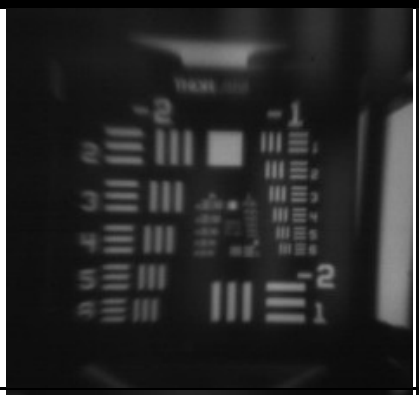	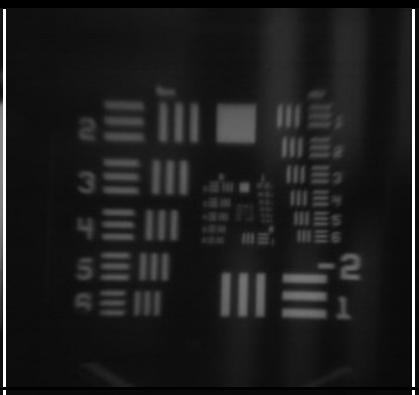	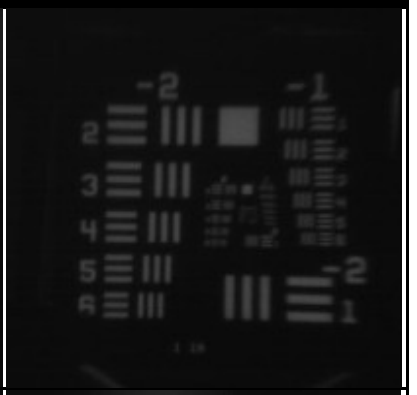
		
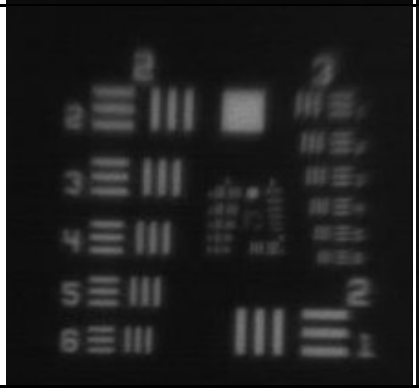	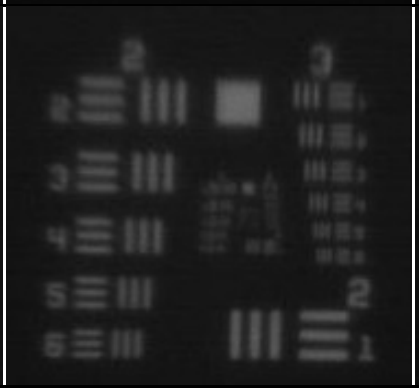	

Slot D seems to be the best followed very close by slot C. In slot B the images are slightly blurrier. Aligning the set-up of the system for capturing the images was also a bit easier when the aperture was in slot D.

Do the MTF curves show this observation?

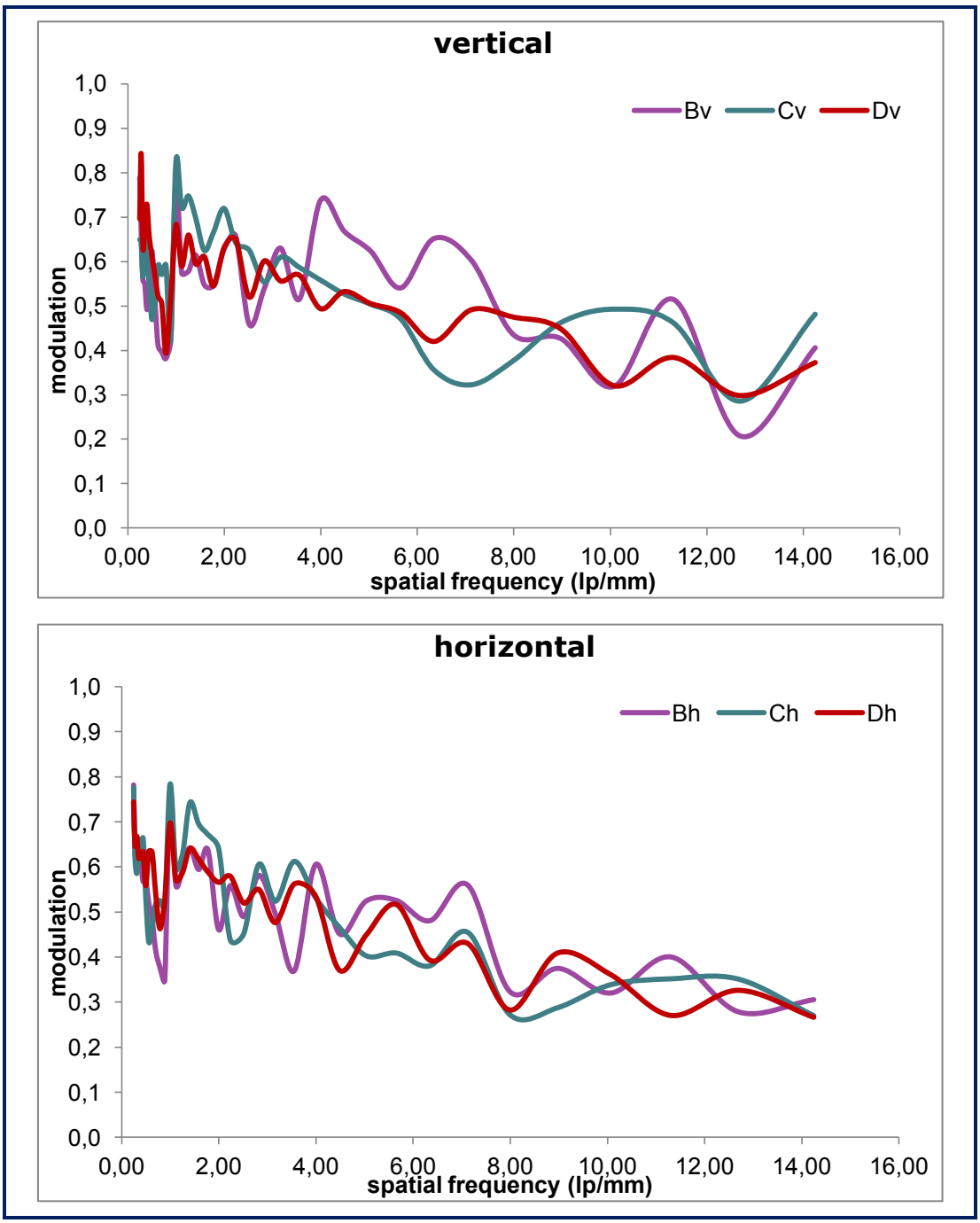

Figure 26. MTF graphs for the third channel when the aperture stop in positioned in the slots B, C or D right.

The curves are not really enlightening: the tendency is quite similar and there are not many discrepancies in the values.

From a first inspection, it is natural focus the gaze on the portion of curve 'Bv' (purple) between frequencies of 4 lp/mm and 8 lp/mm; there is variation of around 10% with respect to the other two curves. The correspondent image shows a larger contrast so the result is acceptable (comparing the image and the correspondent MTF values).

The modulation is in a range of values that varies between 0.3 and 0.8 and the drop is slow. This is in accordance with the lower resolution of this optical channel.

It is common in all the analyzed cases that the MTF is lower for the bars horizontally oriented. This is explained taking into account the situation of the horizontal elements in the USAF chart: are in the external region and higher field points experience more aberrations than on-axis. The system was designed for a single wavelength such the system is diffraction limited. However, in the reality there are more wavelengths (incoherent light source) so the system is not diffraction limited anymore. In the case of the designed system the simulations [9] show a dependency with the position inside the FOV. The higher field points are more affected by diffraction so the MTF is lower than the MTF of on-axis/lower field points.

Another aspect to keep in mind is vignetting, although its effect should not be very significant since the working distances are in the near-field. The point is that the seen effective clear aperture is smaller than the clear aperture of the lower field points.

3.1.2. Lens-stack in slot A

Slot A allows locating the first lens-stack in the left or the right edge or inclining it along the diagonal.

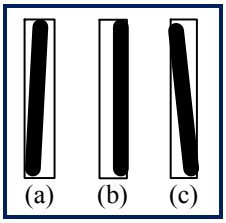

Figure 27. Lens-stack position in the slot A: left (a), right (b), diagonal (c)

Due to the pin-guides and the shape of the supporting base it is not possible to set the lens stack parallel to the left side. The left position (with the lens stack positioned as depicted in Figure 27 (a)) was the position inside the slot A that had the first lens-stack for the analysis carried out in the previous section. In addition, in view of the results obtained slot B has been discarded to house the aperture stop instead slot D was chosen to carry out this second part of the tolerance analysis study.

As in the precedent subsection, the performance of the three optical channels for the made variation will be discussed.

Channel 1

The images are very good: the contrast is very clear. The quality improves if the lens-stack is at the right side and without tilt. However, the signal to noise ratio is the same as in the previous cases, maintaining low levels.

The robustness of this optical channel is also seen again in this case: the comparison of the studied approaches is almost identical. This can be observed in the images of Table5 (only images of the cases (b) and (c) are shown) and in the MTF graph. As seen in Figure 28, placing the lens stack at the right side leads out higher modulation values. That improvement is more significant for higher frequencies (groups 2 and 3 of USAF chart).

Table 5. Images of the different groups of the USAF resolution target by the first optical channel when the lens-stack (slot A) is at the right side of the slot or tilted.

Right D	Tilted D
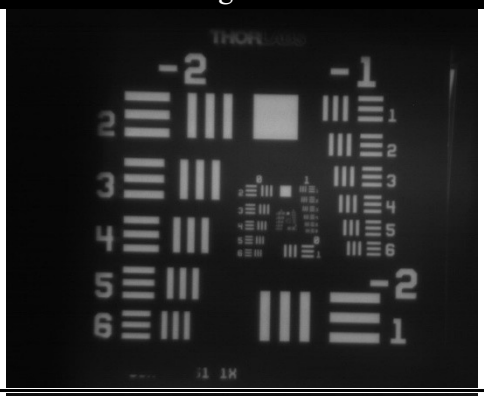	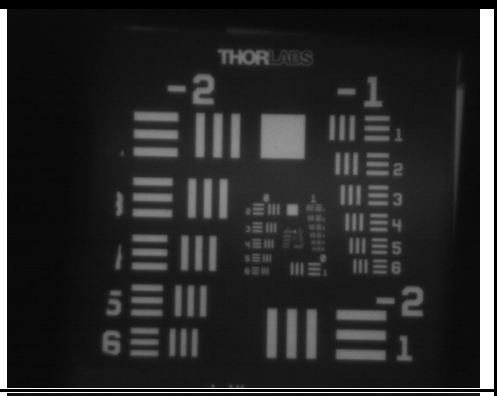
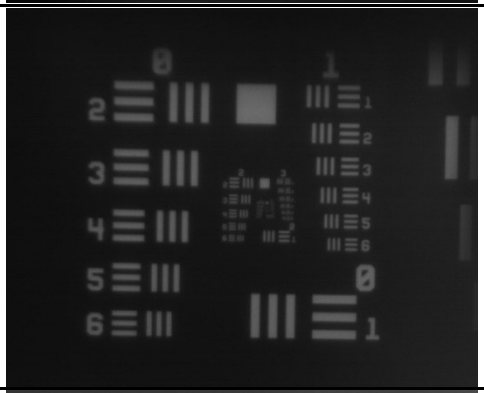	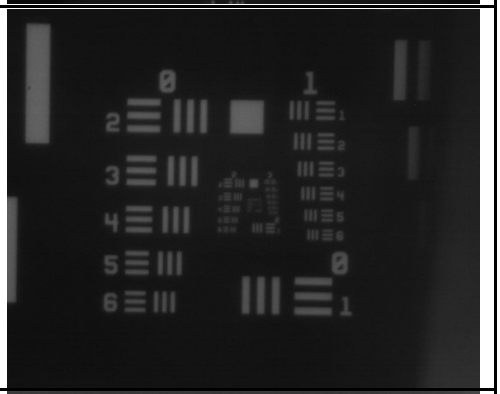
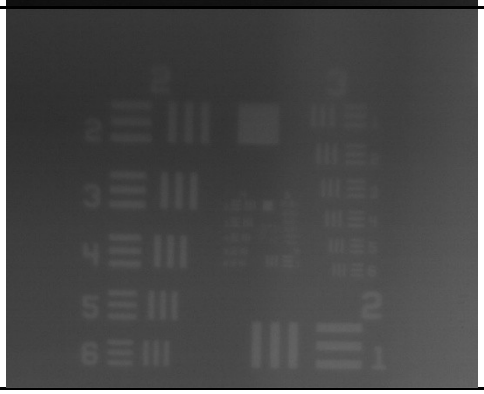	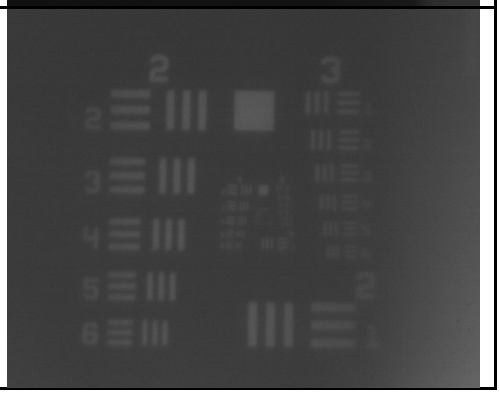

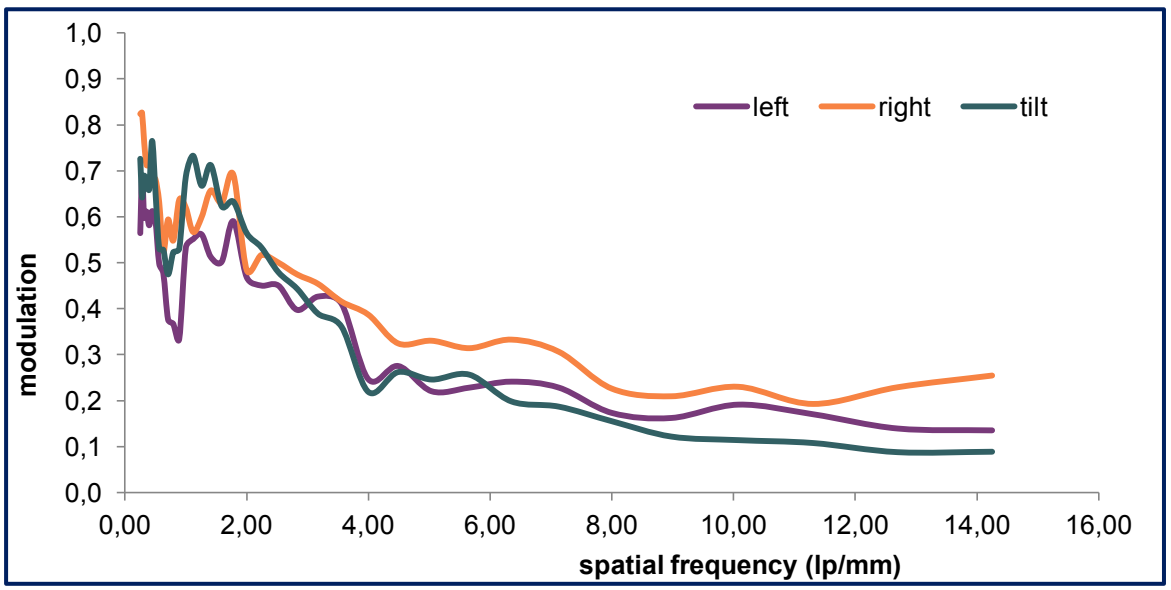

Figure 28. MTF curves of first optical channel when the first lens-stack is in the left, right or tilted.

Channel 2

This channel is a very good example of the dependency of the performance of the imaging system on the alignment of the different components and environmental conditions. The images in the column "Right D" (Table 6) are quite dark and as a result the resolution is low. If the intensity supplied by the source was higher, the outcome would be better. Comparison of the MTF of channel 2 for the three positions of the first lens stack is given in Figure 29. As seen from the figure the MTF for the left position overlaps almost perfectly with the MTF for the right, but there is an offset. Therefore, the system behaves in a different manner depending on the environmental light.

Table 6. Images of the different groups of the USAF resolution target captured by second optical channel in the case that the lens-stack A is at the right side of the slot or tilted.

Right D	Tilted D
	
	
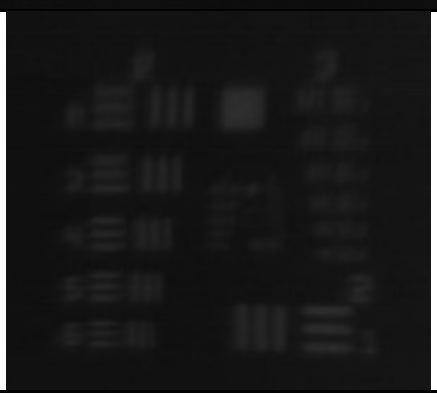	

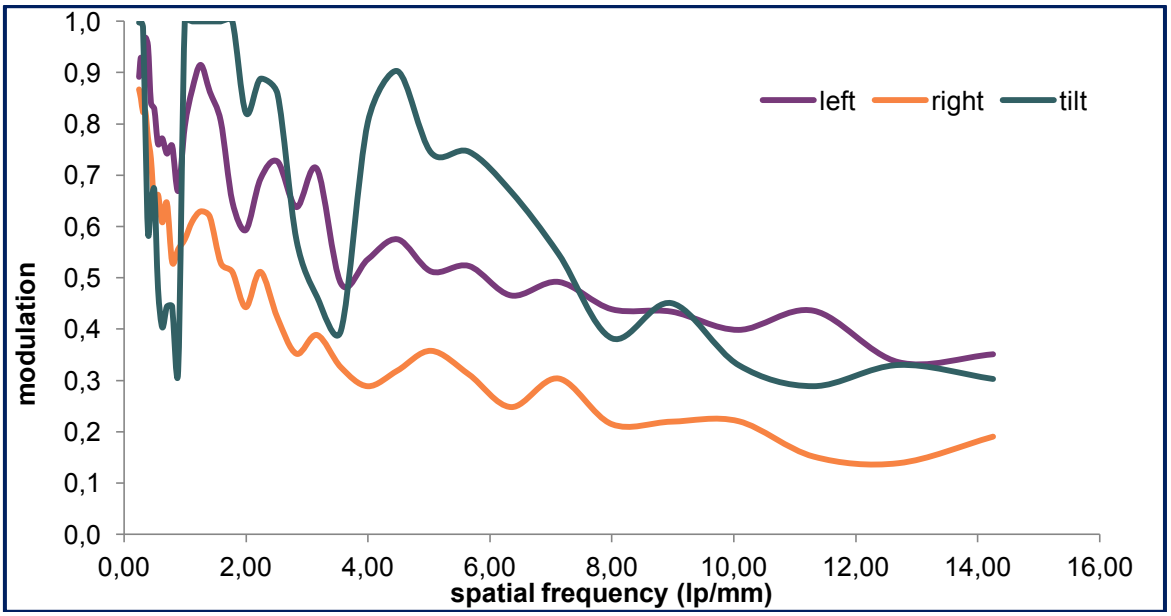

Figure 29. MTF analysis of the images presented in Table 5.

What if the system is able to adapt to the environmental light conditions similar to the iris in human eye? The main function of the iris is to control the amount of light that goes through the eye by changing the size of the central aperture, the pupil. The system could include a resizable aperture in order to adjust the light conditions. At this point, it is important to take into account the fact that the aperture stop determines the system resolution, the light transmission efficiency and the depth of field/focus. It is not interesting to reduce the resolution as the system has been optimized to get the best resolution according to the performance of each channel. Moreover, additional components used for obtaining resizable aperture may t make the system bulkier. Thus, this system has no application at night? What is the minimum amount of light the system needs to work properly? It is something not quantified yet.

This time, let's have a look to column "Tilted D" of Table 5. The black-white contrast is visually elevated and the brightness is also very high, but that is due to the CMOS (uEye) camera detector as properties such as the exposure time, the gain, the pixel clock, etc. can be modified for obtaining a better image. What does that mean? The quality measurements are not really of the system itself but the overall setup. If the light source or the object are not perpendicular to the optical axis there will be errors affecting the outcomes. After all the system is characterized, yet some source of error must be considered.

Back to the images and MTF curves of the second optical channel...
When the lens-stack is tilted the distortion diminishes in a small amount, principally in the top part of the image although the difference is very subtle. On the other hand, the elements of the USAF give the impression of being a bit more blurred for the referenced case. Following with these images: in spite of there are high modulation values, the drop for every pair of groups, i.e. (-2,-1), (0, 1) and (2, 3) is fast and the transition between them is quite abrupt. The explanation is found again in the definition of modulation and the intensity values.

Channel 3

The images look pretty similar (see Table 7). In the first row, the right image shows a darker background and it seems a bit better focused. For the second row there is a slight improvement in the tilted image, it is a bit sharper. The same happens for groups 2 and 3.

In order to take the images, the system was inclined, out of axis and the camera was very close. It could be thought that the tilt of the lens-stack could avoid the rotation of the whole system or the opposite, an extra rotation. It is more or less the same. This pseudo-equality is also found in the MTF analysis; there is a medium-high degree of coincidence between the curves. The biggest discrepancy is in the "tilt" curve in which, as happened in the second channel, the transition between images –meaning the pair of groups is not gradual.

If the MTF analysis is used (Figure 30), there is not a determinant position. If the criterion of direct inspection is considered, the locations at the left edge or along the diagonal of the slot are the best. The decision is actually relative because it is possible to get a better image when the lens-stack is at the right.

Table 7. Corresponding images of the different groups of the USAF resolution target by channel 3 when lens-stack set in the right side of the slot A or tilted.

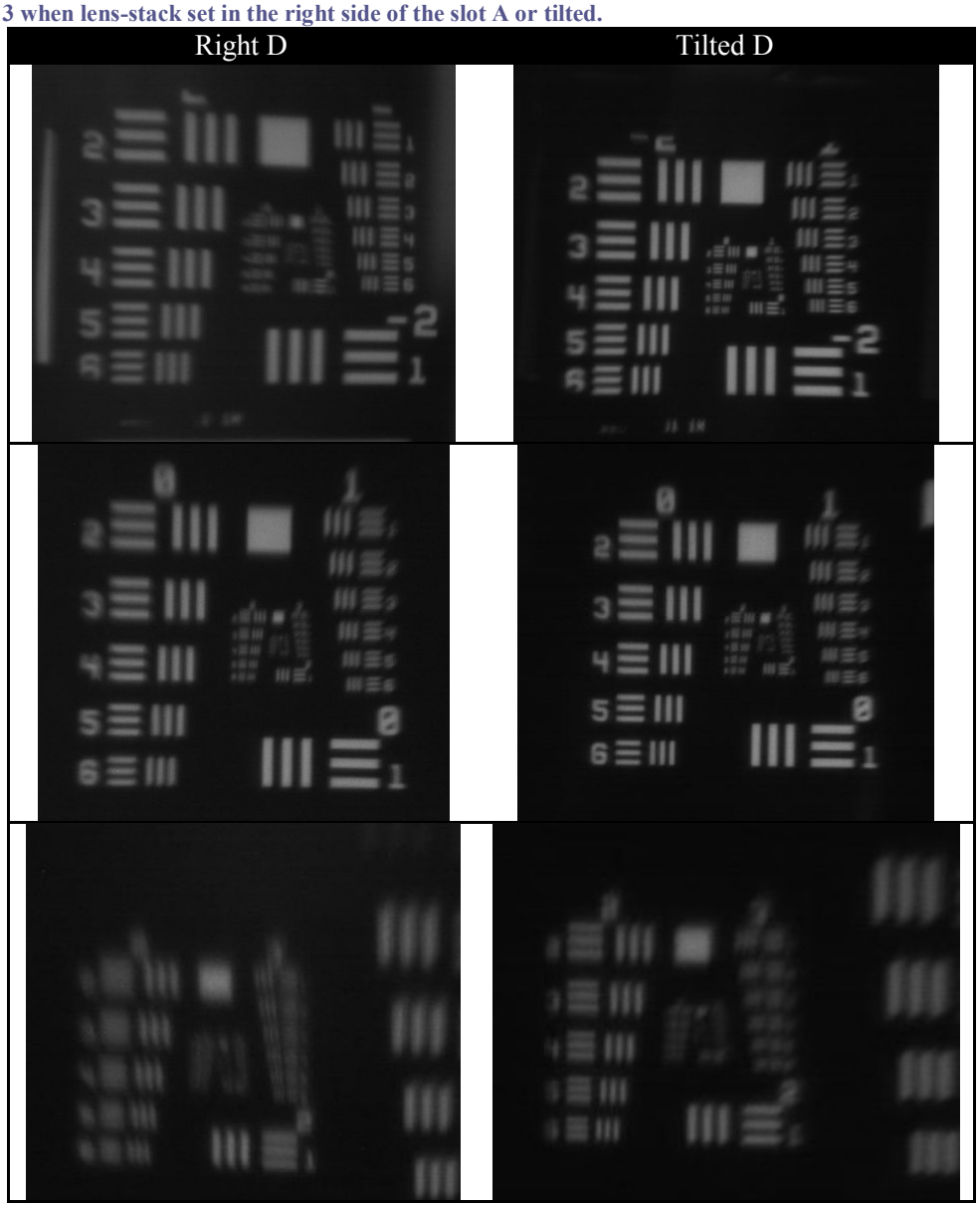

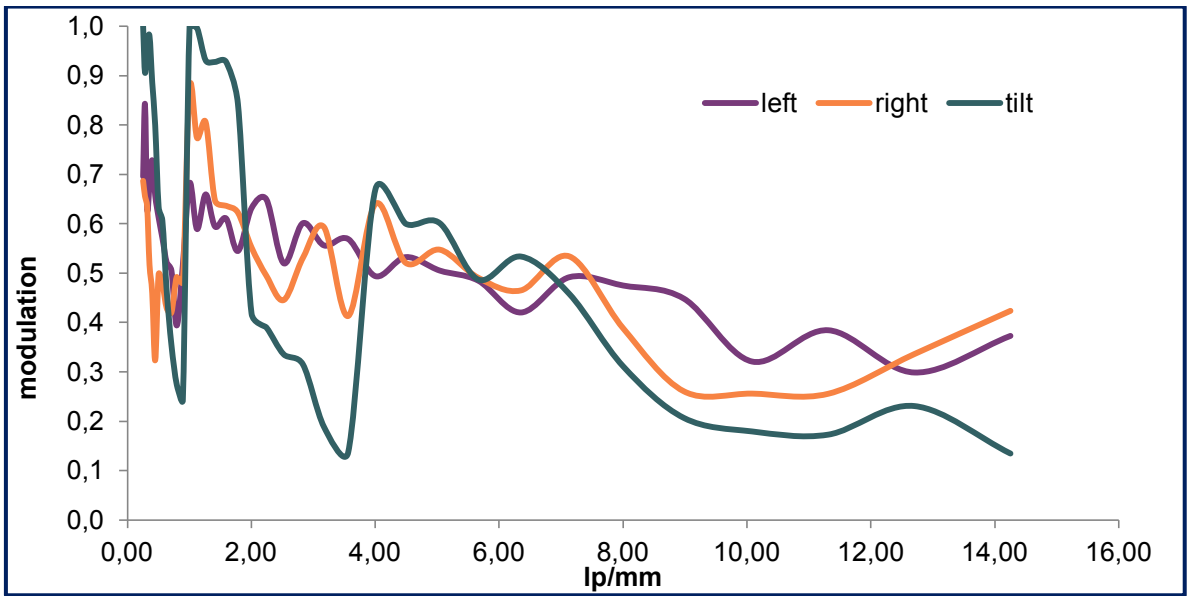

Figure 30. MTF analysis of the images captured by the third channel for the lens-stack located in the left side of slot A, the right side or tilted across the diagonal.

3.1.3. Movement of the tube

The last considered variable is the position of the tube. The first approach is continuing with the longitudinal movement and placing the tube further or closer to the second lens-stack (slot E). The second approach consists of displace the tube transversally in X direction (it is considering that the system is on the plane YZ). Finally, other trials have been carried out with the purpose of studying the influence of the tube's position related to crosstalk –the main aim of the tube is to avoid the crosstalk. The subject of the experiments has been the third optical channel, the one that is affected by the crosstalk.

Longitudinal movement of the tube

There is no much freedom for the movement of the tube as the CMOS detector limits its displacement. What has been observed is that the image quality gets worse as the distance between the lens-stack E and the tube increases. There are not any consequences as the crosstalk is concerned. In addition, the relative position of the system with respect to the optical axis has been modified a little bit in order to find a better image.

Another test done was to move away the detector since the effect is similar to move the tube. The image was blurred after a 2 mm movement; the depth of focus is really small. and thus, the detector must be very close. It has been like that in the previous cases as well. The optimal distance between the tube and the lens-stack E is 1.3 mm, although up to 2 mm is still fine.

Transversal movement of the tube

The supporting base that allows the assembly of the different components has slots, so there is an opportunity of modifying the position of the tube along the X axis (see figure 22). The position is varied in a step of 0.5 mm.

It is obvious that if the movement is negative the system will be inclined; there will be a slope more or less pronounced. The maximum is 12.22º which corresponds to a displacement of 1.5 mm from the original/reference position. It could be supposed that the image quality will drop yet that is not the case even for the larger distance, at least not in a

determinant manner. At this point, another experiment was conducted to check what will occur when the aperture stop moves. The starting point is the slot D and as the aperture goes closer to the lens-stack-A, the sharpness values or the brightness, that would be more precise, is higher but at the expense of a decrease in the quality as the bars are more blurred. According to this result, there are more light rays going through when the aperture stop is closer to the first lens-stack.

It is important that the tube is perfectly parallel to both the Y and Z axis since the image captured by the detector will not be straight. It is better if the tube is slightly raised, in such a way that the tube is fully visible and there is no any hidden part inside the assembly-base.

3.1.4. Other approaches

With the target of finding the optimal position of the different components and observing the effect of the combined changes, different approaches have been made.

- *Lens-stack A: right, aperture stop: slot C, tube: parallel and raised*
  When the lens-stack is a bit raised (it is possible to introduce something, a folded paper for instance, that allows positioning the lens-stack raiser) inside the slot that allows it) in case of channel 2 the images appear more blurred at their bottom region whereas the crosstalk increases in the third channel. If the aperture stop is located in the slot D, the crosstalk is observable again and the second channel performs worse. It is true that slot D seems to be the optima position in view of the above images, but for this particular case an improvement was not achieved locating the aperture stop in slot D. The lens-stack A was not perpendicular to the axis; it was a bit slanted towards the sensor direction which affects the result.

  For the second optical channel when the system is tilted a little (less than 3º), the quality of an image of groups 0 and 1 enhances; in the case of groups 2 and 3, it is necessary to rotate the system considerably.

  In the case of channel 3, a better imaged is obtained when the aperture stop is not perpendicular and is placed between slots C and D. For that position the crosstalk does not disappear when the system is tilted 4º approximately as was explained in the behaviour of the referenced channel in section 2 of this chapter. An extra tilt (a little bit one) is necessary to make sure the crosstalk disappears, although the image quality is worse.

- Regarding reducing the crosstalk of the third optical channel, the fact of positioning the aperture stop in-between slot C and slot D has no really significant effect. Positioning the aperture stop between slots C and D does not affect the crosstalk in the third channel. The first lens-stack is situated at the right side of the slot and the tube is not parallel to the Z axis. For the standard position, the lower elements in the USAF were blurred and with this mounting the problem is partially solved (an improvement is achieved).

- The transversal movement along the Y axis of the first lens-stack (A) or the second lens-stack (E) does not bring a notable improvement in the performance of the imaging system. It seems that the system works better if they are at the left edge. Moreover, since all the components are connected together through the guiding pins, the flexibility is limited and therefore it is complex to move each component in an isolated way without affecting the others; in other case the whole block has to be slanted.

3.2. Conclusion of the tolerance analysis

In view of the results and considering my personal impressions, the imaging system performs best when the lens-stack is positioned at the right side of the slot, the aperture stop in the slot D perpendicular or slightly slanted toward slot C and the tube totally parallel and raised. This last point is quite essential in order to capture a straight image.

The lateral displacement along the optical axis is not as critical as the rotation of the system. Sometimes, it is indispensable to tilt the system to get an image of superior quality or the other way around, the quality deteriorates in front of a tilt.

4. Conclusion about the procedure of the static system

This multi-resolution, multi-channel imaging system performs well in general terms. The first optical channel is most robust to changes. The other two channels have also a low sensitivity however, the distortion in the second channel and the crosstalk in the third optical channel confer some handicaps for an ideal procedure.

The system is robust to longitudinal movements along the optical axis of the several components that compound the system. It has been found that the optimal location of such elements is as follows: the aperture stop has to be in slot D, the tube must be perfectly parallel being even better if it is slighted raised, i.e. the tube should be out of the slot by means of a support. Finally, the quality of the captured images is superior if the first lens-stack is at the right side of the slot. The second lens-stack has no opportunity to vary its position as it fits tightly to the slot.

On the other hand, the tilt of one component of the whole system (or even the tilt of the whole system) affects the performance in a more significant way. Thus, it is essential to achieve an angular alignment as good as possible.

IV. A refocusing imaging system (Dynamic System)

This system is called dynamic because it has refocusing capabilities which means that regardless of the distance of the object with respect to the imaging system, a sharp focused image can be obtained; whereas, in the static system, the focal length remains the same limiting the series of working distances. This ability is achieved thanks to a tunable lens. Thus, the first part of this chapter will focus on the working principle and performance of a tunable lens: first a brief introduction to tunable lenses is presented; followed by the study of the performance of a specific tunable lens. The dynamic system is described in the second subchapter. The next subchapters discuss the experiments that have been done with the refocusing system. Specifically, the third section of the chapter is about the characterization of the fabricated lenses and the last section of the chapter is a proof-of-concept demonstration of the refocusing imaging system.

1. Tunable lenses

1.1. Introduction

As the name denotes, tunable lenses are optical elements with adjustable capabilities. They are able to focus in a series of object positions by varying either the refractive index of the optical medium or the lens curvature.

There are different types of tunable lenses in function of several physical working principles (pressure control, electrowetting control, thermo-optic control, magnetic control, optical control or electro-optic control) such as solid-state tunable lens, which encompasses lens based on electro-active polymers and thermally tunable lenses; liquid crystal tunable lenses or electrically/mechanically liquid tunable lenses.

The type of adaptive lens used in this project is a liquid tunable lens and specifically the Varioptic liquid tunable lens (model *Artic 320*)whose radius of curvature changes and thus, its focal length does so by means of the application of an electric field according to the electrowetting principle. The basic idea of electrowetting lies on the modification of the surface tension of the interface between two immiscible liquids in such a way that they turn miscible. Figure 31 illustrates the manner in which the tunable lens operates.

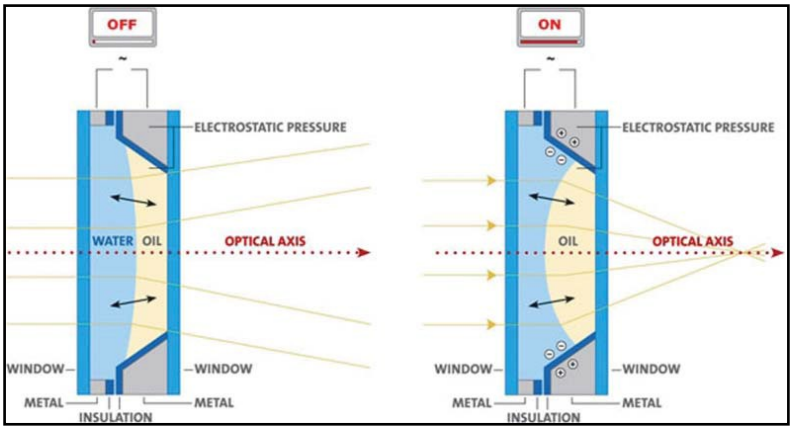

Figure 31. An optical lens consisting of an oil drop in a water medium. When the voltage is on, the oil drop pushed by the water becomes convex and focus the light passing through it. The curvature of the interface between the two liquids (having different refraction indexes) is modified by the application of an electric voltage. This voltage turns gradually the hydrophobic surface into hydrophilic (wettable) since the surface tension changes [22].

The properties of the Artic 320 liquid lens are gathered in Table 8.

Table 8. Properties and appearance of the liquid tunable lens Artic 320

Properties Arctic 320	
Threshold voltage	39.6 Vrms
Pupil diameter	3 mm
Required operating temperature range	-20°C till +60°C
Typical response time	100 ms
Dissipated power	< 1mW
Driving voltage	0 – 60 Vrms
Transmission (@ 587 nm)	> 90 %
Operating cycles	> 1 000 000

The design is compact which facilitates its insertion in systems with reduced dimension as our refocusing imaging system. The time response is relatively fast; so, the adaptation to the potential changes to deal with will be quick and real time response is feasible. Another positive point is the low power consumption. The main shortcoming is the aperture size, 3 mm, but this obeys to the physical constraints of low capillary forces which complicate the building of wider aperture lenses. This lens has been demonstrated and has low wavefront aberration which is translated into a good performance (diffraction-limited) at largest angles and voltages. The focal length varies exponentially with the voltage. For a certain voltage range (50 to 60 Vrms), the curve can be approximated by a line, finding a stable region where the lens performs.

1.2. Study of the performance of the Varioptic Arctic 320 tunable lens

With the objective of understanding the working principle of Varioptic liquid tunable lens and studying its performance, several tasks have been completed:

- Basic setup: illumination source + tunable lens (TL) + CCD
  a) Find the optimal distance between the TL and the detector for different voltages.
  b) For every voltage, move the detector backward and forward the around the optimal position until the image starts to be blurred.
  c) Using the USAF 1951 resolution target determinate the MTF.

- Optics added setup: basic setup + passive lens + beam expander
  a) For different voltages, move the CCD so that the image is sharp.
  b) Obtain a sharp image for several voltage values by moving the object.
  c) MTF Analysis.

The results and a more detailed description of the setups are presented below. Both cases will be compared in order to check the influence of adding other optical elements with respect to the behaviour of the tunable lens itself.

The basic setup consists of a white light source, an object with some characters in it, the tunable lens and a detector. It also includes a beam expander composed of two plano-convex lenses of different focal lengths in conjunction with the source since the diameter (of the source) is not enough to illuminate the object totally. The tunable lens goes into a holder which is connected to a voltage source, so the needed difference of potential is produced.

(a) (b)

Figure 32. Voltage supplier (a)and holder (b) for the tunable lens

The first two tasks can be done together; the procedure is as follows: make a voltage sweep and for every voltage move the detector such that the image is focused. Once a good image is obtained, the subsequent step is to displace again the detector backward and forward until the image starts to become blurred measuring that distance (that is the depth of focus).

The second setup "optics added setup" includes a passive lens between the object plate and the tunable lens. The passive lens is a ThorLabs LE1015-A meniscus lens. The position of this lens is not trivial: the diameter of the meniscus lens is 50.8 mm which provides a large clear aperture; on the other hand, the small diameter of the tunable lens (3 mm) would block part of the rays; as a result, the brightness of the image would be low and the image would be incomplete. Besides, the beam has to fit the sensor dimension (4.6 mm x 4.6 mm) and the focal length of the meniscus lens (199.3 mm) allows achieving it since the rays are converging. This fact is beneficial as well for the tunable lens. These referenced aspects (focal length, image sensor dimension, diameter of the lenses) have influence on the distance between the optical elements.

Actually this setup is the proof of concept (POC) of the designed voltage-tunable refocusing system based on one of the several simulated refocusing configurations considered [23]. This design was optimized to obtain a high angular resolution and a diffraction-limited performance which confers a narrow field of view.

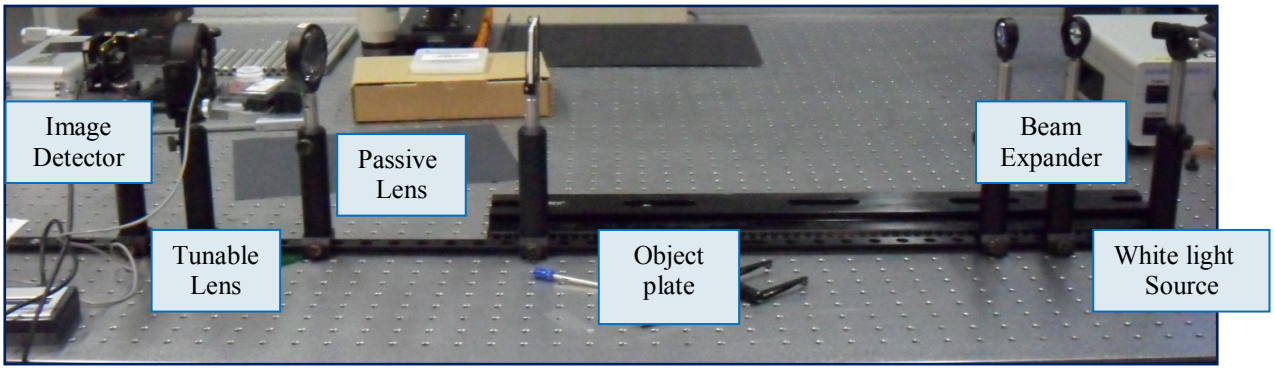

Figure 33. Elements and appearance of the second setup

The procedure is identical to the one related in the basic setup. Nevertheless, there is an extra test in which the object plate varies its position instead of the image detector. The purpose is to evaluate it against the results obtained in the proof of concept.

The sweep spans from 48.2 V to 60.1 V in steps of 1V approximately. The relationship between the voltage and the detector distance is reciprocal: when the voltage is high the distance is short and when the voltage decreases, the distance increases. Therefore, the higher the voltage the closer the detector to the tunable lens should be positioned.

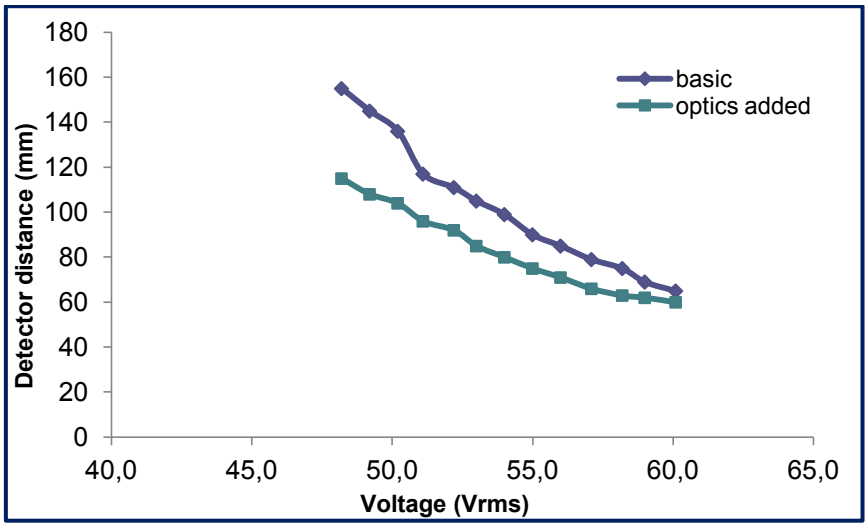

Figure 34. Comparison of the relationship between the voltage and the optimal distance of the detector with respect to the tunable lens for the two considered setups.

When the other optical elements are added, the distance is shorter for the various voltages and as such the difference between both setups increases as the voltage tends to lower values. The second setup seems to be more stable attending to a more developed linearity. The introduced optical components result in a variation of the focal length. This insertion also modifies the depth of focus, that is, the range for which the image is still sharp (or can be considered as sharp). The obtained depth of focus is wider in the second setup; the detector can be displaced more if there are extra elements. This observation is only correct for this particular configuration; depending on the characteristics of the added element(s) and their relative position (tunable lens in front, behind, in-between the element) the result will vary. Again, the higher the voltage the narrower the depth of focus is. As is observed in Figure 35, the displacement is quite small and thus, it is difficult to make an accurate measurement.

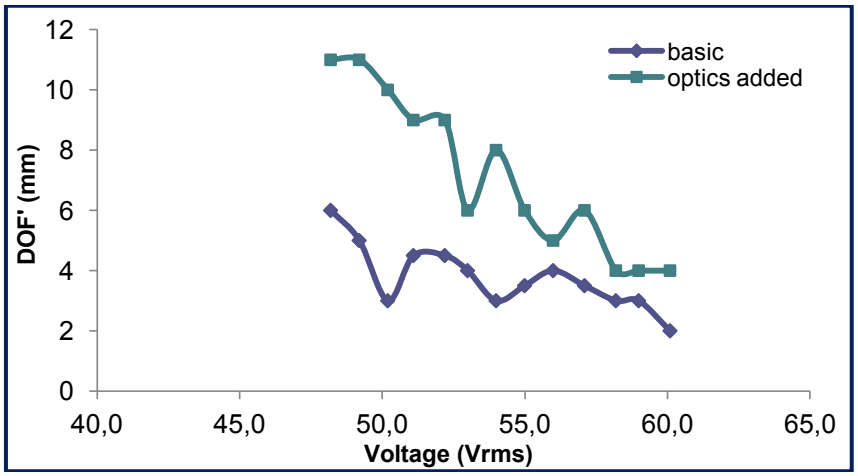

Figure 35. Depth of focus (DOF') as function of the voltage for "basic" and "optics added" setups.

Something similar happens when the object plate is moved instead of the detector. In this case, the distances are larger. The trend obtained in the optics added setup comparing the simulations of the designed refocusing system and the proof-of-concept is analogue. The similarity is major for voltage values over 55.0 Vrms. This region is more stable and reliable.

It is important to point out that the experiment described above is not identical to the POC since the distances between the several involved components are not exactly the same.

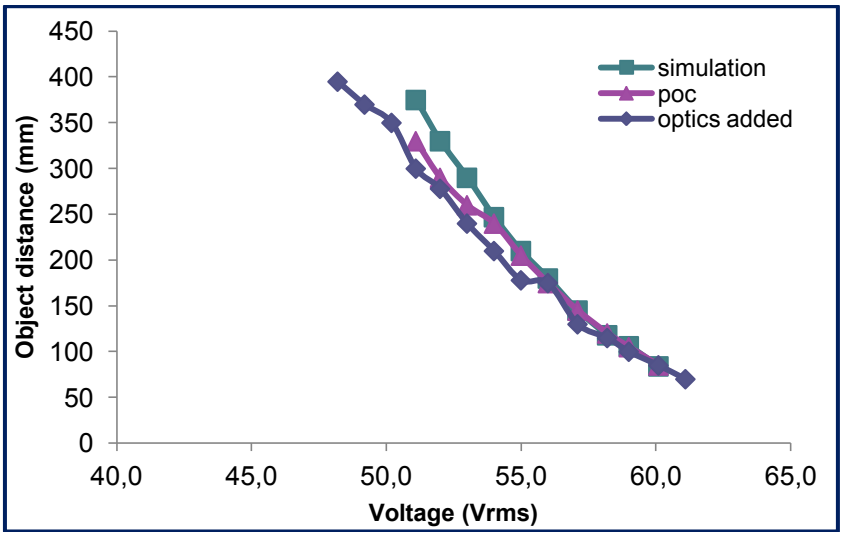

Figure 36. Optimal distance of the object plate measured with respect to the passive lens for a range of voltage values.

In conclusion, the larger the object/detector's distance the wider the depth of field/focus. For shorter object distances to the optical system, a change in that distance has more relevance and it is needed to modify the voltage if a good image is pursued. The behaviour of the tunable lens alone or together with other optical elements changes yet not the working principle.

The MTF is a figure of merit that allows comparing different optical systems. The object utilized is the USAF 1951 resolution target.

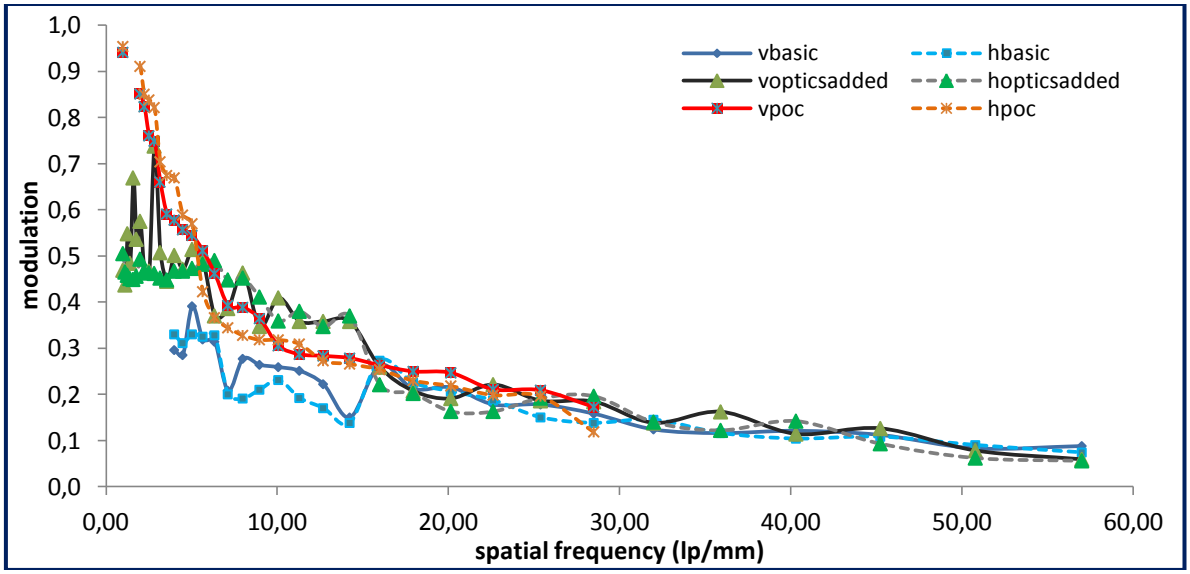

Figure 37. MTF comparison of the three setups

The quality measured in the basic setup is lower than when there are more elements. These extra components improve the angular resolution of the system. The difference is more visible in the range of frequencies that comprises from 4 lp/mm to 15 lp/mm. In the basic setup, it was no possible to take images for the first groups (frequencies from 1 lp/mm to 3.56 lp/mm) in spite of playing with the voltages and the distances because the image magnification prevented to capture the whole USAF. In addition, the sensor size is not large enough to host the whole image. The minimum frequency considered is 1 lp/mm.

2. Description of the dynamic system

As was said in the introduction of the chapter, the dynamic system is a refocusing multichannel system. Refocusing and zooming are not homonym concepts. A **zooming** system is an optical configuration with constant object and image distance. It can give different **magnifications** by modifying the focal length. A **refocusing** system is an optical configuration that has a constant image distance and magnification. It adapts the focal length in order to focus **object**s located at various **distances** from the system.

The design integrates two optical channels in which one of them contains a voltage-tunable refocusing configuration. The first channel is static and corresponds to the third optical channel of the Static System described in the previous chapter. It has large FOV and low angular resolution. The second channel, on the contrary, has a high angular resolution (0.0098º) and low field of view (2x7.52º) and refocusing capabilities by means of the use of a liquid tunable lens (the one described in the previous section). The utilization of this type of tunable lens is really advantageous since in such a way the integration of both channels is easier and the movement restrictions for a mechanical configuration do not exist now. In mechanical refocusing systems, the focusing at different object distance is made by varying the distance between the assembly lens elements out of which the system consists such that the effective focal length is both determined by the focal length of the lens elements and their mutual distance.

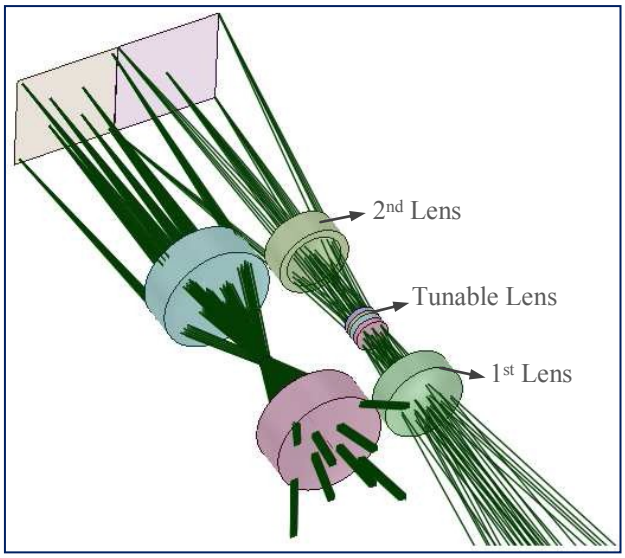

Figure 38. Design of the bi-channel refocusing system. The first optical channel (left) is static. The second optical channel (right) has refocusing capabilities by means of the tunable lens.

As is observed in the above figure, both channels share the same image sensor. The design is for a sensor of dimensions of 1920x960 pixels which is divided into two equal segments of 960x960 pixels. This fact provides major facilities for the integration of both channels in a single entity.

The first optical channel will not be a target of discussion in this chapter; it has already been described in the chapter above the Static System (chapter III). The focus will be on the second optical channel, the channel with refocusing capabilities. Below, the characteristics of this channel are described.

The **refocusing channel** is composed of two lenses ('L1' and 'L2') and the liquid tunable lens ('TL') between them. L1 has two surfaces, 'surface 1' and 'surface 2'; L2, for its part is, is formed by two other surfaces, 'surface 3' and 'surface 4'. Their parameters are shown in Table 9 as designed by Lien Smeesters and al. The thickness of both lenses is 2.8 mm. The centre of the every lens is coincident with the centre of the two lenses of the first optical channel.

All the surfaces are aspheric. An aspheric lens is a rotationally symmetric optical component whose radius of curvature varies radially from its centre. In other words, the radius of curvatures changes with the distance from the optical axis, unlike a sphere, which has constant radius.

Table 9. Parameters of the designed lens surfaces for the second optical channel.

Lens surface	Aperture Radius (mm)	Radius of Curvature (mm)	Conic constant (mm)	4th order aspheric coefficient	6th order aspheric coefficient
Surface 1	3.91	8.33	0.27	$5.34 \cdot 10^{-5}$	$2.87 \cdot 10^{-6}$
Surface 2	3.29	12.13	-0.47	0.0003	$8.43 \cdot 10^{-6}$
Surface 3	2.73	-4.30	0.44	0.0007	$2.22 \cdot 10^{-5}$
Surface 4	3.46	-5.82	-0.14	0.0005	$1.47 \cdot 10^{-5}$

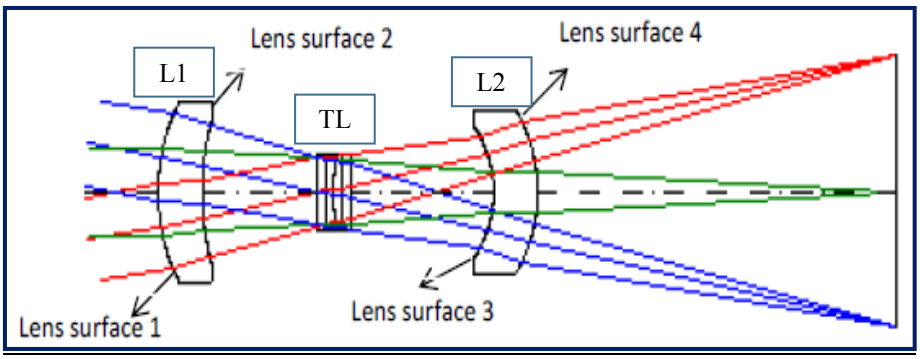

Figure 39. Design of the second optical channel

As the first optical channel was already designed, this second channel has to adapt to this circumstance and therefore, there are some restrictions in the distances between the different components and in the radius of the lenses. The optimal distances obtained in the simulations are the following ones:

- Distance between L1 and TL: 7.29 mm
- Distance between TL and L2: 9.05 mm
- Distance between L2 and image sensor: 22.73 mm

The designed lenses have been fabricated in PMMA by ultraprecision diamond tooling. The next task is the characterization of the fabricated lenses and then building up the structure of the system.

3. Characterization of the fabricated lenses

Once the system has been introduced it is necessary to check if the fabricated lenses correspond to the designed ones for the second optical channel. The characterization is done by means of a measurement coordinate machine (Werth UA 400).

There are three fabricated lenses which contain two surfaces, concave and convex. The results show that there are two identical lenses, so from a vague point of view it seems that the two lenses, L1 and L2 have been manufactured. An exhaustive analysis evidences that surfaces 1 and 2 (L1) and surface 4 (L2) have been made. Thus, surface 3 is missing and instead of this surface, L2 has been fabricated with the parameters of designed surface 2.

The designed profiles are modelled with the sag equation that defines the surface profile of aspheric lenses as:

$$Z(r) = \frac{Cr^2}{1+\sqrt{1-(1-k)C^2r^2}} + A_4r_4 + A_6r_6 + A_8r_8 + \cdots$$

where, Z: sag of the surface parallel to the optical axis,
r: radial distance from the optical axis,
C: curvature, inverse of radius,
k: conic constant,
A_4, A_6, A_8: 4th, 6th, 8th... order aspheric terms.

In the case of the fabricated profiles, the aspheric surfaces are modelled as polynomial surfaces, so the fitting is polynomial. The order of the polynomial chosen is 10th which corresponds to the maximum design order value for a polynomial surface in CODE V (optical design software). The interpolation has been made with the command '*polyfit*' of Matlab which calculates the polynomial that better approximates to the points by least square error. The order of the polynomial is not a minor issue: the reciprocal of the coefficient of second order is the radius of curvature. The higher the fitting order, the more correct is the radius of curvature (with respect to the designed one). However, the influence in the profile curve is almost unnoticeable, less significant.

The next figures compare the designed and fabricated profiles. Figure 40 compares the profiles of the repeated fabricated lenses with designed lens surface 'surface 1' and 'surface 2' that compound the first passive lens. The profile analysis for the second passive lens is depicted in Figure 41.

For the first case, the correspondence of the profiles of the two repeated samples to the profiles of the designed surfaces 1 and 2 is clear and almost perfect. As can be observed in both cases ((*a*) and (*b*)), these two fabricated lenses are identical.

For the second case, the convex surface fits perfectly to surface 4's profile. However the other surface of the lens diverges from the supposed/theoretical designed surface, namely surface 3. The reason is simple: its profile corresponds to parameters of surface 2. Putting side by side the profiles of the concave surfaces of the three fabricated lenses, it is observed that all the profiles are the same (see Figure 42).

Several profile matches have been tried in order to corroborate the result and it is definitive, surface 3 has not been manufactured.

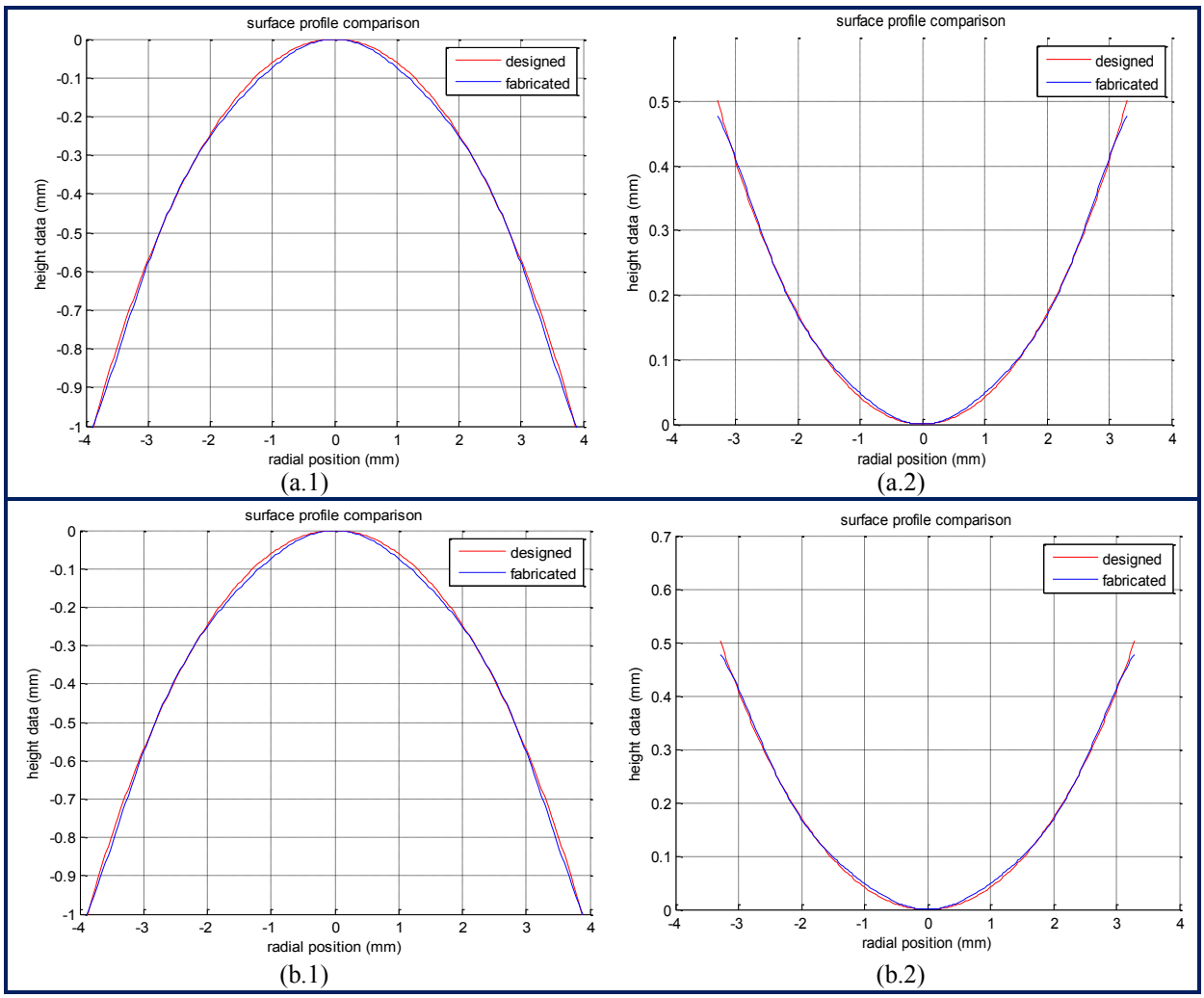

Figure 40. Comparison of two of the fabricated lenses with surface 1 (a.1, b.1) and surface 2 (a.2, b.2)

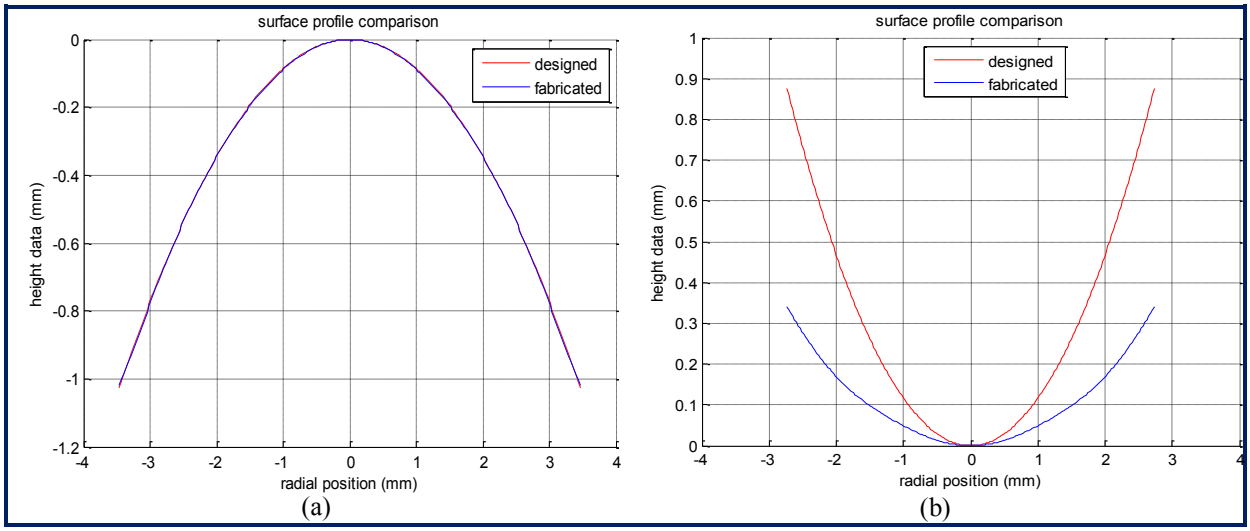

Figure 41. Comparison of the other fabricated lens with surface 4 (a) and surface 3 (b).

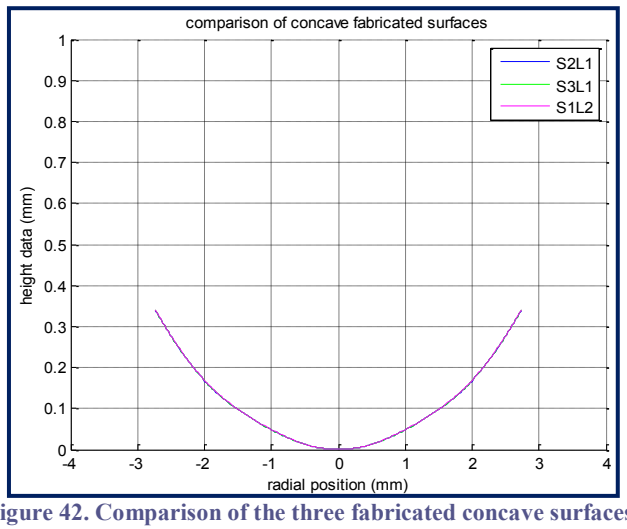

Figure 42. Comparison of the three fabricated concave surfaces.

How will this deficiency affect the performance of the optical channel? It is really transcendental the change in the surface profile as regards to the fulfilment of the desired features (working distances, integration with the firs optical channel) the system has been designed with? The next section will try to figure out the actual influence by the implementation of a proof-of-concept demonstration.

4. Proof-of-concept demonstration of a refocusing imaging optical system

As it is known from the previous section, there is certain discrepancy between the designed and the real system. The designed lens surface 3 has been substituted by a surface with the parameters of designed surface 2. The rest of components are according specifications. Along this subchapter is explained how the setup looks and how the mounted refocusing system performs.

4.1. Building up the setup of the proof-of-concept demonstration

The manner of building the setup is step-by-step, that is setting the several components one after each other. First, L1 is placed and an image is captured (the object to be imaged is the USAF 1951 plate); the focal length of this lens is 58 mm and has been calculated with the object and image distance. The second step is to add the tunable lens at the nominal distance (7.29 mm) and image the object again. At this point, the most important aspect is the alignment of both lenses. The tunable lens has a diameter of 3 mm, so it acts as the aperture stop of the system. It is essential that the centres of both lenses are coincident. The quality of the obtained image is very good. The final step is the inclusion of the second passive lens. According to the design, the distance between TL and L2 is 9.05 mm. Nevertheless it is not possible and the distance must be enlarged up to 17 mm approximately. The main reason for the latter is that the tunable lens is inside a bulky holder (see Figure 44) and the lens is in a holder too. L2 is positioned as close as possible to TL. This is one change with respect to the design. Another variation is the position of the image sensor. At 22.73 mm, for the nominal distance between L2 and the image sensor it is impossible to obtain a good image, even with partial blur. It is necessary to reduce the distance at least to 12 mm to get a sharp image, and even less when applying a voltage sweep. Indeed, if the simulations are redone introducing the new features of lens surface 3, the optimal distance decreases to 9.15 mm. The distance is measured from the vertex of ‘surface 4’ of L2 to the detector surface. At this distance the

image quality is high (high visual contrast of the groups on the USAF plate) although pincushion distortion is found. It has been tried to eliminate the distortion by looking for a better alignment, but the aim has not been achieved.

In addition to the lens elements, there is a laptop with a white screen serving as the light source and the USAF 1951 resolution target as the object to be imaged. The image sensor used is a uEye CMOS detector (the same as used in the Static System). With the purpose of achieving a precise alignment and studying the performance of this refocusing system, both passive lenses, L1 and L2, and the sensor can be moved longitudinally and transversally by means of translation stages. The tunable lens remains fixed and will be used as a reference to measure the object distance. This is because the mounting rail has a ruler incorporated in it and thus it is easier to measure the distances; furthermore, the measurements are more accurate.

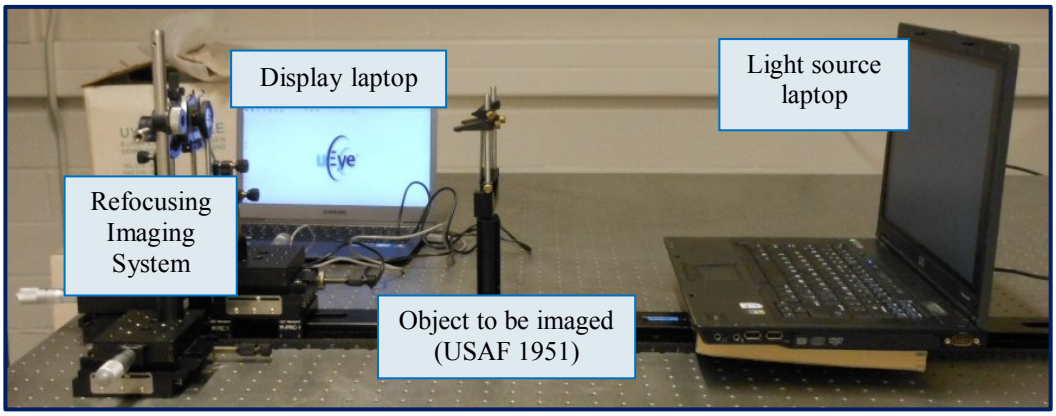

Figure 43. General view of the setup

Both the source laptop and the object can be positioned further away from the imaging system up to two metres approximately. The next pictures show the imaging system in more detail.

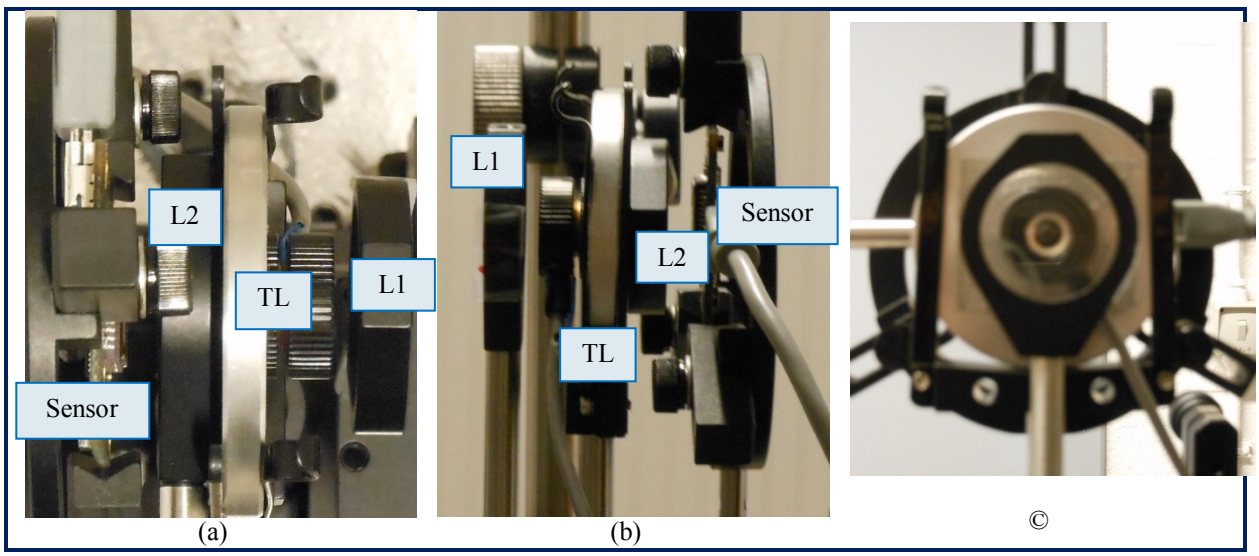

Figure 44. Detail of the refocusing imaging system: top view (a), side view (b) and front view (c)

4.2. Optical performance of the refocusing system

Once the setup is built, the next step is to study the behaviour of the system. In general terms, the image quality obtained are really good. As well as the higher resolution feature is confirmed as the system is able to resolve fine details. Figure 45 is an example of this last statement. Despite the original image (object) is not a good quality one, the image captured by the system is acceptably good since the edges, border lines are perfectly defined and the lines of the blind are absolutely distinguishable. A disadvantage (minor incidence affecting the system) is the presence of pincushion distortion caused by the second lens although it should be noted that it is pretty small and the weight in the degradation of the image quality is almost negligible. So, this aberration can be omitted and the system can be described as without distortion.

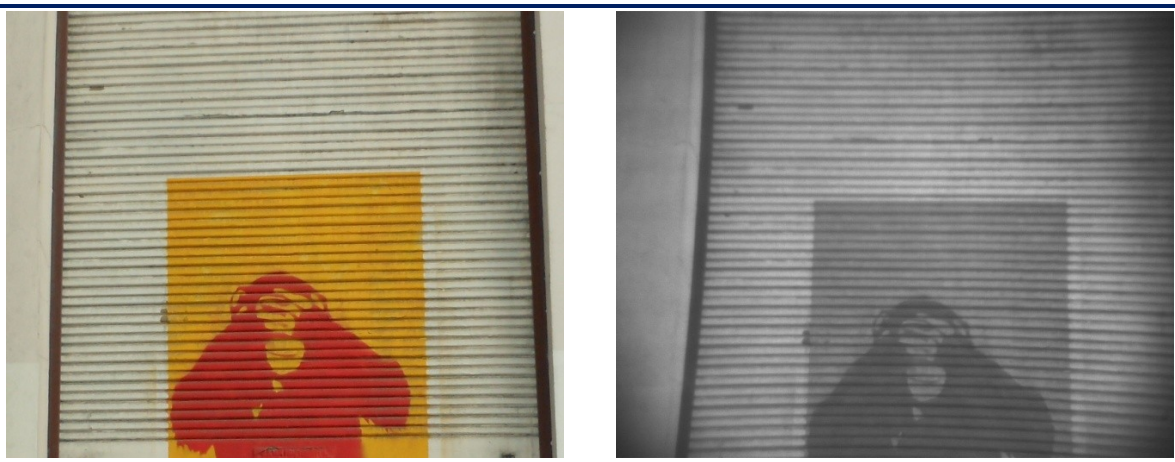

Figure 45. Original image (left) and image captured by the system (right). The system is able to distinguish the border areas and the horizontal lines.

Another aspect that has been observed is related to the slant of the object. When the object (USAF resolution target plate) is not perpendicular to the axis from a top view, the object is tilted, the image in the image plane is tilted too inside the plane. This is expected as the system solely images any object inside its territory (FOV) independent of the inclined or spiral nature of the object. The system has no the ability to change (correct) the shape or orientation of the image of the object as the distortion is very minimal.

The next table (Table 10) shows perfectly how the system performs. The scenario consists of two objects separated around 2.6 m, so one is closer to the system and the other is far away. In function of the applied voltage, the background or the foreground will be in-focus. In order to obtain a sharp image of the closest object, it is necessary to have a short focal length what implies a high voltage value of 57.1Vrms for an object located at 0.32 m. On the other hand, if the target to be focused is in the background the procedure must be opposite: the object distance is further, hence the focal length has to be larger and, thus the voltage level reduces. The central image corresponds to an intermediate voltage. Both objects are out of focus: the front object turns blurred whereas the rear object starts to be sharp. The image sensor is located 7.8 mm from the second passive lens[8].

[8] As will be seen in the subsequent sections the position of the detector has influence in the achievable range of object distances. The chosen distance allows having a wide range of voltages and distances.

Table 10. The refocusing capability allows focusing objects located at different positions.

57.1 Vrms	54.0 Vrms	51.1 Vrms
	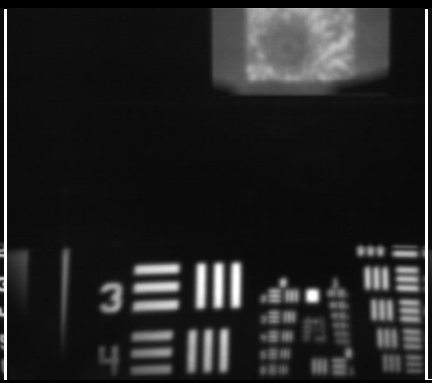	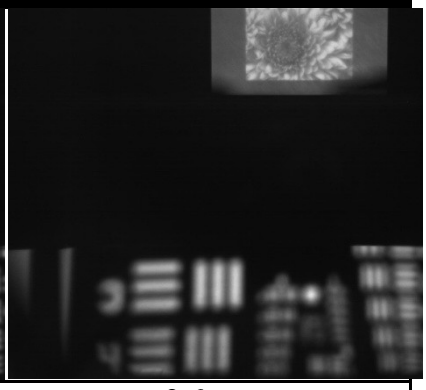
0.32 m	**Object position**	2.6 m

From a qualitative point of view and considering the personal impressions of this thesis author, the system is relatively quite sensitive to variations, especially to the tilt of the elements. The more accurate and precise the alignment, the better the performance; however it is possible a mutual (between the components) compensation of the departure from the ideal position (perfectly orthogonal, on-axis, aligned centres of the lenses). Let suppose that one element is tilted to the left or to the front and the following element is aligned (might be in the same direction or in the opposite) is such a way that the resulting images are perceived as correct (sharp, centred). The system can be assumed as a black box and just paying the attention in the input and the output. Thinking of a ray, what matters is if the ray leaves the system in the optimal (or close to) way not the trip realized for the ray inside the system. A potential drawback in this scenario is that the elements can be perfectly aligned meaning the centres of the lenses converge in a point yet not on-axis, i.e. at 0º. As a consequence the field of view will be shifted some degrees to the left or to the right what could introduce certain aberrations. The key for achieving ideal alignment and location of the optical elements is to have a reliable reference point.

A non rigorous analysis was carried out for observing the effects of moving the first lens (L1) and the second passive lens (L2) (independently) in the general quality performance. In the first case, it was found that the optimal distance L1-TL is 7-8 mm and there is some margin for lateral movement (2.6 mm) (of course the best is a centred position). For the second lens, if the distance to the tunable lens increases it is necessary to bring the detector closer in order to have a sharp image regardless the object distance/voltage. The separation TL-L2 is not infinitely growing, the effective focal length establishes the threshold. The best performance is attained when this distance becomes minimum for this particular setup, that is, as close as possible to the holder of the tunable lens.

What happens in practice? What are the working distances? What is the range of object distance where a sharp image is obtained? Next subsections will try to answer these questions...

4.2.1. Movement of the object for different detector positions

The aim is to obtain the voltage-object distance curve for different positions of the detector, i.e. for various distances between L2 and the detector. The applied voltages extend from 51.1 Vrms to 60.1 Vrms in steps of 1 Vrms, having a total of ten voltage values. Inside this range the behaviour of the tunable lens is linear, stable and more reliable. Furthermore, a few number of points are enough for the curve tracing and the same points were also considered during the simulations.

According to the experiment realized in the study of the behaviour of the tunable lens (section 1.2), it is expected that when the object is closer to the system, the voltage has to be higher and when the object is farther, the voltage level should be lower.

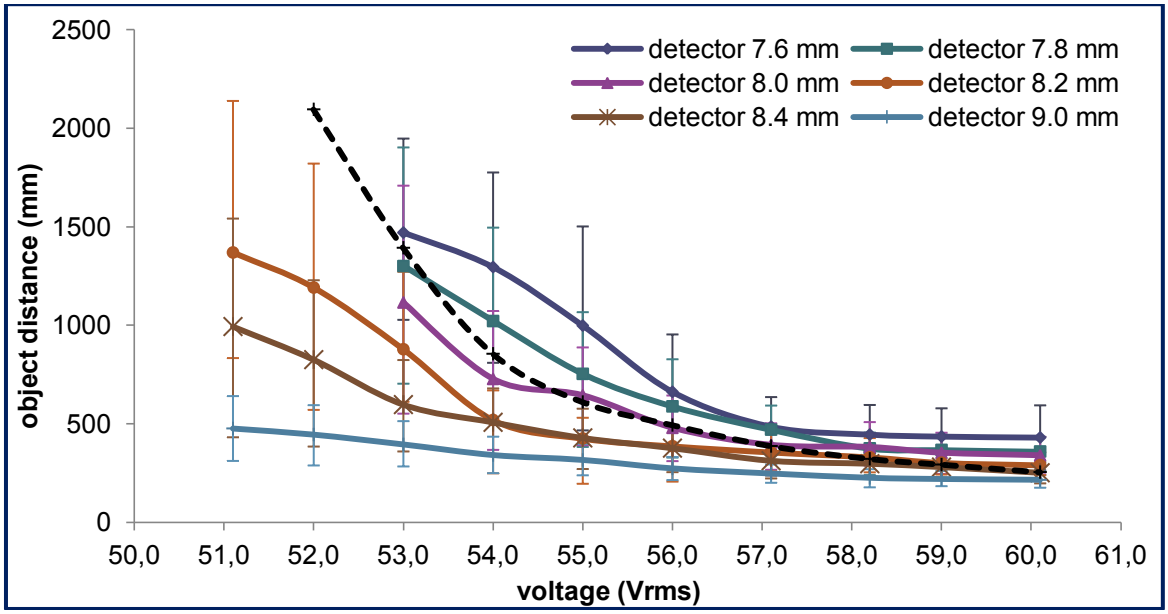

Figure 46. Voltage-Object distance curves for six different detector positions. The vertical bars represent the depth of field.

The predictions are verified: the higher the voltage, the closer the object. Another known behaviour that is also accomplished in this experiment is that the range of object distances for which the image is considered sharp, i.e. the depth of field, is larger when the voltage is lower or the object is closer to the optical system.

This is general for all the curves, what are the differences between them? The first conclusion is that when the image sensor is closer to the second lens, the object can be moved further. In another way, it is possible to focus objects that are located further, at larger distances from the observer (the system). Something similar occurs with the DOF: for instance, at 51.1 Vrms or 52.0 Vrms there is a clear increasing of the width of the bars as the detector is closer. There are some missing points for three detector positions, this is because it was not possible to determine the optimal position of the object neither the limits of the range. Therefore, it is reasonable to infer that for the same object location it will be necessary to reduce the voltage when the sensor is further or, in the other way around, to place the detector at a shorter distance when the voltage is augmented. This will be investigated in the next subsection.

If the depth of field is represented as a function of the object distance a set of Gaussian curves will be seen. The width of the curves will increase as the object distance enlarges. The peaks of the curves correspond to the best performance, which is the optimal detector

distance. The curves overlap in such a way that a constant line can be traced and represents the diffraction limit performance of the system. This edge delimits the DOF.

Putting side by side the experimental and the simulated curves (the simulated corresponds to the original designed system) the largest similarity is found for a detector distance of 8.0 mm, although 7.8 mm is also a good option. In spite of the fact that the difference between the several detector positions is small (0.2 mm) the variation in the object position for the same voltage is larger, especially for the lower voltages where there are differences of hundreds of centimetres. In the same line, the total range of object distance covered by the voltage span is wider.

4.2.2. Movement of the detector for different object positions

Now, the detector and the object play an opposite role with respect to the previous experiment: the object remains fixed and the detector moves closer or further to L2. It is realized for four different object positions.

As is observed in the graph of the figure given below, if the object is closer to the system the detector must be further in order to take a sharp image resulting larger distance for the lower voltages. As the object is located further from the system, the detector distance decreases, although this decreasing is not uniform. For example, between the blue curve (object 595 mm) that will be considered as reference in this argumentation, and the orange curve (object 995 mm) there exists a difference of around 1.5 mm in every point of the horizontal axis, whereas, for the purple line (object 139 mm) the separation with respect to the blue curve increases up to 3 mm approximately and in both cases the distance between the first position of the object (reference) and the second position of it is the same, 0.4 m more or less. The same happens with the largest object position. Nevertheless, linearity is the common trend for the four curves and they are practically parallel thus this separation between the curves can be seen as an offset; an offset that becomes smaller, meaning that the curves will be closer as the object is located further away from the optical system.

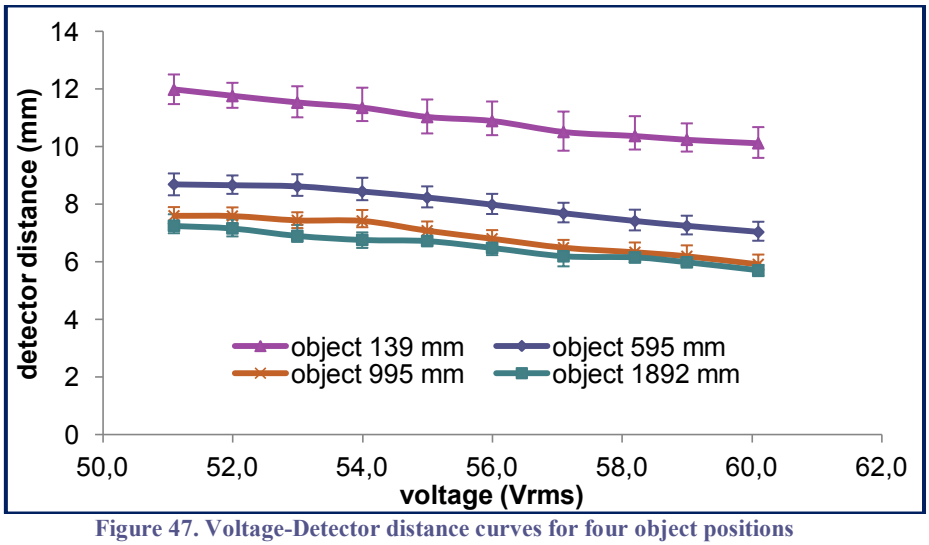

Figure 47. Voltage-Detector distance curves for four object positions

Looking to the vertical bars, which represent the depth of focus (DOF'), one fact stands out: the depth of focus is almost constant for all the voltages in a sweep, that is to say, for a fixed object position. The centre of the range changes as expected since the focal length varies and therefore, the position of the focus shifts. In the study of the tunable lens itself

the DOF' increased as the voltage was lower, although it is true that the span of the range is not too wide. The size of the sensor is constant and thus the circle of confusion as well if the choice is to make the circle's size equal to the diameter of a pixel width (or the whole sensor dimension). Thinking of Gauss ray's construction if a ray is traced from the edges of the lens aperture to the edges of the sensor (four rays in total) the diamond formed will have almost the same shape and dimensions since the variation in the distance (detector position) is quite small. The subtended angles (the origin is the image position) for the different position slightly vary and therefore the focal length is practically the same (focal length can be expressed as a function of that angle). Hence, the depth of focus (limited by the formed diamond) remains almost invariable despite the voltage tuning. From another point of view, the reason of the similarity in the DOF' regardless of the voltage variation could be that the change in the focal length consequence of the voltage tuning, is so small that the depth of focus for each voltage might be close to one another.

The depth of focus is smaller when the object distance enlarges, contrary to the case of the depth of field which is greater. It makes sense in view of the fact that when the object is closer to the optical system, the magnification increases and given that the sensor's size does not change the detector can be moved in a larger space.

4.2.3. Setting the limits for considering an image still sharp

Both the depth of field and the depth of focus have limits, front or rear edges with respect to the optimal position of the object for the first one or the detector for the second one. According to the definition, inside a defined range the images are sharp and in the edges the images start to lose contrast. Which is the criterion to differentiate an acceptable sharpness? Is it immediately after the first imperfection somewhere in the image or after vast percentage of the image blurred? Concerning this point there is a dependency on the detector position involving the way the image gets blurred. The blur is not homogeneous in all the groups of the USAF 1951 plate (object) but the inner groups or the outer groups become hazy earlier (in space). In this way, for a point in the axis the optimal detector distance is 9.15 mm whereas for a point at 4º (the total FOV is 2x7.52º) the highest modulation value is obtained around 7.9 mm; this result is for the simulation and it is valid for all the voltages. In order to smooth out the defocusing shifting for the external and the internal groups a good solution is to position the detector in between the two optimal distances. Hence the investigated detector is positioned as in section 4.2.1. The next pictures depict the images for the case of 56.0 Vrms. Also, in the central image of Table 10 the described defocusing effect is noticeable.

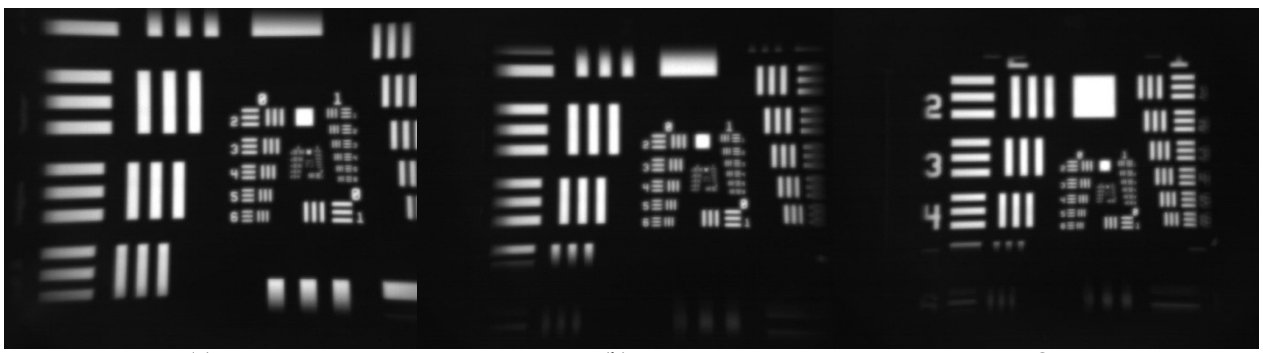

(a) (b) ©

Figure 48. Edge images for different detector positions: 9.0 mm (a), 8.4 mm (b) and 7.8 mm (c)

The dissimilarity is not very clear in the shown images although in practice certain improvement or variation is perceived. Another observation acquired during the experiments is that when the object is displaced from the optimal position to the light source (let's say it is in the front) the blur is more homogenous than when the object is on the rear of the optimal position. There is uniform blurring over the entire image that makes it hazy (not clear). It is like a kind of smudge, a veil over the image as can be noticed in the Figure 49. When the object is further from the system, all part of the USAF plate is imaged because the region in the object space subtended by the FOV of the system is larger in this case; whereas, if the object is closer, the area in the object space which is under the FOV of the system is small, as a result only a small portion (inner groups) of the USAF plate is imaged. In the first case, the background is more evident and the amount of light (diffused) reaching the object is greater. Moreover, the background is out of focus. It seems that the blur of the background (white screen of the laptop) also contributes and is added to the blur of the object in a manner of superimposed planes (the blur of the background is over the image of the USAF groups).

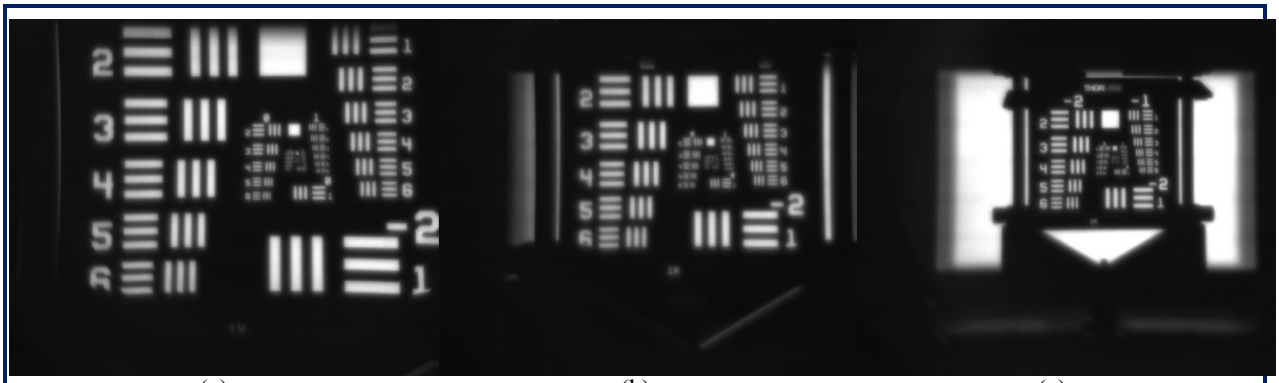

(a) (b) (c)

Figure 49. Front edge images for different detector positions: 9.0 mm (a), 8.4 mm (b) and 7.8 mm (c). The voltage is 56.0 Vrms.

Field curvature or Petzal curvature is one concept that needs to be taken into account in view of the behaviour of the refocusing system under consideration. Field curvature causes a planar object to project a curved image so the object appears sharp just in certain region(s) instead of having uniform sharpness across the image plane. Since the sensor is flat there are points out of focus (coming from off-axis rays). Moving the detector closer a makes that a larger portion of the curve is covered (the difference between the positions in a curved plane and the imaged points positions in a flat plane reduces) and the focus distance turns optimal, as this new situation is closer to the ideal position. That is why there is a quality peak for a relative shifting from the axis (0º). The field curvature can also be 'wavy' provoking that the image is perceived as sharp in the centre and in the corners of the sensor (image plane) yet not in-between.

Comparing figures 48 and 49 is clearly showing the different working distances and the fact that for the same voltage the object can be located closer or further in function of the detector position (distance to L2) in accordance to the above explanations.

4.2.4. Influence of the direction of voltage turning

Does the system always behave exactly in the same manner? Speaking in general terms, the overall quality of the image remains as high as before; yet there are small deviations in distances, in the object/detector position: the second time the object is one centimetre to the left with respect to the first measurement, for example. It is interesting to repeat an experiment in order to reduce the impact of possible errors and know its real weight in the results.

As an example, in Figure 50 is represented the average and the standard deviation for two cases studied in section 4.2.2 of this chapter: the object located at 139 mm and 995 mm. The measurements took place at different moments, not immediately one after the other. So the conditions are not exactly the same.

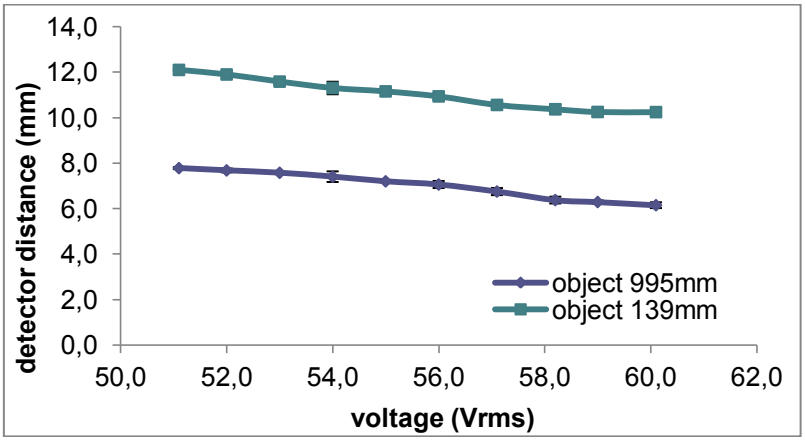

Figure 50. Comparison of repeated measurements for two different object positions

The deviation observed in the graph is pretty small although at 54.0 Vrms is greater in both curves. Why? The tuning direction of the voltage could have influence, so the next step is to examine what happens at 54.0 Vrms starting from a higher or a lower voltage. Table 11 collects the obtained data. For notation: 'down' refers to a voltage diminishing, e.g. from 56.0 to 54.0 Vrms; 'up' is the opposite and denotes a voltage increasing, e.g. from 52.0 to 54.0 Vrms. The terms 'close' and 'far' indicate that the detector is closer or further to the second passive lens (L2) whereas 'optimal' is the detector's position for which the image looks absolutely sharp and well contrasted (black-white).

Table 11. Study of the influence of the direction of voltage turning in determining the position of the detector for a 54.0 Vrms voltage.

	Up			Down		
Object position (mm)	Detector optimal (mm)	Detector close (mm)	Detector far (mm)	Detector optimal (mm)	Detector close (mm)	Detector far (mm)
139	12.57	12.04	12.90	12.20	11.77	12.61
595	8.44	8.14	8.92	8.16	7.81	8.46
995	8.13	7.87	8.46	7.81	7.56	8.20
1892	7.80	7.56	8.13	7.65	7.38	7.83

There are small differences: the optimal position of the detector varies around 0.3 mm that roughly corresponds to half of the whole valid range, i.e. the depth of focus. Is this result translatable to the rest of the voltages? The two graphs below validate the previous outcome. In the left side the voltage sweep is to determine the optimal detector position

when the object is at 595 mm. In the right side the roles of object and detector are swapped; now the detector is fixed at 8.4 mm.

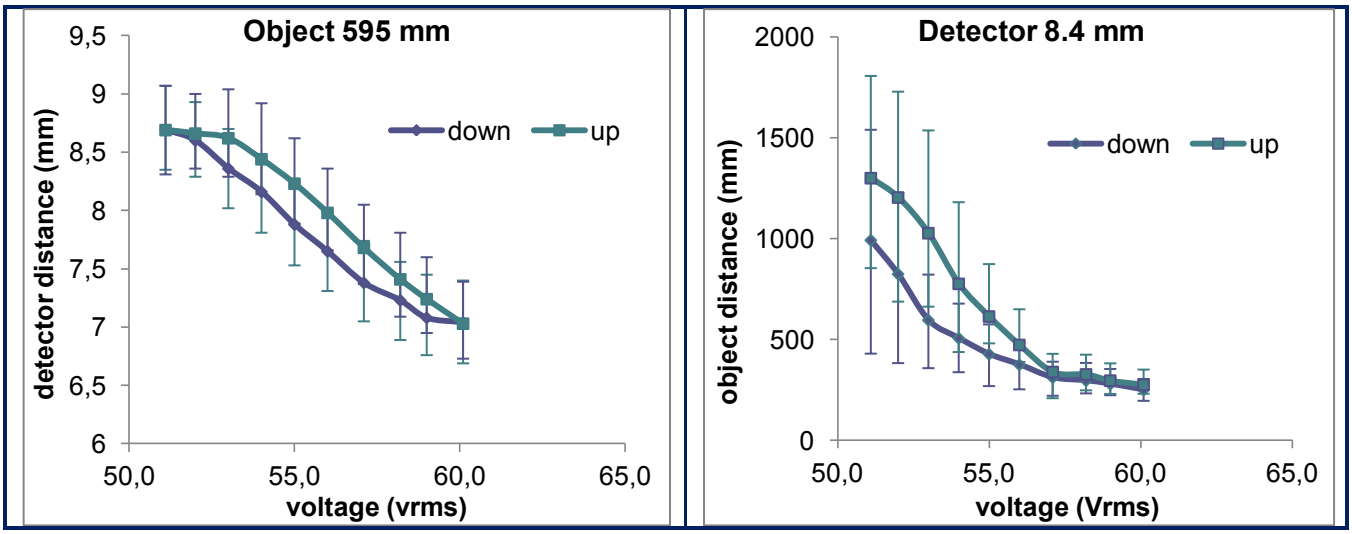

Figure 51. Examples of the dependency of the performance of the refocusing imaging system on the direction of the voltage turning.

When the voltage sweep goes from higher to lower values, smaller distances are obtained. The discrepancy is more significant for low voltage values when the object is moving. This circumstance is the one which could have more weight or demand more attention in this investigation work due to the fact that the purpose of refocusing system is to obtain focused images regardless the object distance by tuning the voltage. From another point of view, this hysterical behaviour could be considered as a minor matter since the distance range in which the image is acceptably sharp is large enough to adapt to several working object distances. In any case, this fact contradicts the reversibility (or hysteresis free) characteristic of the electrowetting fluid actuation stated on the website[9] of Varioptic. There is explained a basic experiment that measures the contact angle versus the voltage obtaining a curve that shows the drop shape variation as a function of voltage during a voltage cycle. The result underlines the reversibility and linearity (precision). This is just an "innocent" and partial remark; a deeper and more accurate investigation is required in order to better discuss the issue. It is not plan of this project.

4.2.5. Quantitative measure of the performance of the Dynamic System

As a kind of example it is shown here in Table 12 the MTF of three images captured by the Dynamic System for a voltage of 55.0 Vrms. The images correspond to three different detector positions: 8.0 mm, 8.4 mm and 9.0 mm.

The number of frequency points is reduced due to the fact that the size of the inner groups is not enough and only have been considered groups -2 and -1 (frequencies up to 1 lp/mm). It is a matter of how the MTF is calculated: magnify the image, i.e. move the object closer in order to analyse the inner groups. It is explained in Chapter II.

The images show a high visual quality although there are some defects, for instance, in the last image (detector 9.0 mm). Distortion is perceptible in all the images. The modulation values are really high for the vertical elements whereas the horizontal elements have lower modulation index as expected since in the outside part (higher points of the field of view)

[9] http://www.varioptic.com/technology/electrowetting/

of the image has poorer quality is. However, there could be an overestimation provoked by the way of calculating the MTF[10]

Comparing the three graphs, they are pretty similar. In the case of the detector positioned at 8.0 mm the values are slightly lower. It could seem that 9 mm is the best distance of the detector to the second lens (L2), but the impressions acquired during the experimentation makes opting for a closer distance. At 7.8mm or 8.0 mm the visual quality for most of the voltage values is quite high and in addition, the object can be moved further away.

Table 12. MTF at 55.0 Vrms for three different detector positions

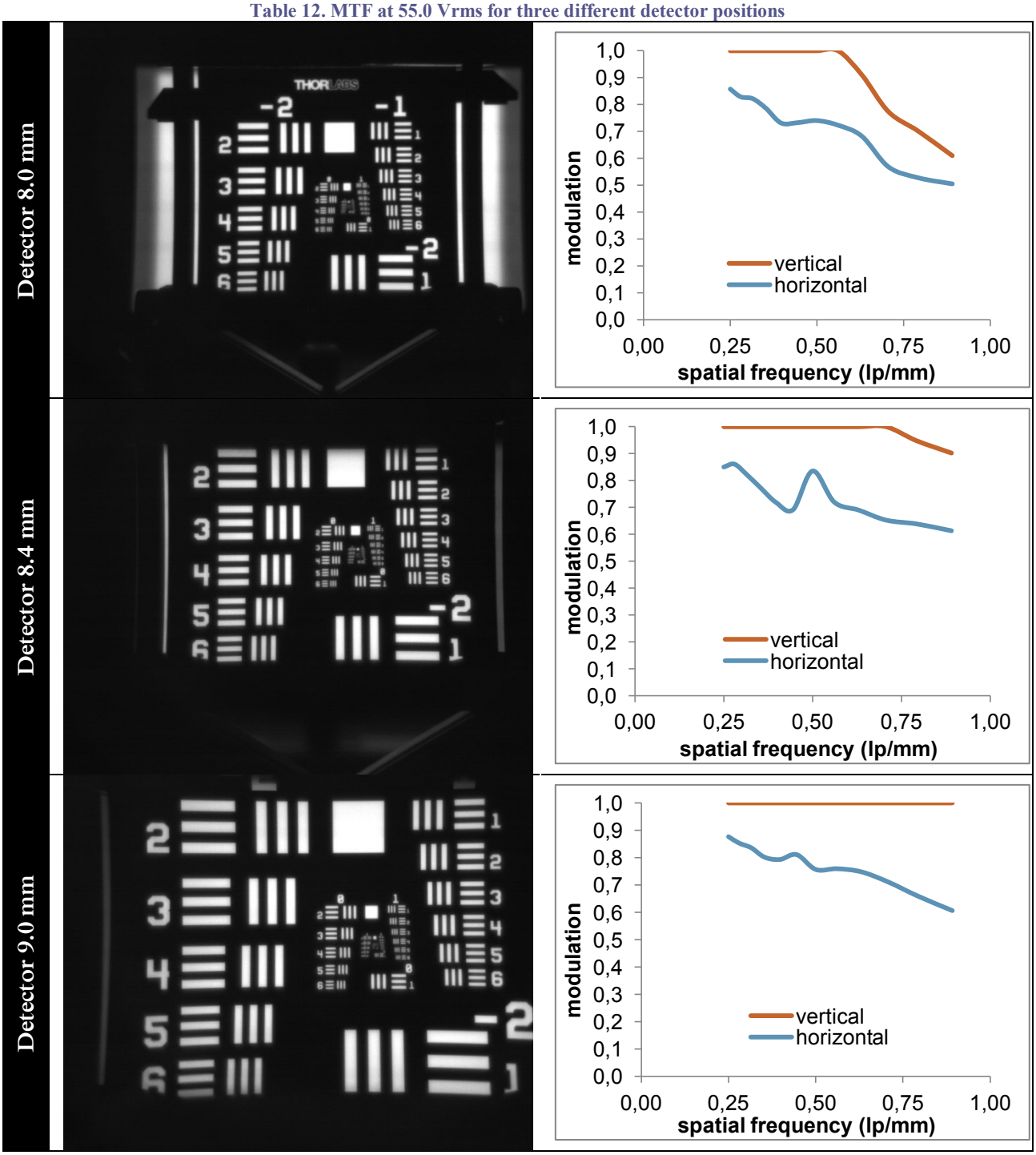

[10] The way of calculating the MTF is considered as valid for the time being yet not definitive and still is being carried out some research.

4.3. Conclusion of the proof of concept demonstration

The Dynamic System is composed of two passive lenses and liquid tunable lens responsible for the refocusing and an image sensor. The designed distances between the elements have changed due to the fact that the fabricated lenses are not the same as the designed ones (run into reality...☺)

The refocusing system captures good quality images (visually) for different object locations. The object distance range extends up to two metres when the object is the USAF 1951 resolution plate and around one metre more for other objects like pictures on a laptop screen. When the object is placed far away from the system, the voltage must be lower (larger focal length) and the opposite, if a high voltage is applied, the object must be near the system. In the same way, when the voltage is in the lower levels (the minimum considered is 51.1 Vrms but it can be lower), the range of object position for which the image is acceptably sharp is larger, i.e. the depth of field is larger.

The range of object distances depends on the sensor position, namely the distance to the second passive lens, in such a way that the closer the detector, the wider the object distance span. The optimal object position is also a function of the direction of the voltage tuning: the position is different (not exactly the same) depending on starting from lower to upper voltages than the other way around. For the latter case, the distances are a bit inferior. This fact also occurs in the case in which the voltage sweep is done for the detector.

For future approaches and taking into account that a compact refocusing system is desired, the whole tunable lens pack, that is, the liquid tunable lens plus the holder and the voltage supplier must be smaller. In that regard, the proof-of-concept has been constrained by the packaging of the tunable lens as it has imposed a restriction on the distance between the tunable lens and the second lens. Nowadays, the field of the tunable lens is quite investigated and finding applications for daily life has paramount importance. Integrating a tunable lens in mobile phone cameras creates an optimistic perspective concerning the miniaturization of the associated circuitry of the tunable lens and the possibility of making compact imaging system more easily. An example of such researching is the work of Hung-Chun Lin and Yi-Hsin Lin where an electrically tunable focusing LC lens with a low voltage and simple planar electrodes has been demonstrated [24]

V. Conclusions and Perspectives

1. Conclusions

In this thesis the proof-of-concept demonstration of two smart optical imaging systems have been accomplished. The first system is a three-channel multi-resolution imaging system (Static System) and the other system is a refocusing imaging system (Dynamic System).

The Static System is composed of three optical channels: the first optical channel has the highest resolution and the narrowest field of view; the third optical channel has opposite properties, i.e. the lowest resolution and the widest field of view; the second optical channel has intermediate properties. The performances of the three channels have been studied showing a good image quality and low sensitivity to changes; the first channel is more robust. The presence of distortion (pincushion) in the second optical channel and crosstalk in the third channel divert the system's experimental performance from the simulation performance. The quality of the images captured by the system has been quantified with a MTF analysis.
The influence of misalignment errors of the components has been investigated. Three variables have been considered: the movement of the aperture stop, the first lens-stack and the tube. The results exhibit robustness against longitudinal movement (along the axis) of the components. However, the system is more sensitive to rotational movements: a tilt of one component or of the whole system affects its performance in a more significant way. The achievement of a good angular alignment becomes essential.

The optimal position of the components have been found, namely: the aperture stop in the slot D, the first lens stack in the right side of the slot A and the tube perfectly parallel to the optical axis, slightly raised (out of the slot) and there must be some separation with respect to the second lens-stack (between 1.3 mm and 2 mm).

The Dynamic System is a voltage-tunable refocusing imaging system consisting of two optical channels. One channel is the third optical channel of the Static System and the other channel has refocusing capabilities thanks to a voltage-tunable liquid lens. In addition to the tunable lens, this channel has four aspheric lens surfaces grouped in pairs (combination of concave and convex). Surface 1 and surface 2 compose a passive lens (first passive lens) and surface 3 and surface 4, another passive lens (second passive lens). The integration of both channels in the same entity has not been realized yet.

Some experiments have been done in order to understand the behaviour and operating principle of the liquid tunable lens (*Varioptic Arctic 320*). An object which is out of focus of an a refocusing system can be made in focus by tuning the voltage applied to the liquid lens. For objects situated far away the system the voltage level is low, whereas, if the object is moved closer, the voltage must be increased. There is a voltage range where the tunable lens behaves in a stable and reliable way.

The fabricated lenses (in PMMA by ultraprecision diamond tooling) of the refocusing channel have been characterized by means of a measurement coordinate machine (Werth UA 400). Three of the four lens surfaces that compose this system have been manufactured correctly. The wrong fabricated surface has been made with the design specifications corresponding to the second designed surface instead of the third designed surface, the correct one.

An experimental setup has been built up to investigate the performance of the refocusing channel. According to the designed system, the tunable lens must be positioned in-between the two passive lenses. It has not been possible to reproduce the nominal (designed) distance between the components in the setup. The first reason is that the optimal position of the image sensor has varied with respect to the original simulations as a result of the modification in the characteristic of one of the lenses. The second reason is that the packaging of the tunable lens imposes a limitation in the available space. Therefore, two distances have been modified: the distance between the tunable lens and the second passive lens (larger) and the distance between the second passive and the image sensor (shorter).

The mounted refocusing system has been demonstrated is able to capture good quality images in a vast range of distances (from 0.15 m up to 3 m approximately) by tuning the voltage in . Moreover, the high degree of detail observed in some captured images corroborates the high resolution property of the second optical channel of the Dynamic System.

Several measurements of the achievable object distances as well as depth of field (DOF) and the depth of focus have been completed, obtaining a voltage-object distance curve or a voltage-detector distance curve. This has been done for various detector (CMOS image sensor) positions (voltage-object distance curve) and object locations (voltage-detector distance curve.) The results show that when the detector is closer to the second passive lens the object can be moved further and the DOF enlarges. In the investigation, it has also been observed that the tunable lens has a hysterical behaviour and as result, the optimal position of the object/detector for a certain voltage is not the same if the voltage sweep goes from higher to lower voltage values or in the other way.

The accomplished proof-of-concept demonstration of the refocusing channel is quite promising for future approaches.

2. Perspectives

The full Dynamic System encompassing the two channels still needs to be demonstrated, i.e., the two optical channels that composes the refocusing imaging system should be integrated. One aspect to consider in such integration is that the packaging of the tunable lens (how the voltage is supplied to the liquid lens) has to be as small as possible. An idea is that the circuitry for creating the potential difference (voltage supplier) and the lens are in the same chip.

The Static System is static because of not only the absence of a refocusing functionality but also the absence of any components which aid to focus the high resolution channel to the desired direction. Currently, it is not possible to obtain detailed information of a desired area of interest unless the whole system is turned to that direction (by moving mechanically). It will be interesting if the system incorporates movement capabilities, for example using actuators or active optics (or at least adapting the concept), so pointing to a particular direction is feasible. Active optics can be also used to reduce or control the amount of distortion as J. Parent and S.Thibault demonstrated with a locally magnifying imager [21].

Thinking in applications, from an artistic point of view it should be curious to use the Static System in cinematography and photography as it is possible to have three images of different resolution (more or less detail) and viewed fields at the same time and space (image sensor). One model is cubism where different perspectives are painted in the same plane. ;-)

Appendix A. Matlab MTF code

```
function [m1,m2] = mtf23 (imagename,nsamples,nitera)

% MTF21
%
%[M1,M2,m1mean,m2mean]=MTF23(IMAGENAME,NSAMPLES,NITERA) Calculates and
%   depicts MTF of an image. Noise treatement for each sample
%   only vertical
%
% Input: image name or path, number of samples to take.
% Output: MTF (values and graphic) Statistics
%         Histogram for input and no noise images.
%
%%%%%%%%%%%%%%%%%%%%%%%%%%%%%%%%%%%%%%%%%%%%%%%%%%%%%%%%%%%%%%%%%%%%%%%%

%initialization
data=zeros(2,nsamples);
m1=zeros(nitera,nsamples);
m2=zeros(nitera,nsamples);
stat=zeros(2,2);

%main program
I=im2double(open_bitfield_bmp_new(imagename)); % read image -> [0..1]matrix
Io=I;
if ndims(Io)==3
    I=rgb2gray(Io);      % treatment for RGB img --> rgb to gray;
end

figure(1); imhist(I); title('general histogram');
fprintf('mean=%d ; std=%d \n', mean2(I), std2(I));

freq=input('Introduce the frequency values [f1 f2 ... fn]: ');
if length(freq)~= nsamples
    disp('Error!:  mismatch n. of freq values "nsamples"\n');
    freq=input('Introduce the frequency values [f1 f2 ... fn]: ');
end

for nit=1:nitera
    fprintf('Loop %d ... \n \n', nit);
    figure(3); imshow(I,[min(min(I)) max(max(I))]);impixelinfo;
    %imshow(I); impixelinfo;
    title('Original image. Obtain the coordinates');
    %improfile(),grid on
  %intensity profile
%     h = imrect(gca, []); %[a b c d]
%     fcn =
makeConstrainToRectFcn('imrect',get(gca,'XLim'),get(gca,'YLim'));
%     setPositionConstraintFcn(h,fcn);
%     pos=getPosition(h);
%     figure(4); xlabel('dist(pixel)'); ylabel('Intensity');
%     [~,name,~]=fileparts(imagename); title({['Intensity values ' name]});
%     plot(I(pos(2):(pos(2)+pos(4)), pos(1):(pos(1)+pos(3))));

    for o=1:2           %vertical=1 / horizontal=2
        if o==1
            fprintf('vertical ||| \n \n');
        else
            fprintf('horizontal =_ \n \n' );
```

```
        end
        for k=1:nsamples
            coord=input('Introduce the coordinates [x0 y0 x1 y1]: ');
            if (coord(3)< coord(1)||coord(4)< coord(2))
                fprintf('Review coordinate values!!!\n');
                coord=input('Introduce the coordinates [x0 y0 x1 y1]: ');
            elseif length(coord)~= 4
                disp('Error!:  not enough values');
                coord=input('Introduce the coordinates [x0 y0 x1 y1]: ');
            end

Isub=get_img_freq(I,freq(k),coord(1),coord(2),coord(3),coord(4),k,o);

            [Imax,Imin]=noise2(Isub); %noise treatment
            modul=modulation2(Imax,Imin,freq(k));
            if o==1
                data(1,k)=modul;
            else
                data(2,k)=modul;
            end;
            fprintf('%d laps to go... \n \n', (nsamples-k));
        end
        m1(nit,:)=data(1,:);
        m2(nit,:)=data(2,:);
    end
    stat(1,:)=[mean(m1(nit,:)) std(m1(nit,:))];     %calc average and
standard deviation
    stat(2,:)=[mean(m2(nit,:)) std(m2(nit,:))];
    fprintf('V: mean = %d ; std = %d \n', stat(1,1), stat(1,2));
    fprintf('H: mean = %d ; std = %d \n', stat(2,1), stat(2,2));

    figure(10); %subplot(4,3,nit);
    plotmtf(freq,m1(nit,:),m2(nit,:),imagename);  %depict  mtf vs
freq(lp/mm)


%export data to a file
    print=[freq; data];
    fid = fopen('mtfvalues.txt', 'w+');    % open file with write
permission
    fprintf(fid,'%4s %10s %10s\r\n','freq (lp/mm)','mod V','mod H');
    fprintf(fid, '%8.3f %14.3f %10.3f\r\n', print);
    fclose(fid);
    type mtfvalues.txt   % view the contents of the file
    f=freq';d=data'; v=[f,d];
    save
('C:\Users\Samsung\Documents\MATLAB\results\dynamicsystem\mtfdata.txt','v',
'-ascii', '-double', '-tabs');
end

**********************************************************************
```

```
function [imf] = get_img_freq (I,f,x0,y0,x1,y1,k,o)
% GET_IMG_FREQ
%
% IMF=GET_IMG_FREQ(I,F,X0,X1,Y0,Y1) the corresponding image part according
% to the frequency values.
% Input: general matrix, initial-final values of submatrix and its
%   associated frequency value
% Output: subimage and submatrix in IMF
%

% error checking
if nargin<7
    disp('not enough arguments');
end

% main program
imf=I(x0:x1, y0:y1);
fprintf('Matrix for frequency %d \n',f);
if o==1
    figure(8); subplot(8,6,k);imshow(imf);impixelinfo;      %vertical
    title({['freq ' num2str(f)]});
else
    figure(8); subplot(8,6,k+24);imshow(imf);impixelinfo;  %horizontal
    title({['freq ' num2str(f)]});
end
```

****

```
function [Imax, Imin] = noise2 (Isub)

% NOISE2
%
% (INTMAX,INTMIN)=NOISE2(ISUB)  Subtract the noise from the image(sample)
%  treating separately black and white
%
% Input:  sample intensity matrix
% Output: maximum and minimun intensity values without 'noise'.
%  Figure/histogram
%
%%%%%%%%%%%%%%%%%%%%%%%%%%%%%%%%%%%%%%%%%%%%%%%%%%%%%%%%%%%%%%%%%%%%%%%%%%%

figure(20); subplot(2,3,1); imhist(Isub); title('sample histogram');
fprintf('mean=%d ; std=%d \n', mean2(Isub), std2(Isub));

maxv=max(Isub); errmax=abs(maxv-mean(maxv));  emax=mean(errmax);    %white
minv=min(Isub); errmin=abs(minv-mean(minv));  emin=mean(errmin);    %black

figure(20); subplot(2,3,4); imhist(errmax); title('error max histogram');
figure(20); subplot(2,3,5); imhist(errmin); title('error min histogram');
fprintf('error max = %d \n', emax);  fprintf('error min = %d \n', emin);

Intmax=max(0,(Isub-emax)); Intmin=max(0,(Isub-emin));  %error subtraction
sample
figure(20); subplot(2,3,2); imhist(Intmax); title('no noise max
histogram');
figure(20); subplot(2,3,3); imhist(Intmin); title('no noise min
histogram');
```

```
figure(21);subplot(1,2,1); imshow(Intmax);impixelinfo; title('error max
subtr');
 figure(21);subplot(1,2,2); imshow(Intmin);impixelinfo; title('error min
subtr');

 Imax=max(0,(max(max(double(Isub)))-emax)); %max intensity value
 Imin=max(0,(min(min(double(Isub)))-emin)); %min intensity value
```

****

```
function [mod] = modulation2 (Imax,Imin,f)

% MODULATION2
%
% MOD=MODULATION2(IMAX,IMIN,F)  Calculation of modulation for a
%  discrete frequency value
%
% Input: min and max intensity values and frequency value for a sample
%
% Output: Maximum and minimun values of intensity. Modulation index.
%%%%%%%%%%%%%%%%%%%%%%%%%%%%%%%%%%%%%%%%%%%%%%%%%%%%%%%%%%%%%%%%%%%%%%%%%%%
% main program
mod =(Imax-Imin)/(Imax+Imin);
fprintf('Imax = %d; Imin = %d \n', Imax, Imin);
fprintf('Modulation index for frequency %d: %d \n',f, mod);
```

****

```
function [] = plotmtf (f,mod1,mod2,imagename)

% PLOTMTF
%
% []=PLOTMTF(MOD,F) Plot the MTF of an image
% Input: modulation and frequency values (matrix/vector)
%
% Output: Plot
%%%%%%%%%%%%%%%%%%%%%%%%%%%%%%%%%%%%%%%%%%%%%%%%%%%%%%%%%%%%%%%%%%%%%%%%%%%
ylim([0,1]);
xlim([0,60]);
xlabel('lp/mm');
ylabel('modulation');
[~,name,~]=fileparts(imagename);
title({['MTF ' name]});
hold on
plot(f,mod1,'-ro','LineWidth',1,'MarkerEdgeColor','k',...
            'MarkerFaceColor','r','MarkerSize',4);
plot(f,mod2,'-gs','LineWidth',1,'MarkerEdgeColor','k',...
            'MarkerFaceColor','g','MarkerSize',4);

legend('vertical','horizontal');
hold off;
```

References

[1] E. Moens, Y. Meuret, H. Ottevaere, M. Sarkar, D. S. S. Bello, P. Merken, H. Thienpont, *An insect eye based image sensor with very large field of view*, Micro Optics 2010, Proc. of SPIE, Vol. 7716.

[2] Duparré, J. and Wippermann, F., *Micro-optical artificial compound eyes*, Bioinsp. Biomim. 1, R1-R16 (2006).

[3] J. Duparré, P. Dannberg, P. Schreiber, A. Bräuer, A. Tünnermann, *Artificial Apposition Compound Eye Fabricated by Micro - Optics Technology*, Applied Optics, Vol.43, Issue 22, 2004, pg. 4303-4310

[4] Marcenaro, L., Marchesotti, L. and Regazzoni, C.S., *A multi-resolution outdoor dual camera system for robust video-event meta data extraction*, Proceedings of International Society of Information Fusion (ISIF), 1184-1189 (2002).

[5] Milojkovic, P., Gill, J., Frattin, D., Coyle, K., Haack, K., Myhr, S., Rajan, D., Douglas, S., Papamichalis, P.,Somayaji, M., Christensen, M. P., and Krapels, K., *Multichannel, agile, computationally enhanced camera based on PANOPTES architecture*, Computational Optical Sensing and Imaging, OSA Technical Digest (CD) (Optical Society of America), paper CTuB4 (2009).

[6] J. Duparré, R. Völkel, *Novel Optics/Micro - Optics for Miniature Imaging Systems*, Proc. of SPIE Vol. 6196, 2006.

[7] J. Parent and S. Thibault, Active imaging lens with real-time variable resolution and constant field of view, Optical Society of America (2010)

[8] Viola, P. and Jones, M., *Robust real-time object detection*, Second International Workshop on Statistic

[9] G. Y. Belay, Y. Meuret, H. Ottevaere, P. Veelaert, H. Thienpont, *Design of a Multi - channel, Multi - resolution Smart Imaging System*, in Proc. SPIE, Vol. 8429-Optical Modeling and Design , 8429-10, 2012.

[10] http://paulbourke.net/miscellaneous/lens/
[11] http://cnx.org/content/m42517/latest/?collection=col11406/latest

[12]

[13] R. Baets, G. Roelkens, *Fotonica Photonics,* Universiteit Gent, (syllabus 2010-2011).

[14] http://www.dvinfo.net/articles/optics/lensdefects.php

[15] L. Qiang, N. M. Allinson, FPGA Implementation of Pipelined Architecture for Optical Imaging Distortion Correction, (2006)

[16] http://spie.org/x34298.xml

[17]http://www.edmundoptics.com/technical-resources-center/optics/modulation-transfer-function/?&pagenum=2

[18] http://www.youtube.com/watch?v=1VgqsMqBpKc

[19] X. Zhanga et al. Measuring the Modulation Transfer Function of Image Capture Devices: What Do the Numbers Really Mean?, Proc. of SPIE-IS&T Electronic Imaging, SPIE Vol. 8293, 829307, (2012)

[20] http://carlesmitja.net/2011/02/06/image-quality-of-photographic-cameras/

[21] J. Parent and S.Thibault, *Locally magnifying imager*, Optical Society of America, 2011

[22] http://www.vision-systems.com/articles/print/volume-15/issue-7/Features/Tunable_Optics.html

[23] L. Smeesters, *Integration of tunable lenses in micro - optical smart camera systems,* Master thesis (Master in de Ingenieurswetenschappen: fotonica) 2011-2012

[24] Hung-Chun L. and Yi-Hsin L., An electrically tunable-focusing liquid crystal lens with a low voltage and simple electrodes, Optical Society of America, 2012.

[25] W. J. Smith, *Modern Optical Engineering* 4th ed., (McGraw-Hill, 2007).

[26] Hecht, O*ptics* 2nd ed.(Adisson Wesley)